. Department of Commerce
Henry A. Wallace, Secretary
tional Bureau of Standards
E. U. Condon, Director

# Journal of Research of the National Bureau of Standards

AUGUST 1946

VOLUME 37

NUMBER 2

UNITED STATES
GOVERNMENT PRINTING OFFICE
WASHINGTON : 1946

# Contents

RP

Page

1730. Viscosity and the extraordinary heat effects in glass. Arthur Q. Tool. (Price 10 cents) 73

1731. An arrangement with small solid angle for measurement of beta rays. Leon F. Curtiss and Burrell W. Brown. (Price 5 cents) 91

1732. Heats, equilibrium constants, and free energies of formation of the alkylbenzenes. William J. Taylor, Donald D. Wagman, Mary G. Williams, Kenneth S. Pitzer, and Frederick D. Rossini. (Price 15 cents) 95

1733. A study of the damaging effect of fatigue stressing on SAE X4130 steel. John A. Bennett. (Price 10 cents) 123

1734. Purification, purity, and freezing points of 31 hydrocarbons of the API-NBS series. Augustus R. Glasgow, Jr., Evelyn T. Murphy, Charles B. Willingham, and Frederick D. Rossini. (Price 10 cents) 141

1735. Absorption measurements for broad beams of 1- and 2-million-volt X-rays. George Singer, Carl B. Braestrup, and Harold O. Wyckoff. (Price 10 cents) 147

. Department of Commerce
onal Bureau of Standards

Research Paper RP1730
Volume 37, August 1946

Part of Journal of Research of the National Bureau of Standards

# Viscosity and the Extraordinary Heat Effects in Glass

*By Arthur Q. Tool*

In accordance with experience concerning the behavior of glass at temperatures within its annealing range, an equation is proposed that relates the various extraordinary heat effects to the inelastic deformability and to the degree of superheating or undercooling. By using this equation in connection with the thermal-expansion curves of a glass within its annealing range, certain constants that are related to the coefficient of viscosity and its changes with temperature and the degree of superheating or undercooling have been determined with reasonable results. Such results make it possible to estimate the inelastic deformability of a glass in its various conditions at all annealing temperatures and are, therefore, valuable in connection with problems that are encountered in the process of annealing glass. The apparent success achieved in applying the proposed equation to experimental data suggests that the concepts underlying this equation are fundamental and must be considered in any theory concerning the constitution of glass or that of any other extremely viscous liquid.

## Contents

| | Page |
|---|---|
| I. Introduction | 74 |
| 1. Superheating and undercooling with accompanying extraordinary effects in viscous liquids | 74 |
| 2. Equilibrium curve of a viscous liquid | 74 |
| 3. Equilibrium temperature | 74 |
| 4. Changes in equilibrium temperature and their relation to inelastic deformability under elastic molecular strains | 75 |
| II. The approach to equilibrium | 76 |
| 1. Differential equations for the rate of approaching equilibrium | 76 |
| 2. Equations modified for linear heating or cooling | 76 |
| 3. Relation of equilibrium temperature to changes in length | 77 |
| III. Application of equations to thermal expansion data | 78 |
| 1. Thermal expansion curves | 78 |
| 2. Method of estimating expansivities | 79 |
| 3. Determination of equilibrium temperatures | 79 |
| 4. Insufficiency of equation 8 which relates viscosity to actual temperature only | 80 |
| 5. Determination of constants in equation 7 which relates viscosity to both actual and equilibrium temperatures | 80 |
| 6. Testing the applicability of equation 7 | 81 |
| (a) First method | 81 |
| (b) Second method | 82 |
| 7. Evidences of plasticity | 83 |
| 8. Use of equation 7 in determining cooling curves | 83 |
| IV. Application of equations to endothermic and exothermic effects | 84 |
| 1. Relation of heat effects to inelastic deformability | 84 |
| 2. Experimental conditions in determining heat effects | 84 |
| 3. Relation between heat effects and changes in equilibrium temperature | 84 |
| 4. Estimated heat effects based on equilibrium temperatures obtained from thermal expansion curves | 87 |
| V. Speculative discussion | 88 |
| VI. Conclusion | 89 |
| VII. References | 90 |

# I. Introduction

## 1. Superheating and Undercooling with Accompanying Extraordinary Effects in Viscous Liquid

As already pointed out [1, 2, 3],[1] there is a possibility that the extraordinary heat effects (including the rapid expansion) of glass in its annealing range result because the high viscosity, which increases rapidly as the temperature decreases, causes glass to become considerably superheated or undercooled even when the rates of heating or cooling are very low. Although the phenomena are related in some respects, the superheating and undercooling of glass are not those experienced when melting and crystallization, respectively, are delayed. Rather, they are effects that may be envisioned as possible even in the most fluid liquid at temperatures far above its freezing point if unattainably high heating and cooling rates could be employed. When a liquid is in equilibrium at any given temperature, there is an average statistical relation between its molecules that is unique, since any change in temperature, even if infinitesimal, will change it accordingly. Such a change in the average statistical relation, which corresponds to an equilibrium condition, presumably requires many processes or readjustments involving the molecules of the liquid. Although some of these adjustments are completed almost instantaneously, time is undoubtedly an important factor in the development of many others, especially if their progress is affected by viscosity. If the time required for the full development of the sluggish readjustments, that are demanded by a given change in temperature, exceeds the time required to accomplish the temperature change, the liquid can be brought to a temperature in a state of nonequilibrium. That is, in the case of heating, the liquid can be superheated and, in the case of cooling, it can be undercooled. Moreover, if the cooling increases the viscosity so greatly that the development of the lagging processes ceases altogether, the liquid (unless reheated) will remain indefinitely in the undercooled state. It may even attain the amorphous solid condition if cooled sufficiently.

When a liquid glass reaches any temperatur a state of nonequilibrium, it might, on thought, seem improbable that this underco or superheated state corresponds closely t equilibrium condition at some intermediate t perature between the temperature reached that at which the liquid was in equilibrium w the cooling or heating was initiated. Doub there are many cases in which such a cor pondence is wanting, but it appears to exis most glasses if the tests are not too search Considerable discussion of this point is inclu in a previous paper [1].

## 2. Equilibrium Curve of a Viscou Liquid

When almost any glass is cooled and hea through its annealing range at a low enough r it is always practically in equilibrium on reach any temperature in that range. By determin the changes in various properties as these tr ments proceed, equilibrium curves can be est lished. A rapid heating or cooling from temperature at which a glass is in equilibri causes departures from such curves. If s departures are caused by sufficiently high rate heating or cooling and if the glass is returned the initial temperature with equal rapidity no other lapse of time, it will be found that glass is still in practical equilibrium at t temperature. However, if the initial heating cooling is comparatively slow, the departures be less marked and a very rapid return of glass to its initial temperature will show tha is no longer in equilibrium there. After a trials in which the same departure is always p duced, it will be found, nevertheless, that glass can be brought rapidly to some other t perature at which it is in practical equilibri This temperature will be higher or lower than initial equilibrium temperature, according a heating or a cooling caused the departure. appears, therefore, that in certain respects th has been no marked departure of the glass fr the equilibrium sequence that it follows on s heating and cooling.

## 3. Equilibrium Temperature

In view of experiences such as those just d cussed, it has been conjectured that glass, w

[1] Figures in brackets indicate the literature references at the end of this paper.

ed or heated very rapidly in the annealing e, behaves in many respects as a solid material, eas it behaves as a liquid when the rate of erature change is low enough. Further- e, it is inferred that the physicochemical ition or state of a glass is reasonably well n only when both the actual temperature that other temperature at which the glass d be in equilibrium, if heated or cooled very ly to it, are known. This latter temperature been termed the equilibrium, or fictive, erature of the glass, and a glass is under- d or superheated according as the fictive erature is reached by the actual temperature ugh heating or cooling, respectively. Ob- sly, the difference between these temperatures measure of the departure of the glass from ibrium. In the following discussion the ibrium temperature will be designated by $\tau$ der to differentiate it from the actual tempera- , $T$.

stated in previous papers [1, 2, 3, 4], the rate hich equilibrium is approached, whenever a rheated or undercooled glass is held at a tant temperature in the annealing range, is hly proportional to the departure of the glass equilibrium. Moreover, if the departures f the same magnitude, and the temperatures different, it seems that the rates of approach in addition, inversely proportional to the vis- y which increases exponentially with decreas- emperature. Thus, although equilibrium may pproximated in a few minutes at the upper of the annealing range, reaching a similar ee of approximation, even when the initial rture is no greater, may require many months e treating temperatures are near the lower of the range.

## Changes in Equilibrium Temperature and Their Relation to Inelastic Deformability Under Elastic Molecular Strains

pecially when subjected to considerable loads, is, to an appreciable extent, still inelastically deformable at temperatures far below its annealing range. At such temperatures and also at temperatures within the lower part of the annealing range there are indications that glass has ceased to be a truly viscous liquid and possibly has assumed a plastic nature [4, 5]. That is, whether the loads are of a purely mechanical or a physicochemical character, it appears that the number of flow planes decreases rapidly with the temperature unless the loads exceed "minimum" limits, which presumably also vary with the temperature and condition of the glass. When flow in a plastico-viscous material is being maintained by stresses of either a mechanical or a molecular nature, the viscous flow that has been proceeding unhampered along certain localized flow planes may become completely blocked at any time because of changed molecular relations, or it may stagnate in a limited locality because conditions in the immediate or surrounding neighborhood have reduced or eliminated the load, at least, temporarily. Likewise, the resistance in a flow plane that has been blocked may break down because the flow in neighboring planes has unkeyed the block or developed stresses that exceed the breakdown limit. As a consequence, some readjustments and molecular processes in a glass approaching equilibrium may not only develop much more rapidly than others, but some may also become completely blocked at low annealing temperatures. The discussion [1] of some peculiarities observed in the exothermic effects yielded by samples of a chilled glass, that were only partially annealed at low annealing temperatures, was based on this concept of the behavior of glass at low annealing temperatures. Furthermore, according to this concept, it is obvious that any theory based on the assumption that glass is a purely viscous liquid will not be applicable at temperatures below the annealing range. The effects caused by the development of a plastic condition are demonstrated in the following pages. However, such effects are simply modifications of the heat effects, density changes, etc., that would have occurred if the elastic molecular strains had relaxed because of viscous flow alone.

# II. The Approach to Equilibrium

## 1. Differential Equations for the Rate of Approaching Equilibrium

According to the introductory statements relative to the rate of approaching equilibrium,

$$d\tau/dt = K_\tau(T-\tau). \quad (1)$$

In this relation $K_\tau$ is a factor that is inversely proportional to the viscosity as long as there is little change in the coefficient of elasticity, and $d\tau/dt$ and $T-\tau$ are, respectively, the time rate of change in the equilibrium temperature, $\tau$, and the departure of this fictive temperature from the actual temperature, $T$. Assuming the empirical relation suggested by Twyman [6] for the dependence of viscosity on temperature in the case of a glass in its annealing range, it appears that

$$K_\tau = Ke^{\tau/k}. \quad (2)$$

In this expression, $k$ is Twyman's constant, and $K$ is obviously the value of $K_\tau$ when $T=0$. Thus, $K$ is an extrapolated coefficient that relates to the inelastic deformability at 0° C. Experience indicates that $K$ is approximately the reciprocal of the Maxwellian relaxation time for mechanical stresses, and it is, consequently, extremely small for glass at ordinary temperatures. This apparent similarity between the approach to equilibrium and the relaxation of ordinary elastic strains first suggested that the relaxation of certain elastic molecular strains effects the approach to equilibrium.

On combining eq 1 and 2, the expression

$$d\tau/dt = K(T-\tau)e^{\tau/k} \quad (3)$$

results. Even in the annealing range, eq 2 and 3 yield only a very rough fit when they are applied to data procured on an annealing glass. For example, $d\tau/dt$ will decrease somewhat more slowly with time in an undercooled glass and somewhat more rapidly in a superheated one than eq 3 allows. One purpose of this paper is to demonstrate this inadequacy of eq 3 when it is applied to the extraordinary contraction and expansion and to the exothermic and endothermic effects of a glass that is being heated through its annealing range.

That eq 2 and, consequently, eq 3 are not adequate is not surprising as the effect of a changing $\tau$ on the viscosity is ignored. From experience it seems that the manner in which a property is affected by a change in $\tau$ is very similar to that in which it is affected by a change in $T$. For reason it has been assumed in previous cases that eq 2 would be more nearly adequate had the form

$$K_\tau = Ke^{\tau/g}e^{\tau/h}$$

and $g$ and $h$ were analogous to Twyman's stant $k$. Equation 3 then becomes

$$d\tau/dt = K(T-\tau)e^{\tau/g}e^{\tau/h}.$$

By this means the above-mentioned inadequ in expressing the change in $\tau$ at all ordinary a ing temperatures seem to be removed. How more precise data on the changes that are c in various properties and effects must be pro before a final decision on this point is rea In any case, it is obvious that eq 4 and 5 a inadequate as soon as glass ceases to be a p viscous liquid and assumes a definite pla viscous nature. That is, eq 4 does not take account the possibility that the coefficien inelastic deformability may depend on the Moreover, this equation may not be adequa express the changes in viscosity over wide te ature ranges.

## 2. Equations Modified for Linear He ing or Cooling

In many heating tests, $T$ is increased at a stant rate that considerably exceeds that at w $\tau$ decreases at temperatures below the ann range even if the initial $\tau$-value was high. in the plastico-viscous range of a glass, the tion between $T-\tau$ and $T$ diverges compara little from a linear one during any given t which the heating rate is relatively high constant. The absolute value of the factor as it appears in eq 3 and 5 may be thought possessing some of the qualities of a mecha load, especially in its relation to the ina deformability of a plastico-viscous glass. is, as this factor increases, the deformabili creases. If the change in the plastic deforma is an exponential function of the load, and i special heating condition mentioned above i in any test, then eq 5 should be modified fo plastico-viscous range by introducing the f $e^{(T'-T)/g'}$. In this exponential factor, $T'$ is sumably near the upper limit of the range in w the glass is appreciably plastic.

When a glass is being heated or cooled constant rate ($dT/dt = \pm R$, respectively) in

being held at a constant annealing temperature, 3 and 5 become

$$d\tau/dT = \pm(K/R)(T-\tau)e^{T/k} \quad (6)$$

d

$$d\tau/dT = \pm(K/R)(T-\tau)e^{T/k}e^{\tau/h}. \quad (7)$$

If $T$ and $d\tau/dT$ are given, $T-\tau$ is definitely termined according to eq 6, and the equation also easily solved in terms of exponential inte-ls. That is, if $y=(T-\tau)/k$ and $\pm x=(K/R)ke^{T/k}$, $d\tau/dT=\pm xy$ and

$$Ei(\pm x)-Ei(\pm x_0)=ye^{\pm x}, \quad (8)$$

ce $dy \pm ydx=(dx)/x$. In this equation, $x_0$ is the lue of $x$ for some particular temperature, $T_0$, which the glass was in equilibrium. (For the ndition that equilibrium does not exist at $T_0$, e right-hand member becomes $ye^{\pm x}-y_0e^{\pm x_0}$.) viously, the negative sign before $x$ is used in the se of cooling, and $y$ is positive or negative cording as the glass is superheated or under-oled.

With respect to eq 7, assigning values to $T$ and $/dT$ leaves $T-\tau$ indeterminate, since, under rtain conditions, $\tau$ may have, from a physical as ll as from a theoretical standpoint, either of o values,[2] depending on $\tau_0$, the initial value of $\tau$. though no simple solution for this relation is ailable, the course followed by $T-\tau$ during any heating or cooling is quite definite for any given set of initial conditions. Since $(1/g)+(1/h)=1/k$, as previously shown [4], eq 7 becomes $1/x-(h/k)dy/dx=\pm ye^{-y}$ if substitutions,[3] $y=(T-\tau)/h$ and $\pm x=(K/R)\ he^{T/k}$, are made. However, from a practical standpoint, neither this nor any of the numerous other forms that can be obtained by various substitutions and transformations seem to possess advantages over eq 7. Although a solution of this equation is lacking, it as well as eq 8 can be tested by the use of thermal expansion data and also by a study of their significance with respect to the endothermic and exothermic effects observed in glass.

## 3. Relation of Equilibrium Temperature to Changes in Length

When $\tau$, that is $T-ky$, has been computed by means of eq 8 for various temperatures through the use of assumed or determined values for $k$, $K$, $x_0$, and $R$, the computed results may be compared with experimental data obtained on any property that is subject to the extraordinary changes observed when a glass is heated or cooled through its annealing range. For example, the linear thermal expansion curves may be used, although it is difficult to determine precisely the expansivities for those values of $T$ and $\tau$ that are in that part of the practical annealing range where softening begins. It appears that no great errors are introduced by assuming that the linear expansivities ($a$ for varying $T$ and constant $\tau$, and $\alpha$ for varying $\tau$ and constant $T$) are approximately constant throughout the annealing range and have values that can be determined with reasonable precision near the lower limit and sometimes even throughout the lower half of that range. Thus, it appears that the linear expansion per unit length through the annealing range is expressed approximately by

$$(L-L_0)/L_0=a(T-T_0)+\alpha(\tau-\tau_0) \quad (9)$$

if $L_0$ is the length of the glass sample when $T=T_0$ (a temperature that will usually be chosen at some point within or just below the annealing range and that may or may not be that for which $x=x_0$ and $\tau=\tau_0$). The use of eq 9 in conjunction with eq 7 is considered in the following section.

When $y$ or $(T-\tau)/h$, has the value +1, the product $e^{-T/k}d\tau/dT$ has only one e, the maximum possible. If, in addition, $d\tau/dT=+1$, then $y$ is at a imum and $e^{T/k}=Re/Kk$. Furthermore, $T=k$ ln $(Re/Kk)$ is the minimum perature, $T_m$, for which $d\tau/dT$ can be +1. That is, $ye^{-y}<e^{-1}$ if positive $y$ ther greater or less than unity, and $T>k$ ln $(Re/Kk)$ if $d\tau/dT=1$ at the e time.

Then $ye^{-y}$ has a positive value less than $e^{-1}$, it is obvious that $y$ has a pair ossible values, one greater and one less than unity. If $T$ is the same in h cases, $d\tau/dT$ will also be identical and, moreover, it is obvious that the es of $y$, under such conditions, correspond to different heating curves. at is, the larger value corresponds to a curve procured on a comparatively l-annealed sample of glass ($\tau_0<T_m$), whereas the lesser corresponds to a ve obtained, under the same standard conditions of test, on a less well aled sample of the same glass ($\tau_0>T_m$). Furthermore, if $d\tau/dT=1$ these values of $y$, it follows that the common temperature, $T$, for the two e is greater than $T_m$. When the usual heating rate (3° to 6° C/min) is loyed, it will be found that the condition $y=1$ and $d\tau/dT=1$ usually rs when the sample has been moderately well annealed. Since the heat t (endothermic effect, for instance) is just getting under way when $T$ is unity, it often appears that the beginning of the endothermic (or d expansion) effect in a moderately annealed sample occurs at a somewhat er temperature than in either less or more thoroughly annealed samples. mples of series of curves that present this appearance are found in figures d 8 of a previous publication [1].

For the chilled and annealed samples that were used in the expansion tests e described in this paper, the temperatures at which $d\tau/dT$ equaled y were estimated to be 586° and 578° C, respectively. When $T_m$ was puted by using the values found for $k$, $h$, and $K$ (or $R/K$), the value 9° C was obtained.

f eq 8 were applicable, there would be no $T_m$ above which the maxima of endothermic effects must be reached, and consequently they would not confined to a limited range. Experience shows that the temperature ge in which these maxima occur is limited, even if the treatment of a glass aried greatly.

[3] In making these substitutions, use is made of the identity $e^{T/k}e^{\tau/h}=e^{T/h}e^{(\tau-T/k)}$. However, when appearing in an exponent as in this case, $T-\tau$, although its magnitude is presumably proportional to certain molecular strains, cannot be considered as necessarily having an effect that is analogous to that of a mechanical load in its relation to inelastic deformations.

# III. Application of Equations to Thermal Expansion Data

## 1. Thermal-Expansion Curves

In a progress report [2] made to the Glass Section at the Cincinnati meeting of the American Ceramic Society in 1942, the inadequacy of eq 6 and 8 was shown by applying them to experimental expansion data. It was also pointed out, although not shown definitely, that much of the discrepancy between experimental and computed results could be eliminated by assuming that the viscosity of glass is affected by changes in $\tau$ very much as it is affected by changes in $T$. In the following, a résumé of that report and a fuller discussion of the effect of changes in $\tau$ are presented.

The expansion data used for this purpose were obtained on two samples of a borosilicate crown that was of the usual kind employed in thermometers that are graduated to temperatures that exceed 500° C. One of the samples was treated at a high temperature (approximately 850° C) and cooled rapidly in moving air in order to prevent $\tau$ from falling below 650° C. In fact, the cooling rate of this treatment was such that the red g of the small sample in a comparatively dark r disappeared in about 5 seconds. The other sa was treated for several weeks at 500° C in orde reduce $\tau$ to that temperature. Each sample c sisted of three small pyramids of a type th suitable for expansion measurements by the in ferometric method and that makes very r cooling possible after treatments at high t peratures. The expansion measurements tended from room temperature to the softe point near 620° C and were made by James Saunders according to the weighted-spacer met that he has described [7].

The portions of the resulting expansion cur between 260° and 620° C are shown in figure and 2 (curves 1 and 1′). The relative placem of the two expansion curves (curve of the chil sample above that of the annealed) was determi by making them practically coincide at ab 615° C, where both samples were just entering range of slight but noticeable softening. In t range the $\tau$-values of the two samples were p sumably almost equal, and the values of $T-\tau$ w doubtless not much greater than a degree, as t heating rate used in these tests was only 3 deg min. That is, within the range of appreci softening, it is difficult to maintain $T-\tau$ at va exceeding 1 degree unless the rates of heatin cooling are exceptionally high. In other wo if deformation of the samples had not taken pl the expansion curves presumably would h practically coincided with the equilibrim cu from this point upward. This curve is represe by the line $EE'$, and it intersects the expan curve of the annealed sample at 500° C bec up to that point there was no appreciable cha in the $\tau$-value of that sample. However, if t heating rate from this point had been made w low, the resulting expansion curve on the anne sample would have coincided approximately w $EE'$ from 500° C until the temperature of app ciable deformation was reached. Doubtless line (such as $EE'$) representing the sequence equilibrium conditions in terms of change length should be somewhat curved; but in t purely demonstrational presentation, relati minor details of this nature will be ignored for t purpose of simplicity.

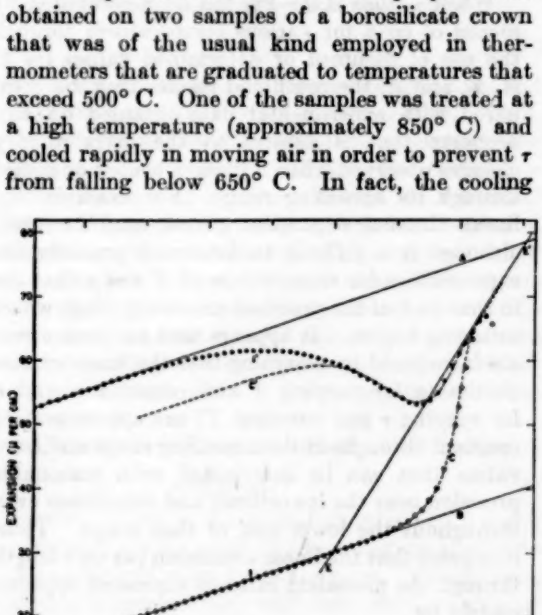


FIGURE 1.—*Comparison of computed and experimentally determined thermal-expansion curves for a borosilicate thermometer glass.*

1 and 1′, Experimental curves for an annealed sample (circles) and a chilled sample (dots), respectively; $A$ and $B$, tangents to curves 1′ and 1, respectively, at points near 370° C; $EE'$, the approximate thermal-expansion curve of the glass when it does not depart from equilibrium because the heating and cooling rates are very low; $C$ and $C'$, computed thermal-expansion curves (broken lines) corresponding to 1 and 1′. These curves were computed in accord with eq 7, and the departure of $C'$ from 1′ below 500° C results presumably because the equation is inapplicable while a glass is in its visco-plastic stage.

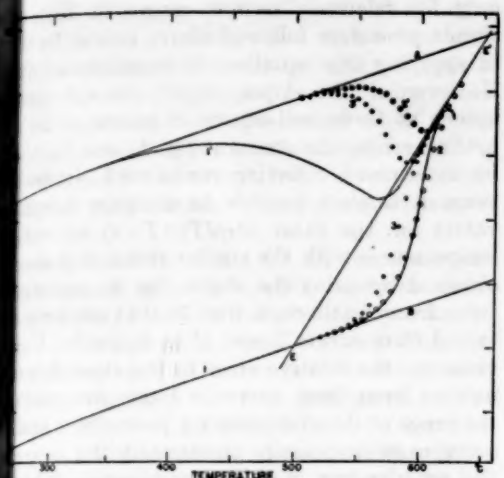


URE 2.—*Comparison of thermal-expansion curves determined experimentally and computed in accord with uation 8.*

*A*, *B*, and *EE'*, Reproduced from figure 1; 2 and 2' (large circles and large s, respectively), correspond to curves 1 and 1' and were computed on the umption that the necessary constants were $k=15$ degrees, $K=e^{-37.5}$, $T_1=500°$ C, and also that the initial $\tau$-values were 500° C and 653° C the annealed and chilled samples, respectively; 3 and 3' (small les and small dots, respectively), similarly computed except that the stants $k=13.57$ degrees, $K=e^{-40.4}$, and $T_1=544.1°$ C were used. This parison of experimental and computed curves indicates that eq 8 is tisfactory, probably because the viscosity varies as the equilibrium perature changes.

## Method of Estimating Expansivities

Between 300° and 500° C the expansivity of the nealed sample was found to be about 0.066 m)/deg C, but below this range the average s less than 0.063. Although the expansivity a severely chilled glass is usually increased a percent at atmospheric temperatures, the ansivity of the chilled sample also appeared e about 0.066 at 300° C. If a line coinciding h the expansion curve of the chilled glass and ing this slope (0.066 $\mu$/deg) is extended to high peratures, it intersects *EE'* at 653° C, which resumably the initial value of $\tau$ in the chilled ple and also its value during the earlier steps the expansion test and until the equilibrium dition of the sample began to change appreably—as it appears to have done immediately ve 340° C. This temperature is about 150 below the lower limit of the practical annealing ge of this glass, and is, therefore, far below the ge in which purely viscous flow is presumed to possible.

If the relative placement of the two curves is approximately correct, the difference (653 to 500 deg) between the initial $\tau$-values of the two samples produced a difference in length of 38.4 $\mu$/cm. This corresponds to a linear expansivity of 0.251 ($\mu$/cm)/deg C change in $\tau$. In the usual units, this value also corresponds to a volume expansivity of $0.75\times10^{-4}$ for a 1-deg change in $\tau$, and it is about 0.7 as large as the value found by testing a borosilicate optical glass. The sum, $0.251+0.066=0.317$, is presumably $10^4$ times one-third of the volume expansivity of the glass when it behaves as a liquid within its annealing range—that is, when this particular glass follows its equilibrium curve (line *EE'*).

## 3. Determination of Equilibrium Temperatures

Knowing the expansivities and the initial $\tau$-values, it is a simple matter to compute the $\tau$-value at any temperature, $T$, from the expansion curves. Thus, for the chilled glass, $\tau=653°-[0.066(T-300)-(L_T-L_{300})/L_T]/0.251$ (see eq 9) and, for the annealed glass, the expression is the same except that 500° replaces 653° C. In figure 3 (curve 1, circles, annealed; curve 1', dots, chilled glass), the $\tau$-values so obtained are plotted against $T$.

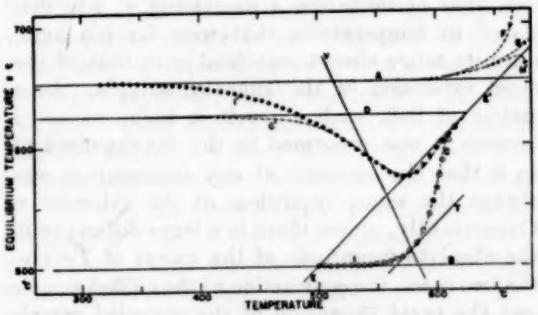


FIGURE 3.—*Curves relating to changes in the equilibrium temperature as a glass is heated or cooled.*

1 and 1' (Circles and dots, respectively), equilibrium temperatures computed in accord with eq 9 from the corresponding experimental curves 1 and 1', figure 1; *C* and *C'* (broken lines), equilibrium temperatures that correspond to curves *C* and *C'* of figure 1 and were computed by a step-by-step method based on eq 5; *B*, *A*, and *D*, tangents ($d\tau/dT=0$) to equilibrium temperature curves 1 and *C*, 1', and *C'*, respectively, at points near 300° C; *EE'*, trend of the equilibrium temperature (slope $d\tau/dT=1$) when glass remains in constant equilibrium because the rate of heating (or cooling) is very low; *T* (parallel to *EE'*), tangent to curves 1 and *C* when degree of superheating (or $T-\tau$) reaches a maximum; *V*, one of a family of curves indicating conditions for constant viscosity; *F*, *G*, and *H*, approximate courses that would be followed by the equilibrium temperature during cooling if the cooling rates (30, 37.5, and 40 deg *C*/sec, respectively) from comparatively high temperatures prevented the equilibrium temperature from falling below 653° C when *T* became zero.

## 4. Insufficiency of Equation 8 Which Relates Viscosity to Actual Temperature Only

In view of the temperature range involved and the form of the $\tau$-curve for the annealed glass, it is comparatively easy to select values for $K$ and $k$ that make it possible to compute, by means of eq 8, a curve that follows the experimental curve moderately well. By introducing the $\tau$-values so computed into eq 9 and thus transforming to expansions again, the computed results shown in figure 2 (curve 2) were procured. To delay the beginning of the rapid expansion to the point indicated by the experimental curve, it was necessary in computing these $\tau$-values and expansions to assume that $K_\tau$ possessed the value unity (reciprocal of 1 hour) at a rather high temperature (560° C). Furthermore, it was then necessary to assign a rather high value (15 deg) to $k$ in order to prevent the rapid expansion from developing too rapidly when $T-\tau$ reached the rather large values indicated by the experimental results. As a result, when this difference became comparatively small at high temperatures, the rate of expansion was too low as a comparison of curves 2 and 1 (fig. 2) indicates. Moreover, when the values assigned to $K$ and $k$ were used to compute 2′ for the chilled sample, the contraction effect, that accompanies a decreasing $\tau$, was displaced to temperatures that were far too high, since its range almost coincided with that of the rapid expansion of the annealed sample. As a matter of fact, such a result is to be expected because it was presumed in the development of eq 8 that the viscosity at any temperature was always the same, regardless of the value of $\tau$. Consequently, unless there is a large difference in the absolute magnitude of the values of $T-\tau$ in the two cases, the contraction of the chilled sample and the rapid expansion of the annealed sample will begin at about the same temperature. Also, the maximum rates of contraction and expansion in these cases will be attained at temperatures that are not materially different.

## 5. Determination of Constants in Equation 7 Which Relates Viscosity to Both Actual and Equilibrium Temperatures

As differential eq 7 has not been solved explicitly for $\tau$ (except in the form of series suitable only for relatively narrow ranges in $T/g$), the simple procedure followed above cannot be used in applying this equation to experimental data. However, if the slopes, $d\tau/dT$, are well enough known at three well-separated points in the annealing range, the constants, $g$, $h$, and $K/R$, can be determined. Having made such determinations, it is then possible to compare computed values for the ratio $(d\tau/dT)/(T-\tau)$ at various temperatures with the similar ratios that can be obtained by using the slopes (fig. 4) and departures from equilibrium (fig. 5) that are both obtained from curves 1 and 1′ in figure 3. Unfortunately, the relative error in the slope determinations from these curves is large over much of the range of the extraordinary heat effects and, in some cases (especially throughout the range of the superheating of chilled specimens), the relative errors in determining $T-\tau$ are also rather large. Nevertheless, it is considered that the data obtained for $d\tau/dT$ and $T-\tau$ (figs. 4 and 5) are adequate for the purpose, because this paper is purely a demonstrational presentation without pretense of high precision.

The three ranges in which these data seemed to be comparatively good were near the respective temperatures (1) at which $d\tau/dT=1$, (2) at which this slope attained a maximum in the case of the superheated annealed sample, and also (3) near the temperature at which the slope reached a minimum (maximum negative value) in the case of the undercooled chilled sample. Letting $p$ and $d$ symbolize slope $(d\tau/dT)$ and departure from equilibrium $(T-\tau)$ and the subscripts $c$ and $a$ indicate the chilled and annealed samples, respectively, the data in the first two cases were: $p_a=1.00$, $T_a=578.0°$ C, $\tau_a=513.0°$ C, and $d_a=65.0°$ C; and (2), $p_a=5.37$, $T_a=603.0°$ C, $\tau_a=578.0°$ C, and $d_a=25.0°$ C. In the third case the data at a point chosen near that of the ma-

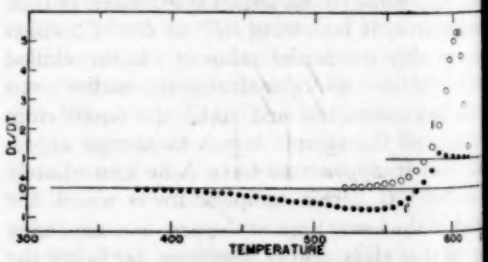


FIGURE 4.—*Slopes of the equilibrium temperature curves and 1′, figure 3, at various actual temperatures.*

were (3), $p_e=-0.72$, $T_e=542.9°$ C, $\tau_e=$ 7° C, and $d_e=-46.8$. Use of the first and of these sets of data with eq 7 gives the result $=(\tau_e-\tau_a)/(T_a-T_e)=2.185$.[4] On using this in connection with the second set of data, llows that $g=19.78$, $h=43.22$, and $k=13.57$. value of $k$ is rather high, but it is by no means xtreme as the value 15 that appeared neces- for eq 8.

using the value found for $h/g$ in connection the second set of data, advantage was taken e fact that $p_a=5.37$ was presumably a maxi- n. At such a point, $dp/dT=0$, and thus, on rentiating eq 7, it follows that for this condi- $h=(p+h/g)d/(p-1)$ and that $p=(1+d/g)/$ $d/h$). These equations also hold for a mini- n in $p$. The fourth set of data was chosen at int where such a minimum appeared to be was as follows: (4) $p_e=-0.73$, $T_e=540.0°$, 591.6°, and $d_e=-51.6°$, and it was found the expression relating $p$ and $d$ was reason- well satisfied by these data without changing d $g$.

aving determined $g$ and $h$, any of these sets of can be used to determine $K/R$ and also $T_1/k$

Introducing two sets of data (such as the first and third presented into eq 7 and by equating the logarithms of the ratios of the correspond- mbers of the two resulting equations, a rearrangement of the result $h/g=(\tau_3-\tau_1)/(T_1-T_3)+(h/(T_1-T_3))$ ln $(p_1d_3/p_3d_1)$. In the above case rd set of data was taken at a point such that $p_1/d_1=p_3/d_3$ approximately. quently the logarithmic term disappeared.

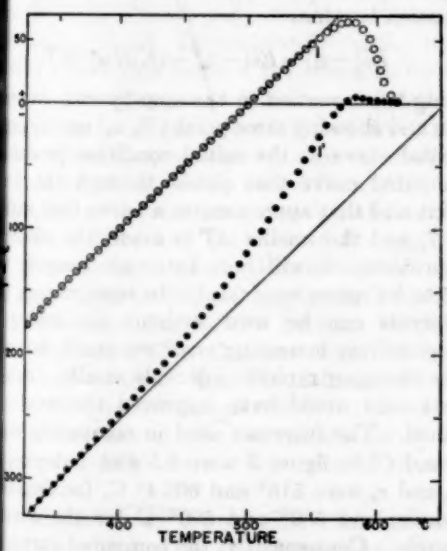


RE 5.—*Degrees of undercooling and superheating* $(T-\tau)$ *indicated by curves 1 and 1' in figures 1 and 3.*

if $T_1$ symbolizes the temperature for which the glass, when in equilibrium ($T=\tau$), has a relaxation time, $1/K_T$, equaling 1 hour. That is, $K=(pR/d)e^{-T/k}e^{-\tau/h}=e^{-T_1/k}$. Since $R=180$ deg/hr (3 deg/min), the two values for $K$ are $K_a=e^{-40.20}$, and $K_e=e^{-40.05}$ if the second and fourth sets of data are used. The corresponding values for $T_1$ are 545.6° and 543.5° C. Two such sets of data should give the same values for $K$ and also for $T_1$ if eq 7 is applicable, regardless of the treatment received by the glass, and the fair agreement found here exceeds what should be expected in view of the unreliability of the $d$- and $p$-determinations. Besides, there is the probability that $R$ varied more than was apparent during the tests.

After these constants are determined for a glass, the relaxation times, $1/K_T$, can be obtained for all conditions and temperatures in the annealing range. Even the viscosity coefficients, $\eta$, can be estimated if the elastic modulus, $E$, is known within reasonable limits. That is, $\eta=E/K_T$.

## 6. Testing the Applicability of Equation 7

### (a) First Method

From eq 7 it is apparent that a straight line should result if ln $(d/p)-d/h$ is plotted against ln $(R/K)-T/k$. That is, as long as the viscosity varies approximately as assumed (and also provided that the relation between it and the extraordinary expansion and contraction is that assumed), there should be within the annealing range no departures from this straight line that are not ascribable to uncertainties in the data. For this test, the $p$ and $d$ values from figures 4 and 5 and the $h$, $k$, and $K$ (average) values given above were used. (Since the rate of heating was 180 deg/hr, $R=e^{5.193}$ and ln $(R/K)=45.320$.)

The results of this test are shown by curve $E$ in figure 6. Between 600° and 500° C the departures from a straight line are reasonably small, except in a few cases in the range where the chilled glass became superheated and the procurement of data without very large relative errors was impossible. However, beginning near 500° C and extending to lower temperatures, there is a steadily increasing departure from a straight line by the results for the chilled glass. The sense of the departure indicates that $d\tau/dt$ at temperatures below the annealing range has absolute values

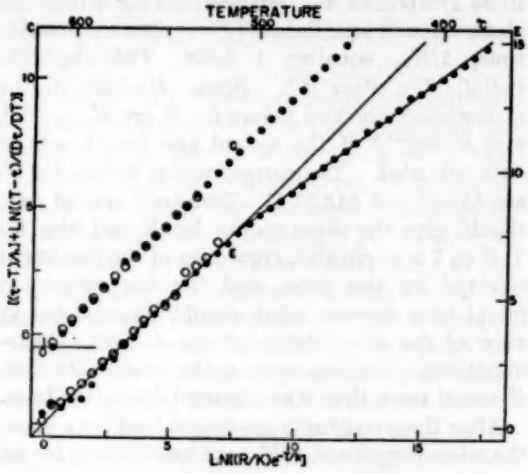


FIGURE 6.—*Test of the degree to which changes in equilibrium temperature satisfy eq 7.*

*E*, Tests of results (curves 1 and 1′ in figs. 3, 4, and 5) derived from thermal-expansion data (curves 1 and 1′ in fig. 1), ordinates on the right. *C*, tests of data derived from curves *C* and *C′* in figure 3 (displaced ordinates on the left). (Circles and dotes, annealed and chilled glass in both cases.)

(at least when $\tau - T$ is large) that are greater than they would have been if the deformability had continued to decrease with decreasing temperature according to its manner of decrease within the annealing range. That is, the relatively distended glass of the chilled sample under heavy loads collapsed more readily at these relatively low temperatures than it would have collapsed if it had retained an almost purely viscous character with a viscosity coefficient that continued to decrease with $T$ and $\tau$ as in the annealing range. This result was expected, because experience in attempts at establishing equilibrium conditions at such relatively low temperatures led to the conclusion that the rate of collapse at these temperatures is no longer roughly proportional to the load, as in the annealing range, but decreases so much more rapidly as the collapse progresses that—in the case of a glass approaching equilibrium at a constant temperature—the product of $e^{(T-\tau)/k}/(T-\tau)$ and $d\ (T-\tau)/dt$ decreases rapidly (instead of remaining constant, as it would if the glass were purely viscous) as $(\tau - T)$ becomes small. That is, when a glass is at a temperature such that it is definitely plastic, this product exceeds or falls short of $Ke^{T/k}$ in magnitude according as the physicochemical "load" (as represented by $(T-\tau)$) is large or small.

### (b) Second Method

As figure 6 indicates that the chilled sample does not behave as required by eq 7 until 500° C is exceeded, it becomes a matter of interest to determine approximately how much lower than 630° the initial $\tau$-value would have been if the glass had behaved according to that equation throughout the heating. Such a determination can be made by laborious step-by-step computations.

If the temperature is constant, eq 5 can be written in the form $e^{-z}dz/z = -Ke^{T/k}dt$, in which $z=(\tau - T)/h$. The solution of this for any interval of time, $\Delta t$, for instance, is $Ei(-z_1)-Ei(-z_0) = -Ke^{T/k}\Delta t$, in which $z_0$ and $z_1$ are the values of $z$ at the beginning and end of the time interval. Consequently, the $\tau$-value reached by a treatment at $T_0$ is $\tau_1 = hz_1 + T_0$. Assuming, now that the temperature is changed so sharply from $T_0$ to $T_0+\Delta T$ at the end of this first step, that $\tau$ remains unchanged, it follows that $e^{T_0/k}$ is changed to $e^{(T_0-\Delta T)/k}$ and that $z_0$ is changed from $(\tau_0 - T_0)/h$ to $z_1 - \Delta T/h$ for the second step in which the glass is treated for an interval, $\Delta t$, at an increased temperature. If $z_2$ is the $z$-value reached at the end of the second time-interval, the $\tau$-value reached is $\tau_2 = hz_2 + T_0 + \Delta T$, and after $n$ such step-by-step treatments, $\tau_n = hz_n + T_0 + (n-1)\Delta T$.

By making $\Delta T/\Delta t = R$, the rate of heating in degrees per hour, the above exponential integral equation becomes

$$Ei(-z_1) = Ei(-z_0) - (K/R)e^{T/k}\Delta T.$$

Using this equation in the step-by-step computation and choosing some point $(T_0, \tau_0)$ on the experimental curve as the initial condition produces a computed curve that passes through this initial point and that approximates a curve that satisfies eq 7, and the smaller $\Delta T$ is made, the closer the approximation will be. Intervals ranging from 0.5 to 6 degrees were tried. In some ranges, large intervals can be used without developing progressively increasing error too much, but where $\tau$ is changing rapidly, intervals smaller than the least used would have improved the results obtained. The intervals used in computing curves $C$ and $C'$ in figure 3 were 0.5 and 1 degree, $T_0$ and $\tau_0$ were 516° and 608.4° C, for the chilled sample, and 530° and 500° C for the annealed sample. Consequently, the computed curves and the $\tau$-curves derived directly from the experimental data intersect at these points.

puted curves, $C$ and $C'$, indicate in both cases the glass at temperatures above 516° C ved very nearly as eq 7 requires.

hen the previously employed test—made by ing ln $((d/p)e^{-d/k})$ against ln $((R/K)e^{-T/k})$—applied to these computed curves, the results n by curve $C$ in figure 6 were obtained. In of the fact that intervals no smaller than alf degree were used, these results are as factory as could be expected, and they ate that the computed curves, $C$ and $C'$ 3), throughout most of their courses are not om curves that fully satisfy eq 7.

## 7. Evidences of Plasticity

figure 3 the trend of curve $C'$ when compared at of curve 1′ at temperatures below the an- ng range suggests that 653° C is about 28 deg r than the initial $\tau$-value required if eq 7 expressed reasonably well the behavior of the d sample at temperatures below as well as in the annealing range. In accord with iously expressed surmises, this difference be- n the actual and required initial $\tau$-values is umably the result of the failure of eq 7 to into account the increased mobility of plastic when subjected to very large loads. In connection, curve $E$ of figure 6 indicates that points that were obtained below 516° C, re $T-\tau$ is almost proportional to $T$, would been alined approximately with those ined above that point if the abscissas for the of these ranges had been computed by s of the expression ln $(R/K)-T/k-(513-$ 2.6. It is to be presumed that the values of the tants $T'$ and $g'$ of this added term (513° and in this particular case) depend, at least, on initial $\tau$-value and the rate of heating. In of previous mention that an added term ining such constants might be indicated r certain conditions, the manner in which results below 516° C depart from the basic ght line suggests that the deformability of in its plastico-viscous condition is an ex- ntial function of the load as well as of the erature. This possibility merits further tigation.

is discussion of the possible characteristics his particular glass at temperatures below C must not be taken as a suggestion that it rgoes some sudden and definite change at that point. It is more probable that all changes that take place in ordinary glasses while heating or cooling do so gradually over a considerable temperature range. That is, this point for the upper limit of the plastic range has about the same significance as the softening point or the point chosen as the beginning of the rapid expansion range.

## 8. Use of Equation 7 in Determining Cooling Curves

Since the magnitude of the cooling rate that produced an initial $\tau$-value of 653° C was a matter of some curiosity, approximations to cooling curves (as shown in fig. 3) were also computed by the step-by-step method [5] and on the assumption that $\tau$ had fallen to 653° C by the time that $T$ had fallen to 550° C, below which there had been no further appreciable change in $\tau$. It was thought that the cooling rate might have been about 40 deg/sec, since it appeared that the sample in cooling from 850° C had lost all redness in about 5 sec. However, the cooling curve procured for that rate suggests a lower rate, because it indicates a crossing of the equilibrium curve at a temperature slightly above 670° C rather than at 850° C. When a rate of 30 deg/sec was used in the computation, the resulting curve began at about 655° C to diverge from the equilibrium curve instead of continuing to approach it. That is, this rate

[5] Equation 8 can be used to determine directly a rate of cooling that is definitely lower than the required rate to produce a given $\tau$-value ($\tau'$) when $T$ becomes zero. When $T$ reaches zero, $z=Kk/R$ and is very small unless $R$ has a very low value. Consequently, $e^z=1$ and $Ei(-z)=\ln(Kk/R)+\gamma$ approximately. (Euler's constant, $\gamma=0.5772+$.) Thus, eq 8, for cooling from an equilibrium temperature, $T_0$, to zero degrees becomes $-\tau'/k=\ln(Kk/R)+\gamma-Ei(-z_0)$ which, since $z_0=(Kk/R)e^{T_0/k}$, may be changed so as to become $[(T_0-\tau')/k]-\gamma=\ln z_0-Ei(-z_0)$. From this equation, $z_0$ is easily determined approximately when the left-hand member is known and adequate tables of exponential functions and integrals are available. Thus, $R$ is known if $T_0$ and the necessary constants of the glass are known. Moreover, $z_0$ is so large, when the starting temperature, $T_0$, is high and $R$ is not too great, that $Ei(-z_0)$ is negligible. Consequently, for such cases $R=Kke^{\tau'+\tau'/k}$. Using the values previously found for $K$ and $k$, and assuming that equilibrium was established when cooling began at a starting point near 850° C, it is apparent that $z_0$ is large for this case and that $R=19.9$ deg/sec, approximately. Thus, a rate computed in this manner and known to be too low, is about one-half of the rate indicated by the step-by-step computation described above.

Occasionally it is desirable to estimate a minimum for the rate at which a glass in equilibrium at some temperature, $T_0$, can be cooled to room temperature without material change in $\tau$ from $\tau_0=T_0$. In such a case, $R$ must be so large that $z_0$ becomes very small. It then becomes obvious, on expanding $Ei(-z_0)$ in the above equation for determining $z_0$, that $T_0-\tau'=kz_0$, approximately, and that $R=Kk^2e^{T_0/k}/(T_0-\tau')$. That is, if eq 8 were applicable, $R$ is the minimum rate necessary to prevent $\tau_0-\tau'$ from exceeding some small assigned value. If $k$ is replaced by $g$, and $K$ by $Ke^{\tau'/k}$, the result is that which would have been obtained if eq 7 had been used for the same purpose and on the assumption that $\tau$ varied so little that $e^{\tau'/k}$ could be treated as constant. The ratio of these results for $R$ is $g^2/k^2$ and the smaller result, at least, is much lower than required, but such computations aid in estimating the cooling rates required to obtain desired $\tau$-values.

was much too low unless a much higher rate preceded it from 850° to about 660° C, for instance. Without using very small intervals in the computation, it also appears that a rate of 37.5 deg/sec is somewhat too low. Thus, it seems that probable average rate of cooling in the ch treatment was slightly under 40 deg/sec. curves *F*, *G*, and *H* in figure 3.

# IV. Application of Equations to Endothermic and Exotherm Effects

## 1. Relation of Heat Effects to Inelastic Deformability

As previously stated [4, 5], the manner in which strain is dissipated in annealing glass and the character of the exothermic and endothermic effects, observed when chilled and annealed glasses are heated, suggest the gradual development and disappearance of a degree of plasticity in glass as cooling and heating, respectively, proceed within and especially below the practical annealing range. As for the expansion effects, so also in that of the endothermic effect, the degree of plasticity that develops within the useful annealing range can apparently be ignored. However, at unusually low and, for most purposes, impractical annealing temperatures, it seems necessary to assume the existence of a considerable degree of plasticity in seeking an explanation for the progressive changes which appear in the exothermic effect of samples of a glass that, subsequent to a severe chilling from a high temperature, have been annealed for different periods of time at a very low annealing temperature. Curves showing such effects have previously been presented [1], and the progressive changes are believed to indicate that some molecular readjustments leading to equilibrium conditions develop rather readily at low treating temperatures, whereas others develop very slowly or not at all until the glass is subjected to higher treating temperatures. Such differences in the rates of development are easily explained if it is assumed that only a portion of the flow-surfaces normally available at temperatures in the annealing range are still open at lower temperatures for viscous flow while other portions are either entirely closed or are practically so unless exceptional loads are applied.

Careful consideration will show that the heat generated by the flow, as the elastic molecular strains (which are excessive because of superheating or undercooling) are relaxed, is probably negligible compared to the heat effects observed. These considerations then lead to the conclu that the observed heat effects are the result rapidly changing specific heat as the equilib temperature changes.

## 2. Experimental Conditions in Det mining Heat Effects

For understandable reasons, the actual co tions that exist in obtaining curves that s exothermic and endothermic effects are alw very different from the idealized conditions sumed in discussing the methods of test. G erally, it is assumed that the test sample i small that any temperature gradients withi while heating or cooling at a considerable can be neglected. Actually, this condition seldom approximated and, as a result, the obse heat effects are blunted and spread over a tem ature range that is somewhat too broad.

In tests of this kind the well-known differe thermocouple method is commonly used. hot junction of this couple is in the test sam whereas the other is either in the wall that plies the heat to the heating sample and supposedly conforms to an isothermal surfac it is in a so-called neutral body that is encl in contact with the sample, by the same isot mal wall. Also, supposedly, there is no tra of heat from one of these junctions to the o that would appreciably affect the magnitud the heat effects that are sought. At best, t ideal conditions are only approximated and, result, any improvement in the test condit usually accentuates the effects as they are sh by heating curves.

## 3. Relation Between Heat Effects a Changes in Equilibrium Temperat

If $T$ is the temperature of the test sample at instant and if the simultaneous temperatur the isothermal wall is $T_w$, the rate of heat ($H$)

to the sample is $dH/dt=A(T_w-T)$. Under lized conditions, the factor $A$ in this relation e product of the area and the so-called external ductivity of the contact between sample and l. If the sample weighs 1 gram, the rate of heat absorption equals this rate of supply and $''dT/dt+\sigma d\tau/dt$ for glass. In this expression, the heat absorbed per degree increase in $\tau$, $s''$ is the normal specific heat. Both of these fficients, like the expansivities, are functions $\tau$ and $T$. Thus, $s''=s(1+bT+\beta\tau)=s'+s\beta\tau$ es as a first approximation for the change in specific heat with these temperatures. In the ond form of this approximation, $s'$ is pre-ably independent of $\tau$ and is, consequently, same for all samples of a glass whether chilled annealed. The normal specific heat of a mate- represents (in the case of heating) both the gy required to increase the thermal agitation that expended in expanding the material inst the so-called intrinsic pressure that results m the molecular attractions. Increases in $\tau$ not affect the thermal agitation but are normal- accompanied by expansions that generally re- e the intrinsic pressure somewhat, since a aration of the molecules usually reduces their tual attraction. Consequently, $\sigma$ represents y an energy of separation and $\beta$ is normally gative.

By equating the heat supplied to that absorbed d introducing the first approximation for $s''$, the ation $T_w-T=(R/A)(s'+s\beta\tau+\sigma d\tau/dT)$ is ob-ned and, for the neutral body, which pre-ably has no peculiar characteristics in the mperature range of the tests, the corresponding uation is $T_w-T_n=(R_n/A_n)s_n'$ if $R$ and $R_n$ the heating rates of the sample and neutral dy, respectively. It is helpful in practice if $=s'$, and $A_n=A$ approximately. In that case, follows that

$$T-T_n=(R/A)(s'(-1+R_n/R)-s\beta(\tau-\tau_a)-\sigma d\tau/dT)=G. \quad (11)$$

this equation, $\tau_a$, the $\tau$-value for a very well nealed sample, is introduced because $\tau$ never be reduced to zero in ordinary glasses.

In the following discussion, $G$ represents the perimental results found for $T-T_n$. Ordi-rily these experimental results are greatly fected by gradients, and consequently seldom proximate the values that $T-T_n$ should have under ideal conditions. For example, in testing a well-annealed sample, $T-T_n$ should approximate zero throughout the range between the temperature at which a steady heating condition is first established and that at which the endothermic effect begins. This is obvious because $R_n=R$, $\tau=\tau_a$, and $d\tau/dT=0$. However, $G$ may have a fairly large value that is either positive or negative, depending on the characteristics of the heating furnace and the manner of packing the sample and neutral body. When proper care is taken, these disturbing gradients do not change materially between the time a steady condition is first developed and that at which granular samples show a considerable degree of sintering. As a disturbing degree of sintering seldom takes place below temperatures that are well above those required for the completion of the endothermic effect, a second steady condition of heating is usually developed. In these ranges of steady heating, the $G$-values change very slowly and only because $A$, $s'$, and $\sigma$ change slightly as $T$ (and also $\tau$ when the second steady condition is reached) increases. Thus, when the results for $G$ are plotted against $T$, the curves show two distinct levels, one preceding and the other following the heat effects. If these levels are represented by $G_1$ and $G_2$, repeated tests on identical samples show that $G_1-G_2$ does not vary greatly if proper precautions are taken. For this reason it will be considered that $G$ properly represents $T-T_n$ plus an error that is practically constant and can be neglected at least as long as only differences in the determinations of $G$ for a single test are considered.

When several samples of a glass are tested, they will all have attained approximate equilibrium when the second level is reached and the several curves can properly be made to coincide approximately in this region, although the $G_2$-values may be quite different because of the errors just mentioned. Because the variation in $G_1-G_2$ is usually small in the case of identical samples, the initial levels of the curves will then almost coincide unless there is a wide spread in the initial $\tau$-values of the several samples. That is, when the spread is not large, the effect of the differences in the initial $\tau$-values is often masked by the errors in determining $G_1-G_2$, but this masking is insufficient to hide the effect of differences as large as those found between the $\tau$-values of severely chilled and

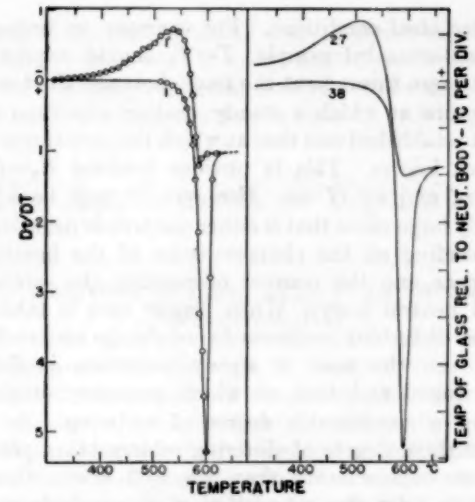


FIGURE 7.—*Exothermic and endothermic effects.*

27 and 38, Observed effects on heating chilled and annealed samples, respectively, of a borosilicate optical glass; 1 and 1′, indicate approximately the heat effects which, according to curves 1 and 1′ in figure 1 and curves 1 and 1′ in figure 4, should be found for annealed and chilled samples of the borosilicate thermometer glass if the decrease in specific heat with increasing equilibrium temperature were insignificant. The separation between curves 27 and 38 below 400° C is mainly the result of a comparatively low specific heat when $\tau$ is high.

well-annealed samples (fig. 7, curves 27 and 38). (See also ref. 1, fig. 8.)

The significance of the difference between the initial levels of these curves is at once apparent from eq 11 when it is considered that $d\tau/dT$ is approximately zero and unity in the ranges of the first and second levels, respectively. To make this significance more apparent, it will be assumed that the change in $A$ with temperature is negligible. In that case, $G_1-G_2=(R/A)(s\beta(\tau_2-\tau_1)+\sigma)$, since $R_n/R=1$ at both levels. Thus, by neglecting the relatively small $\beta$-term, the difference between the levels is approximately $R\sigma/A$, but as $\beta$ is negative, there is some increase in $G_1-G_2$, as the initial $\tau$-value, $\tau_1$, is increased and thereby causes the $\beta$-term to decrease. The $\tau$-value, $\tau_2$, is that of the temperature at which all of the various curves, when plotted to show the results of a series of tests, are brought into coincidence in the range of the second level. Unless $R$ is very low or the glass has been chilled very severely, $\tau_2$ is greater than $\tau_1$.

When $d\tau/dT$ reaches its maximum negative and positive values in the temperature range between the first and second levels, the heating curves (as plotted) attain, respectively, their maxima (exothermic effects), which are observed in chilled glasses only, and their minima (endothermic effects), which are very pronounced in all annealed glasses. During the endothermic and exothermic effects, $(R_n/R)-1$ takes on small positive and negative values, respectively. Consequently, in both cases, the effect of the $s'$-term, eq 11, is to detract somewhat from the effect of the $\sigma$-term. However, as when developing the approximate relation, $G_1-G_2=R\sigma/A$, the $s'$- and $\beta$-terms, being relatively small, may again be neglected for simplicity. Then, if the values obtained for $T$-$\tau$ at the peaks of the endothermic and exothermic effects are designated by $G_3$ and $G_4$, respectively, it follows that $G_3-G_1=-(R\sigma/A)(d\tau/dT)_{min}$ and $G_4-G_1=-(R\sigma/A)(d\tau/dT)_{max}$ roughly approximate actual conditions. As estimated from curves 27 and 38 in figure 7, it appears that the three differences, $G_1-G_2$, $G_3-G_1$, and $G_4-G_1$ are about 1.0, 1.0, and −8.0 deg C, respectively. Consequently, $(d\tau/dT)_{min}=-0.55$, and $(d\tau/dT)_{max}=4.4$. When compared to the respective values −0.73 and 5.37 found from the expansion curves of the thermometer glass, these values obtained from the differential heating curves of the borosilicate optical glass appear rather low. However, this result is to be expected since experimental conditions prevent the heating curves from showing the full magnitude of the heat effects.

If the full magnitude of the endothermic effect and the corresponding change in $\tau$ could be well determined (especially in the case of a thoroughly annealed glass), it seems that it should be possible to determine the ratio $s''/\sigma$, since the relation between the relative cooling of the glass and the change in $\tau$ should be expressed approximately by $s''(G_1-G_4)=\sigma(\tau_4-\tau_1)$, in which $\tau_4$ is the maximum of $\tau$ when the relative cooling reaches its peak. A rough estimate, which could be 30 percent or more in error, gave the result $s''/\sigma=140$. In arriving at the estimate of 140 deg as the value of $\tau_4-\tau_1$, it was considered that the initial equilibrium temperature, $\tau_1$, of the sample that yielded curve 38 was probably somewhat below 460° and that $\tau_4$ was not far below 600° C, because the difference between the actual and equilibrium temperatures is not great when the endothermic effect reaches its maximum.

As the heating rate in obtaining the heating curves under consideration was about 6 deg/min, it follows that $\sigma/A=(G_1-G_2)/R=1.8/0.1$ and from this result and the above ratio, that $s''/A$

. Thus, for any probable value of $s''$ at tematures in the annealing range, the order of $A$ pears to be in the neighborhood of $10^{-3}$. This gh approximation is not a wholly improbable ue, since $A$ (instead of possessing its idealized nificance in these tests) was concerned with the nduction of heat from some undermined surface the furnace through a wall that was of uncertain a and was composed of a thin layer of burned estos paper and an undetermined thickness of nular glass or alundum. However, this uncerinty is of minor significance, as the chief purpose introducing the very rough approximations, that re obtained as described in the immediately ceding paragraphs, is to give a clearer picture the significance of the curves that result from s rather complicated type of test which, although cellent in a qualitative sense, does not lend itself precise determinations.

## Estimated Heat Effects Based on Equilibrium Temperatures Obtained From Thermal Expansion Curves

Besides the reproduced curves 27 and 38 (which re obtained by tests in which $R=6$ deg/min), ure 7 also contains curves obtained for comrison by plotting the data, shown in figure 5 for $/dT$, according to the manner and scale used in otting the experimentally determined differential ating curves. Although the two glasses were like, the treatments that they had received re not too dissimilar. Consequently, it seemed at their observed exothermic and endothermic fects should have had about the same magnitude the heating rates had been the same. To make $-G_1$ and $G_4-G_1$ approximate 1 and $-8$ deg, spectively, for the synthetic curves (right-hand ale of fig. 7), it was necessary to multiply the lues of $d\tau/dT$ by 1.48. This factor corresponds $R\sigma/A$, since $d\tau/dT$ is zero in the range of the st and unity in that of the second level. How-er, when the difference in the heating rates is nsidered, it is seen that the factor in this case s very little definite significance, since halving e heating rate changes the magnitude of the at effects appreciably. Nevertheless, a survey the heating curves obtained on a number of dinary glasses indicates that the average agnitude of $G_1-G_2$ is near 1.5 deg.

In preparing curve 1′, the $s\beta(\tau_2-\tau_1)$-term was eglected. As a result, $G_1-G_2$ is the same for both synthetic curves, 1 and 1′ (fig. 7). That is, the decrease in $s''$ (at low temperatures) as $\tau_1$ is increased was ignored. In all other respects the two sets of curves, experimental and synthetic, are quite similar in form.

In figure 8 the synthetic differential heating curves 2 and 2′ (for chilled and annealed samples, respectively) correspond to the curves with similar designations in figure 2, and are replicas of those shown before the Glass Section at the previously mentioned Cincinnati meeting of the American Ceramic Society [2]. As then, these curves are now presented to show that the form of the exothermic effect, if the viscosity of glass depended only on the actual temperature, would not be that of the experimentally determined effect. Also, it is apparent that, contrary to experience, the exothermic and endothermic effects of a chilled sample would then occur exactly within the temperature range of the endothermic effect of a well-annealed sample. In plotting these curves, $d\tau/dT=\pm xy$ (see eq 8) was also

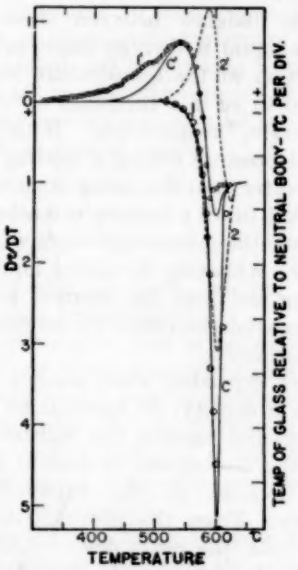


FIGURE 8.—*Comparison of computed exothermic and endothermic effects.*

1 and 1′, (Large and small circles, respectively) same as 1 and 1′ of figure 7; $C$ and $C'$, computed effects in accord with computed curves $C$ and $C'$ of figures 1 and 3. The failure of eq 7 to account for the plasticity of glass below the annealing range presumably causes the divergence between $C'$ and 1′ below 500°C. 2 and 2′, (broken lines) computed heat effects in accord with curves 2 and 2′ in figure 1. The wide divergence between these curves and 1 and 1′ presumably is caused by the failure of eq 8 to account for both the plasticity of the glass below 500° C and the decrease in the viscosity as the equilibrium temperature increases.

multiplied by the factor 1.48 to bring them into conformity with the other curves of figure 7.

Curves $C$ and $C'$ correspond to the similarly designated curves in figures 3 and 1. These curves were obtained from the values of $d\tau/dT$ that were procured by the previously described step-by-step computations, and they show a definite approach to the form and relative placement of the experimental curves. They also closely resemble the synthetic heating curve (fig. 7) that were derived more directly from the expansion data, except that much of the heat developed in the plastic range is not represented. That is, the dependence of the viscosity on $\tau$ both broadens the exothermic effect and displaces it somewhat toward temperatures below those of the endothermic effects of annealed glasses, even if plasticity is not taken into account.

## V. Speculative Discussion

In addition to the external pressure which is comparatively quite small, there are two pressures to be considered in relation to liquids, (1) the thermal pressure arising from the collisions of the thermally agitated molecules, and (2) the so-called intrinsic pressure arising from the mutual attraction of the molecules. On the average, these opposed pressures are equal when a liquid is in an equilibrium condition at any temperature. Cooling or heating a viscous liquid rapidly from a temperature at which equilibrium has been reached disturbs the balance between these pressures because the liquid is then no longer in an equilibrium condition at the temperature reached and may be said to be in a condition of "distension" or "compaction," respectively. If the change in the thermal pressure during a heating or cooling is always greater than that in the intrinsic pressure, it follows that (until a balance is reached between the pressures) the intrinsic pressure will gradually compress the relatively distended liquid after an undercooling and that the thermal pressure will gradually expand the relatively compacted liquid after a superheating.

The work expended when such a compacted liquid with a density, $D$, expands at a constant temperature and against the intrinsic pressure, $P$, equals the mechanical equivalent of the heat absorbed because of the expansion. Thus, $Pdv=JD\sigma d\tau$. From the previous discussion of expansion tests, the result $dv/d\tau=0.75\times10^{-4}$ was obtained for the glass tested. For the same glass, $D=2.5$ approximately, and according to the previous very rough estimate, $\sigma=s''/17.5$. Although $s''$ for this glass is unknown, it appears from a summary [11] of the results of a number of investigations that the specific heat for the average glass at temperatures in its annealing range is somewhat in excess of 0.2. On the basis of these rough values, $P=1.6\times10^{10}$ dynes/cm.$^2$ That is, the intrinsic pressure of glass in its annealing range appears to exceed $1.5\times10^4$ atmospheres and, as previously pointed out [3], this is the same order of magnitude as that of values that have been mentioned as possible for the intrinsic pressure of water [8]. If it becomes possible to obtain really dependable values for the intrinsic pressure of glasses and other viscous liquids by this or other means, the values will be of considerable interest, since this theoretical pressure is closely related to surface tension and to certain other properties. It is also to be hoped that speculations of this sort may help in those theories that are based on X-ray studies of glass. This hope rests on the assumption that the very excessive compactions and distentions found in extremely viscous liquids when superheated and undercooled are in some comparatively simple manner concerned with the character and size of the larger molecules in these liquids.

Such molecules not only add to the viscosity and thus hamper the readjustments of smaller molecules to temperature changes but, when present in relatively large numbers, probably form comparatively extended frameworks [9] (supermolecules) that also become too compacted (or distended) whenever the temperature is rapidly raised (or lowered) and that are delayed in correcting this incompatibility by the viscosity and plasticity to which they presumably contribute so greatly. As previously pointed out [3], chain- or ring-like molecules [10] and some other forms of extended molecular structures that often have been discussed as possibilities (for references see [10, 11]) might easily be subject to such incompatibilities whenever there is a temperature change.

Within the annealing range, these extended lattice-like structures formed from simpler molecules are presumably unstable in the sense that

ey (individually but not on the average if uilibrium exists) are being continually altered form and size by the thermal agitation of the mponents. However, the rate of alteration is esumably so low that the structures not only ange comparatively little during a rapid heat- or cooling over even considerable temperature tervals but also persist in a compacted or dis- ded state for appreciable periods after the d of the heating or cooling, respectively.

As the thermal agitation decreases in a cooling quid, the persistence of such structures pre- mably increases rapidly and the rate of increase oubtless parallels that at which the viscosity creases. Furthermore, the structures gradually come permanent and probably attain a con- derable elasticity of form if the cooling is tended to temperatures considerably below e practical annealing range. At this stage e liquid is overly distended and the intrinsic essure exceeds considerably the thermal pres- re. Consequently, much of the contraction on oling consists of something akin to an elastic mpression in which the structural members ffer various excessive elastic distortions or molec- ar strains.

As the thermal pressure decreases toward zero n continued cooling, the elastic resistance of the tructures becomes a greater and greater factor in balancing the intrinsic pressure. However, it seems that their elastic coefficients should also be increasing quite rapidly at very low temperatures. In that case, the increase in compression per degree decrease in temperature decreases, and the increase in the elastic coefficients may even be sufficient at low temperatures to cause the strains, that have been building up, to diminish. Furthermore, the expansivity of the vitreous solid may become negative if the expansion caused by this diminution in strain more than offsets the contraction which accompanies the decreasing thermal pressure. That is, many, if not all, vitreous materials may yield expansivity curves that, in this respect, resemble the expansivity curve of vitreous silica at very low temperatures [12].

The compacted condition as caused by rapid heating can be produced to an appreciable degree only in the annealing range. In this condition the excessive thermal pressure may also be regarded as the cause of elastic molecular strains. That is, the excess of the thermal over the intrinsic pressure is balanced by the elastic resistance of molecular structures to distortion. Even after equilibrium is established, molecular strains are doubtless present and continually varying about an average as one after the other of the pressures becomes temporarily the greater in limited elements of the whole volume of liquid.

## VI. Conclusion

Practically speaking, glass at temperatures ithin and above its annealing range is a purely iscous liquid that is easily undercooled or super- eated because its viscosity is so very high. owever, at temperatures far below its annealing nge, glass behaves as an elastic solid although here is an intermediate range in which it possesses he characteristics of a plastico-viscous material.

Although the condition of an undercooled glass s not one of equilibrium at the actual temperature f that glass, it usually corresponds to one of quilibrium at some temperature within the nnealing range and, if the actual temperature is aised quickly enough to that point, the glass ill be practically in equilibrium there. A cor- esponding relation exists between the condition f a superheated glass and some equilibrium emperature within the annealing range. The egree of undercooling (or superheating) is measured by the difference between the actual and equilibrium temperatures.

The properties of a glass are affected not only by changes in the actual temperature but also by changes in the equilibrium temperature. Thus, a glass expands when the equilibrium temperature increases as well as when the actual temperature rises, and lowering either temperature increases the viscosity very rapidly.

Ordinarily, the equilibrium temperature changes at a perceptible rate only when the actual temperature exceeds the lower limit of the annealing range; but, if the degree of undercooling is very high as in quenched glasses, it decreases at appreciable rates even when the actual temperature is in the immediately lower range within which glasses take on a plastic character.

The rate at which the equilibrium temperature changes is proportional to the degree of under-

cooling (or superheating) and also to the inelastic deformability. Moreover, for the same departure from equilibrium, the rate increases very rapidly as the inelastic deformability is increased by raising the actual temperature. As this deformability also increases as the equilibrium temperature increases, the manner of approaching equilibrium from an undercooled condition differs somewhat from the manner of approach from a superheated condition at the same actual temperature.

In approaching equilibrium from an undercooled condition, a glass contracts and evolves heat, whereas it expands and absorbs heat in approaching equilibrium from a superheated condition. The rates at which these heat effects develop depend on the rate of approaching equilibrium and are therefore also controlled by the inelastic deformability.

In view of the foregoing conclusions, an equation has been proposed that relates these various rates to the inelastic deformability. It is found that this equation is applicable to experimental data on the extraordinary expansion and contraction effects and on the exothermic and endothermic effects of glass in its annealing range. As the equation is based on the concept that glass is a purely viscous liquid, it is not applicable to data on changes taking place while a glass is within its plastico-viscous stage in which the inelastic deformability increases with the load.

By using this equation in connection with the usual expansion curves that are obtained by heating a glass to temperatures just above its annealing range, reasonable results are found for constants that are related to the coefficient of viscosity and its changes with the actual and equilibrium temperatures. These constants would make it possible to determine this coefficient if the modulus of elasticity were known for the glass at these high temperatures.

The behavior of glass at temperatures within and immediately below its annealing range indicates that the various heat affects appear because the balance between the average intrinsic pressure (which arises from the molecular attractions) and the average thermal pressure (which arises from the thermal agitation) is disturbed during superheating and undercooling. This disturbance of the normal balance of the pressures in a liquid causes elastic molecular strains that are abnormal. When such abnormal elastic strains exist in a glass within its annealing range, they relax gradually at rates that are governed by the inelastic deformability which also governs the rates of relaxation of ordinary strains in annealing glass.

# VII. References


[1] A. Q. Tool and C. G. Eichlin, J. Am. Ceramic Soc. **14**, 276 (1931); BS J. Research **6**, 523 (1931) RP292.

[2] A. Q. Tool, Bul. Am. Ceramic Soc. **21**, 13 (Apr. 15, 1942).

[3] A. Q. Tool, Bul. Am. Ceramic Soc. **22**, 92 (Apr. 15, 1943).

[4] A. Q. Tool, J. Research NBS **34**, 199 (1945) RP1637.

[5] A. Q. Tool and J. Valasek, Sci. Pap. BS **15**, 537 (1920) S358.

[6] F. Twyman, J. Soc. Glass Techn. **1**, 61 (1917).

[7] J. B. Saunders, J. Research NBS **23**, 179 (1939) RP1227.

[8] H. S. Taylor, Treatise on physical chemistry 1, 141–43 (D. Van Nostrand Co., New York, N. Y., 1925).

[9] A. Q. Tool and C. G. Eichlin, J. Am. Ceramic Soc. **8**, 13 (1925).

[10] E. Preston, J. Soc. Glass Techn. **26**, 82 (1942).

[11] G. W. Morey, Properties of glass, p. 212–18 and 531–39 (Reinhold Publishing Corporation, New York, N. Y., 1938).

[12] R. B. Sosman, Properties of silica, p. 352–67 (Chemical Catalog Co., New York, N. Y., 1927).


WASHINGTON, March 1, 1946.

. S. Department of Commerce
ational Bureau of Standards

Research Paper RP1731
Volume 37, August 1946

Part of Journal of Research of the National Bureau of Standards

# An Arrangement with Small Solid Angle for Measurement of Beta Rays

*By Leon F. Curtiss and Burrell W. Brown*

An arrangement using a Geiger-Müller counter with small aperture with a radioactive source at some distance from it is described for counting beta particles. Sources emitting only beta rays with maximum energies above 1 million electron volts of the order of 1 millicurie can be measured in terms of the disintegration rate from the observed counting rate and the solid angle as calculated from the dimensions of the apparatus. An independent check of the arrangement shows that this can be done reliably. A suggestion for discarding the use of the curie and substituting a unit consisting of $10^6$ disintegrations per second to be called the "rutherford" is made. The curie is properly applicable only to members of the radium family.

## I. Introduction

The development of improved methods for the production of radioisotopes, resulting in an increase in the use of such radioactive materials, has led to a demand for better methods of measurement. In the simple case where a radioelement emits only beta particles of fairly high energy, as in the case of $P^{32}$, it should be comparatively easy to measure the strength of radioactive sources in terms of disintegrations per second, even for fairly strong sources. This has not yet been accomplished, however. Disagreements of the order of 300 percent have come to the attention of the authors. The need for reliable methods of measuring the strength of sources of $P^{32}$ is accentuated by its newly developed use in the treatment of leukemia. It is of considerable importance that the amounts of $P^{32}$ as measured by various laboratories should be in reasonable agreement. Otherwise, clinical results obtained in various parts of the country from the use of this element cannot be compared.

The writers have undertaken to develop an arrangement, comprising a Geiger-Müller counter and source holder, with a sufficiently low solid angle that sources of the order of 1 millicurie can be counted in it directly. The number of disintegrations per second will then be obtained from the observed counting rate and the solid angle determined from the dimensions of the arrangement.

### Contents

| | Page |
|---|---|
| I. Introduction | 91 |
| II. Geometrical arrangement | 92 |
| III. Independent check on solid angle | 93 |
| IV. Use of the curie | 94 |

## II. Geometrical Arrangement

Figure 1 is a diagram of the counter, chamber, and source holder built to test the effectiveness of this method of measuring beta-ray sources. A brass tube approximately 60 cm long and 4-cm internal diameter constitutes the chamber. In this a number of baffles, *B*, are mounted with a movable shutter, *Sh*, of 3-mm brass at the end where the source, *S*, is mounted. This shutter permits a measurement of background with a source in place. The opposite end of the chamber is closed by a steel plate, *P*, 6 mm thick with an aperture, *A*, 4 mm in diameter in the center. A counter, *C*, is mounted concentric with *A*, which is covered by a mica window of approximately 2 mg/cm$^2$. The chamber can be evacuated during observations. The construction of the source holder is shown in figure 2. It is made of Plexiglas and designed to reduce back-scattering from various parts.

The most important spurious effect to be anticipated in this arrangement is small-angle scattering from the walls of the tube. The very small solid angle used makes this a serious difficulty. Consequently, a series of studies was made of the effect of baffles of various materials, at different locations in the tube, on the counting rate. These studies revealed that Plexiglas and soft-wax baffles were equally effective in producing a definite minimum counting rate when the source was in full view of the aperture.

Typical results are shown in table 1 for equally spaced baffles, consisting of disks ¼ in. thick closely fitting the internal diameter of the tube with a central hole ½ in. in diameter. The diameter of the source was 1 cm.

The optimum diameter of the circular opening in the baffles was found to be slightly greater than the diameter of the source. Small changes at this approximate diameter had no effect on the counting rate.

TABLE 1.—*Relative scattering for different arrangements of baffles*

| Material | Number of baffles | Relative counting rate |
|---|---|---|
| | 0 | 1.27 |
| Brass | 3 | 0.58 |
| Plexiglas | 3 | .50 |
| Do | 4 | .50 |
| Do | 12 | .56 |
| Wax | 3 | .50 |

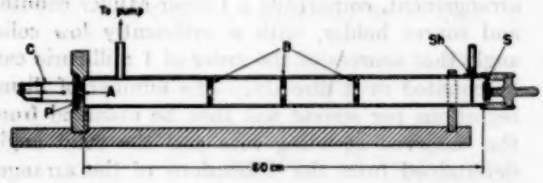


FIGURE 1.—*Arrangement of counter, vacuum chamber, and source holder.*

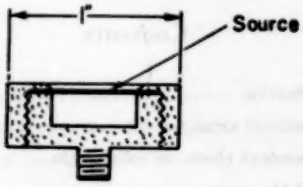


FIGURE 2.—*Beta-ray-source holder*

The effect of internal scattering along the tube was further tested by changing the source-to-aperture distance from 60 to 40 cm by mounting the source on a rod extending 20 cm into the tube. The counting rate observed under these conditions agreed within less than 1-percent with that calculated from the ratio of the calculated solid angles and the counting rate observed at 60 cm.

From the actual dimensions of the aperture, diameter $=4.06 \pm 0.01$ mm, and source-to-aperture distance equals $60.0 \pm 0.2$ cm, the solid angle divided by $4\pi$ is computed as $2.86 \times 10^{-7}$. Multiplying the observed counting rate by the reciprocal of this number, $3.49 \times 10^5$, gives the number of disintegrations per second. If it is desired to express this value in millicuries, the observed count is multiplied by $9.44 \times 10^{-7}$, assuming the curie as $3.7 \times 10^{10}$ disintegrations per second. This practice of expressing source activities in terms of curies is to be condemned, as will be explained later.

There are at least three disturbing effects common to all Geiger-counter measurements of beta rays, which must be considered in connection with the present arrangement. These are back-scattering from the source and support, absorption in the mica window and in some cases self-absorption in the source. In the present case the back-scattering from the support for the source was reduced to a minimum by the selection

Plexiglas with a considerable cavity behind the source to reduce this effect. The sources were deposited on aluminum 0.00035 in. thick. However, the material of the source itself would cause considerable back-scattering, as the phosphorus used did not have a high specific activity, and there also would be some self-absorption. These effects tend to counteract each other.

## III. Independent Check on Solid Angle

A number of $P^{32}$ sources were measured in the arrangement as described. The values obtained were in general agreement with those expected, but it became obvious that some independent check was required to establish the reliability of the measurements. For this purpose a thin mica-window counter of the bell type was constructed and arranged so that a source could be mounted very close to the window in an accurately reproducible location. This was achieved by mounting the counter with the mica window up and laying the sources, properly centered, directly on the counter. The curvature of the mica window provided a small but definite separation between it and the source. This arrangement is represented in figure 3, where $S$ is the source and $M$ the mica window.

To determine the solid angle for this position of the source a sample of RaD was prepared from lead extracted from pitchblende to be used as a standard. The radium content of this ore was carefully measured, and the total amount of lead was determined quantitatively. From the above data and the known weight of lead in the standard, the number of beta rays per second from the RaE in equilibrium with the RaD could be calculated.

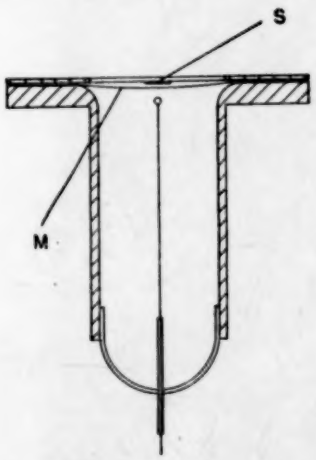


FIGURE 3.—*Mica-window counter.*

The ratio of the observed number of counts to this calculated value gives the effective aperture of the counter. With this information available, an aliquot was taken from one of the $P^{32}$ solutions, of such amount to give a convenient counting rate in the inverted mica-window counter. The counting rate multiplied by the above ratio gives the number of disintegrations per second in the aliquot of $P^{32}$. Multiplying again by the aliquot ratio, the number of disintegrations is obtained in the original $P^{32}$ sample, which had previously been measured in the chamber with small solid angle. In making these measurements in comparison with the RaD+E standard, care was taken to deposit the $P^{32}$ on the same backing material as was used for the standard and over the same area. This reduces the back-scattering correction to a small value, dependent only on the difference in energies of the RaE and $P^{32}$ beta rays. The mica window had a thickness $\sim$ 6 mg/cm$^2$, so that the absorption corrections would also be nearly the same.

When comparing the measurements in the arrangement with large solid angle with those obtained in the apparatus with small solid angle, it is to be noted that whereas the effect of back-scattering in the former has been reduced, this is not true for the small-angle arrangement as there were several milligrams of phosphorus in the sources of approximately 0.5-millicurie strength. Therefore, we would expect the value obtained in this case to be somewhat higher than that obtained from comparison with the RaD+E standard. On the other hand, for the large solid angle arrangement there is almost no self-absorption of beta rays in the material of the source due to the smallness of the sample, whereas in the small solid-angle apparatus a source of approximately 0.5 mc weighs about 30 mg and extends over a little less than a square centimeter. The self-absorption will be considerable under these conditions. A measurement gave 0.489 mc for 30 mg in the high, large solid-angle arrangement and 0.488 mc for the low solid-angle arrangement. Under the conditions of these measurements the

results can only be explained if the back-scattering effect was approximately offset by self-absorption within the source. The agreement might be regarded as fortuitous. Therefore, the comparison was repeated from the beginning, using freshly prepared sources from the same original solution of $P^{32}$ in both pieces of apparatus. The measurements gave 0.504 mc in the large solid-angle counter and 0.502 mc in the low solid-angle arrangement. This makes it quite certain th the low solid-angle chamber gives a relia measurement of beta rays from $P^{32}$ or any sour emitting only beta rays of approximately th same energy. Furthermore, this counting arrang ment is independent of any standard and giv the disintegration rate simply by multiplying th observed counting rate by the solid angle com puted from the dimensions of the apparatus.

## IV. Use of the Curie

It has become the practice to express the strength of all radioactive sources in terms of curies. Actually, the curie can be applied logically only to members of the radium family. This arises from the fact that the curie was originally defined as "That quantity of radon in equilibrium with 1 of radium." Therefore, only members of the radium family in equilibrium with 1 g of radium can have this disintegration rate. A further disadvantage in the use of this unit is that it is uncertain to at least 4 percent and values are in current use which fall well outside these limits.

The solution of this difficulty is remarkably simple. The intensity of radioactive sources is measured actually in terms of disintegrations per second. Therefore, all that is required is to designate some convenient rate and give it a name. We suggest that a convenient rate is $10^6$ disintegrations per second, and that the unit be called a "rutherford," abbreviated as "rd." The microrutherford then is the amount undergoing disintegration per second and a kilo rutherfor $10^9$ disintegrations per second. In the future i is anticipated that even those nucleii havin fairly complex disintegration schemes will b measurable in terms of disintegrations per second and many can already be treated in this way Thus all confusion that has arisen from the fals application of the curie can be eliminated.

This subject has been discussed by the Nationa Research Council Committee on Radioactivity which, in turn, has suggested that the Nationa Bureau of Standards recommend the use of th "rutherford" as a general unit for the measure ment of radioactive sources. This recommenda tion was published in Science **103,** 712 (1946), and will appear shortly in other journals.

WASHINGTON, May 23, 1946.

S. Department of Commerce
National Bureau of Standards

Research Paper RP1732
Volume 37, August 1946

Part of Journal of Research of the National Bureau of Standards

# Heats, Equilibrium Constants, and Free Energies of Formation of the Alkylbenzenes[1]

By *William J. Taylor*,[2] *Donald D. Wagman, Mary G. Williams*,[2] *Kenneth S. Pitzer*,[3] *and Frederick D. Rossini*

For benzene, toluene, ethylbenzene, the three xylenes, normal and isopropylbenzene, the three methylethylbenzenes, the three trimethylbenzenes, and the higher normal alkylbenzenes, values are presented for the following thermodynamic properties for the gaseous state to 1,500° K: The heat-content function, $(H°-H°_0)/T$; the free-energy function, $(F°-H°_0)/T$; the entropy, $S°$; the heat content, $H°-H°_0$ the heat capacity, $C°_p$; the heat of formation from the elements, $\Delta Hf°$; the free energy of formation from the elements, $\Delta Ff°$; and the logarithm of the equilibrium constant of formation from the elements, $\log_{10} Kf$.

Equilibrium constants and concentrations are given in tabular and graphical form for the isomerization of the four $C_8H_{10}$ alkylbenzenes and for the eight $C_9H_{12}$ alkylbenzenes as a function of the temperature to 1,500° K. Equilibrium constants are also given in tabular and graphical form for some reactions involving alkylation (addition of olefin to benzene to form alkylbenzene), cyclization (conversion of paraffin to alkylbenzene plus hydrogen), and trimerization (of acetylene to form benzene and of methylacetylene to form 1,3,5-trimethylbenzene).

## Contents

| | Page |
|---|---|
| I. Introduction | 96 |
| II. Units and constants | 96 |
| III. Heat-content function, free-energy function, entropy, heat content, and heat capacity | 96 |
| 1. Translational and free rotational contributions | 96 |
| 2. Vibrational contributions | 98 |
| (a) Benzene, toluene, the xylenes, and mesitylene | 98 |
| (b) Ethylbenzene | 98 |
| (c) 1,2,3- and 1,2,4-trimethylbenzenes | 98 |
| 3. Restricted rotational contributions | 99 |
| (a) Symmetry of potential barriers | 99 |
| (b) Reduced moments of inertia | 100 |
| (c) Calculation of potential barriers from experimental entropies | 100 |
| (d) Calculation of potential barriers from experimental heat capacities | 100 |
| (e) Selected values of potential carriers | 101 |
| 4. Calculations by the methods of increments | 102 |
| 5. Tables of values of the thermodynamic properties | 102 |
| IV. Heat of formation, free energy of formation, and equilibrium constant of formation | 108 |
| 1. Method and data use in calculations | 108 |
| 2. Results | 108 |
| V. Free energies and equilibria of isomerization | 115 |
| VI. Equilibrium constants for some reactions involving alkylation, cyclization, and trimerization | 118 |
| VII. References | 122 |

[1] This investigation was performed jointly by the American Petroleum Institute Research Project 44 on the "Collection, Analysis, and Calculation of Data on the Properties of Hydrocarbons" and the Thermochemical Laboratory at the National Bureau of Standards.

[2] Research Associate on the American Petroleum Institute Research Project 44 at the National Bureau of Standards.

[3] Associate Supervisor of the American Petroleum Institute Research Project 44; Professor of Chemistry, University of California, Berkeley, Calif.



702005—46——4

# I. Introduction

As part of the work of the American Petroleum Institute Research Project 44 and the Thermochemical Laboratory at the National Bureau of Standards, values have been calculated for the heat-content function, free-energy function, entropy, heat content, and heat capacity for the 14 alkylbenzene hydrocarbons through $C_9H_{12}$, and for the higher normal monoalkylbenzenes, in the gaseous state to 1,500° K. These data have been combined with values of heats of formation at 25° C to calculate values of the heats, free ene ties, and equilibrium constants of formation these compounds in the gaseous state to 1,500° K. Equilibrium constants have been calculated fo some reactions involving alkylation (addition o olefin to benzene to form alkylbenzene), cyclizat tion (conversion of paraffin to alkylbenzene plu hydrogen), and trimerization (of acetylene to form benzene and of methylacetylene to form 1,3,5-trimethylbenzene).

# II. Units and Constants

The unit of energy, atomic weights, and values of the fundamental constants used in this report are the same as those previously described [1][4]

[4] Figures in brackets indicate the literature references at the end of this paper.

# III. Heat-Content Function, Free-Energy Function, Entropy, Heat Content, and Heat Capacity

The thermodynamic functions for benzene, toluene, *o*-, *m*-, and *p*-xylenes, and mesitylene were published by Pitzer and Scott [9]. The present calculations include minor revisions in these values to take account of more recent data, but they primarily concern the remaining alkylbenzenes through $C_9H_{12}$ and the higher normal monoalkylbenzenes. The detailed methods, in which contributions from translation, over-all and internal rotation, and vibration are considered, were used for benzene and all its methyl derivatives and for ethylbenzene. The calculations for ethylbenzene and all methylbenzenes with ortho methyl groups contain certain additional approximations. The functions for *n*-propylbenzene and the higher normal alkylbenzenes, isoproplybenzene, and the three methylethylbenzenes, were estimated by a method of increments from the functions for the normal paraffin hydrocarbons and the lower alkylbenzenes.

## 1. Translational and Free Rotational Contributions

For this series of molecules the potential barriers to internal rotation are relatively low, and the moments of inertia are always fairly large; consequently, it is convenient to calculate the classical free internal rotational contribution and then to correct it in all cases for the potential barrier present. The alternate procedure of calculating directly the thermodynamic contributions for restricted internal rotations would be equally correct.

All the molecules considered in this section fall in the class studied by Pitzer and Gwinn [5], (symmetrical tops attached to a rigid frame) except ethylbenzene. However, it may be considered as a methylene group with a symmetrical methyl group and a balanced, but unsymmetrical phenyl group attached. By the term "balanced" it is meant that the center of gravity of the phenyl group is on the axis of rotation but that the two moments of inertia of the phenyl group perpendicular to the axis of rotation are not equal. An analysis of this type of problem, which shows that in such cases the various moments of inertia should be calculated for the equilibrium configuration of the molecule, is to be published elsewhere [4]. Although more general formulas are given there, they reduce to those already published [5] for this case.

The formulas of Pitzer and Gwinn [5], with the new physical constants mentioned above, combined with the equations for translation and over-

rotation [1], yield the following equations for total contribution of translation, over-all ation, and free internal rotation:

$$(H°-H_0^\circ)/T=C°_p=7.9787+0.9936m \quad (1)$$

$$-(F°-H_0^\circ)/T=C_1 \log_{10} T+C_2 \quad (2)$$

$$C_1=18.3026+2.2878m \quad (3)$$

$$C_2=6.8635 \log_{10} M+ 2878 \log_{10} A+2.2878 \log_{10} B-4.5757 \log_{10} \sigma -2.5342m-10.2960. \quad (4)$$

these equations, $m$ is the number of internal tations in the molecule; $M$ is the molecular eight; $A$ is the product of principal moments inertia for over-all rotation, each in units of $^{-39}$ g cm$^2$; $B$ is the product of reduced moments inertia for internal rotation, each in units of $^{-40}$ g cm$^2$; and $\sigma$ is the total symmetry number, e product of the over-all rotation symmetry mber and all internal rotation symmetry mbers. The reduced moments of inertia for ternal rotation were calculated from equations b and 1c of Pitzer and Gwinn, which give a cond approximation to the reduced moments r molecules with several tops. However, for e molecules considered here, except perhaps hylbenzene, there is no significant difference tween the second approximation and the first proximation given by equation 1a of these thors.

The values for the bond lengths used in the calculations were chosen after a consideration of the published X-ray and electron-diffraction data. The benzene ring was assumed to be a plane hexagon, with carbon-carbon bond lengths of 1.39 angstroms. The other bond lengths, in angstroms, were 1.54 for the carbon-carbon bonds in the alkyl groups, including the bond joining the group to the ring [7], 1.09 for the carbon-hydrogen bonds in the alkyl groups, and 1.08 for the carbon-hydrogen bonds on the ring. Tetrahedral angles were assumed in the alkyl groups. These dimensions yield for the moment of inertia of the methyl group about its axis of rotation $5.30\times10^{-40}$. However, the moment of inertia of ethane about its threefold axis [8] should be double that of a methyl group giving for the latter $5.52\times10^{-40}$. Although no definite decision can be reached at this time, the larger value was used in all calculations for the methyl derivatives of benzene. The calculations for ethylbenzene had already been made with the smaller value and have not been changed.[5]

The values of the constants in eq 1 to 4 are summarized in table 1.

[5] The use of the higher value of the methyl moment of inertia for ethylbenzene would increase the entropy for free rotation by 0.04 cal/deg mole at all temperatures. As a result the potential barrier for the rotation of the phenyl (or ethyl) group evaluated later in this report from the experimental entropy would be increased from 1,080 to 1,130 cal/mole, which is well within the limit of other errors.

TABLE 1.—*Constants for the calculation of the translational and free rotational contributions to the thermodynamic functions*

| Quantity | Symbol | Benzene | Toluene | Ethylbenzene [b] | o-Xylene | m-Xylene | p-Xylene | 1, 2, 2-Trimethylbenzene | 1, 2, 4-Trimethylbenzene | 1, 3, 5-Trimethylbenzene |
|---|---|---|---|---|---|---|---|---|---|---|
| Number of rotors | $m$ | 0 | 1 | 2 | 2 | 2 | 2 | 3 | 3 | 3 |
| Symmetry number | $\sigma$ | 12 | 6 | 6 | 18 | 18 | 36 | 54 | 27 | 162 |
| Molecular weight | $M$ | 78.108 | 92.134 | 106.160 | 106.160 | 106.160 | 106.160 | 120.186 | 120.186 | 120.186 |
| Principal moments of inertia x10$^{39}$ [a] | $I_x$ | 14.62 | 15.15 | 18.50 | 26.32 | 23.47 | 15.68 | 38.08 | 28.41 | 48.13 |
| | $I_y$ | 14.62 | 33.15 | 56.71 | 39.07 | 47.61 | 58.24 | 48.13 | 65.34 | 48.13 |
| | $I_z$ | 29.24 | 47.77 | 68.51 | 64.32 | 70.02 | 72.86 | 84.62 | 92.16 | 94.67 |
| Product of principal moments of inertia x10$^{117}$ | $A$ | 6,252 | 24,000 | 71,920 | 66,140 | 78,240 | 66,550 | 155,100 | 171,000 | 219,300 |
| Product of reduced moments of inertia [a, c] | $B$ | ---------- | 5.319 | 180.1 [d] / 173.2 | 29.31 | 29.23 | 28.33 | 161.7 | 159.6 | 162.5 |
| Constant of eq. 2 [c] | $C_2$ | −0.422 | −2.666 | −4.763 / [d] −4.802 | −8.834 | −8.670 | −10.239 | −15.214 | −13.752 | −17.048 |

[a] All moments of inertia for internal rotation are expressed in units of 10$^{-40}$ g cm$^2$.

[b] For the configuration in which the carbon atoms of the ethyl group lie in a plane perpendicular to the plane of the benzene ring.

[c] For the moment of inertia 5.52 for the methyl group; unless otherwise indicated.

[d] For the moment of inertia 5.30 for the methyl group; this value was used in the calculation of the thermodynamic functions for ethylbenzene.

[e] The principal $z$-axis is perpendicular to the plane of the benzene ring, except for ethylbenzene, for which it makes an angle of 11° with the perpendicular. The orientation of the principal $x$- and $y$-axes may be determined by inspection, except for 1,2,4-trimethylbenzene, for which the projection of the $x$-axis on the plane of the benzene ring makes an angle of 13° with a line passing through the 1 and 4 positions on the ring.

## 2. Vibrational Contributions

### (a) Benzene, Toluene, the Xylenes, and Mesitylene

The vibrational assignments of Pitzer and Scott [9] for benzene,[6] toluene, the three xylenes, and mesitylene, were accepted without change. Such new data as have become available would not appear to make a complete reconsideration of the spectra of these compounds at this time worthwhile. However, the harmonic oscillator contributions to the thermodynamic functions were recomputed at 250° K and at 100-degree intervals from 300° to 1,500° K, using the tables of Sherman and Ewell [3] and the new values of the physical constants [1].

### (b) Ethylbenzene

The vibrational frequencies of ethylbenzene were assigned on a semiempirical basis that involved a detailed consideration of only the lowest frequencies of vibration of the benzene ring and also of the frequencies associated with vibration of the ethyl group. The remaining frequencies were taken from the assignment for toluene [9]. A complete frequency assignment for ethylbenzene at this time is impracticable. The details of this assignment, together with the method of calculation, will be presented elsewhere [6]. The resulting frequencies as used in the thermodynamic calculations are listed in table 2.

### (c) 1,2,3- and 1,2,4-trimethylbenzenes

The total vibrational contributions to the thermodynamic functions of 1,2,3- and 1,2,4-trimethylbenzene were estimated empirically from the values calculated for 1,3,5-trimethylbenzene (mesitylene) and the three xylenes. The differences in the vibrational contributions for the three xylenes are small, as may be seen from the values given in table 3 for the heat-content function, free-energy function, and heat capacity, at several temperatures. In view of the small differerences in the functions obtained with the methyl groups ortho-, meta-, or para- to one another, it seems reasonable to conclude that these positional effects are approximately additive. This view does not take account of the effect of molecular symmetry on the vibrations. However, symmetry affects the over-all distribution of frequ

TABLE 2.—*Vibration frequencies of the ethylbenzene molecule*

| Type of vibration [a] | Symmetry [b] | Frequency |
|---|---|---|
| | | $cm^{-1}$ |
| Vibrations principally characteristic of the benzene ring or phenyl radical: | | |
| 11 ($C_6H_5$ rocking) | A′ | 3 |
| 18b ($C_6H_5$ rocking) | A″ | 3 |
| 16a | A″ | 4 |
| 16b | A′ | 4 |
| 6a | A′ | 4 |
| 6b | A″ | 5 |
| 4 | A′ | 6 |
| 10b | A′ | 7 |
| 12 | A′ | 7 |
| 10a | A″ | 8 |
| 17b | A′ | 9 |
| 5 | A′ | 9 |
| 17a | A″ | 9 |
| 1 | A′ | 1,0 |
| 18a | A′ | 1,0 |
| 15 | A″ | 1,0 |
| 9b | A″ | 1,1 |
| 9a | A′ | 1,1 |
| 7a ($C_6H_5-C_2H_5$ stretching) | A′ | 1,2 |
| 3 | A″ | 1,2 |
| 19b | A″ | 1,3 |
| 19a | A′ | 1,4 |
| 8b | A″ | 1,5 |
| 8a | A′ | 1,6 |
| 14 | A″ | 1,6 |
| 13 | A′ | 3,0 |
| 7b | A″ | 3,0 |
| 2 C−H stretching | A′ | 3,0 |
| 20a | A′ | 3,0 |
| 20b | A″ | 3,0 |
| Vibrations principally characteristic of the ethyl group: | | |
| $C_6H_5-CH_2-CH_3$ angle bending | A′ | 2 |
| $CH_2$ rocking | A″ | 7 |
| $CH_2-CH_3$ stretching | A′ | 9 |
| $CH_3$ rocking | A′ | 1,0 |
| $CH_2$ rocking | A″ | 1,1 |
| $CH_2$ twisting | A″ | 1,2 |
| $CH_2$ rocking | A′ | 1,3 |
| $CH_2$ symmetrical bending | A′ | 1,3 |
| $CH_2$ symmetrical bending | A′ | 1,4 |
| $CH_3$ unsymmetrical bending | A′ | 1,4 |
| | A″ | 1,4 |
| $CH_2$ symmetrical stretching | A′ | 2,9 |
| $CH_2$ unsymmetrical stretching | A″ | 2,9 |
| $CH_3$ symmetrical stretching | A′ | 2,9 |
| $CH_3$ unsymmetrical stretching | A′ | 2,9 |
| | A″ | 2,9 |
| Internal rotations: | | |
| $C_6H_5-C_2H_5$ rotation | A″ | |
| $CH_3$ rotation | A″ | |

[a] The numbers refer to the normal modes of vibration for the benzene molecule, as given in figure 6 of reference [9].

[b] The ethylbenzene molecule, in the equilibrium configuration assumed, has the symmetry $C_{1h}$, with the symmetry plane perpendicular to the plane of the benzene ring. Vibrations of the type A′ and A″ are symmetric and antisymmetric, respectively, to reflection in the symmetry plane.

[6] The recent vibrational assignment of Herzfeld, Ingold, and Poole [27] yields thermodynamic properties for benzene which do not differ significantly from those presented here. The largest differences are about 0.1 cal/deg mole in the entropy and heat capacity.

es, and therefore the vibrational function, to a uch smaller extent than it does the individual equencies. It is easily verified that, on the asis of the assumption that positional effects are dditive, the proper formulas are

$$(1,2,3\text{-trimethylbenzene}) = (1,3,5\text{-trimethylbenzene}) + 2[(o\text{-xylene}) - (m\text{-xylene})] \quad (5)$$

$$(1,2,4\text{-trimethylbenzene}) = (1,3,5\text{-trimethylbenzene}) + [(o\text{-xylene}) + (p\text{-xylene}) - 2(m\text{-xylene})] \quad (6)$$

The vibrational functions for 1,2,3- and 1,2,4-rimethylbenzene were calculated by means of hese formulas at each temperature. The result-ng functions are compared with those for 1,3,5-rimethylbenzene at several temperatures in able 4.

## 3. Restricted Rotational Contributions

The calculation of the translational, total free (over-all and internal) rotational, and vibrational contributions to the thermodynamic functions have been described in the preceding sections for benzene, toluene, ethylbenzene, the three xylenes, and the three trimethylbenzenes. This completes the calculation for benzene and leaves only the restricted internal rotational contributions for the other molecules. The potential barriers restricting internal rotation of the methyl groups in toluene and the three xylenes have been determined by comparison with the experimental entropies and heat capacities. The potential barrier for the methyl rotation in ethylbenzene was assigned a reasonable value empirically, and the barrier for the ethyl rotation was then obtained from the experimental entropy. The barriers for the methyl rotations in the trimethylbenzenes were assigned on the basis of the barriers in the xylenes. The details of these calculations will be presented in this section.

### (a) Symmetry of Potential Barriers

The usual assumption has been made that the potential barrier for each internal rotation may be approximated by an $n$-fold cosine function and that interaction terms in the potential energy between different internal rotations may be neglected. The barrier for the methyl rotation in toluene is sixfold ($n=6$), and the barriers for the methyl groups in $p$- and $m$-xylenes must have essentially the same magnitude and symmetry as the barrier in toluene. The situation in $o$-xylene has been discussed by Pitzer and Scott [9], and their recommendation that the methyl groups be treated as independent rotors, with $n=3$, has been fol-

TABLE 3.—*Vibrational contributions for the xylenes*

| $T$ | Vibrational contribution in cal/deg mole | | | | | | | | |
|---|---|---|---|---|---|---|---|---|---|
| | $(H°-H0)/T$ | | | $(F°-H0)/T$ | | | $C_p°$ | | |
| | o-Xylene | m-Xylene | p-Xylene | o-Xylene | m-Xylene | p-Xylene | o-Xylene | m-Xylene | p-Xylene |
| °K | | | | | | | | | |
| 300 | 7.92 | 7.88 | 7.98 | −4.62 | −4.13 | −4.33 | 19.88 | 20.30 | 20.13 |
| 500 | 16.40 | 16.58 | 16.52 | −10.63 | −10.17 | −10.39 | 37.76 | 38.30 | 37.93 |
| 1,000 | 34.54 | 34.84 | 34.66 | −27.96 | −27.60 | −27.80 | 63.93 | 64.24 | 64.03 |
| 1,500 | 46.55 | 46.83 | 46.66 | −44.40 | −44.25 | −44.29 | 75.76 | 75.93 | 75.83 |

TABLE 4.—*Vibrational contributions for the trimethylbenzenes*

| $T$ | Vibrational contribution in cal/deg mole | | | | | | | | |
|---|---|---|---|---|---|---|---|---|---|
| | $(H°-H0)/T$ | | | $(F°-H0)/T$ | | | $C_p°$ | | |
| | 1,2,3-Trimethylbenzene | 1,2,4-Trimethylbenzene | 1,3,5-Trimethylbenzene | 1,2,3-Trimethylbenzene | 1,2,4-Trimethylbenzene | 1,3,5-Trimethylbenzene | 1,2,3-Trimethylbenzene | 1,2,4-Trimethylbenzene | 1,3,5-Trimethylbenzene |
| °K | | | | | | | | | |
| 300 | 10.27 | 10.34 | 10.19 | −6.77 | −6.48 | −5.79 | 23.70 | 23.94 | 24.52 |
| 500 | 19.65 | 19.76 | 20.00 | −13.96 | −13.72 | −13.06 | 43.62 | 43.79 | 44.69 |
| 1,000 | 40.36 | 40.49 | 40.97 | −34.35 | −34.20 | −33.80 | 74.44 | 74.55 | 75.06 |
| 1,500 | 54.38 | 54.49 | 54.93 | −53.55 | −53.45 | −53.25 | 88.61 | 88.67 | 88.94 |

lowed. The barrier for the ethyl (or phenyl) group rotation in ethylbenzene is twofold ($n=2$). Although the barrier in this case may deviate considerably from the simple cosine form, sufficient calorimetric data are not available to justify a more detailed treatment.

### (b) Reduced Moments of Inertia

Although only the product of reduced moments of inertia was needed for the free-rotation calculation, individual values are required for restricted rotation calculations [5], since the partition function for each individual rotation is needed. In terms of our constants it is

$$Q_f=2.7935\ (10^{38}IT)^{\frac{1}{2}}/n, \qquad (7)$$

where $I$ is the reduced moment of inertia, $T$ the absolute temperature, and $n$ the symmetry number. The values of $I$ were calculated from eq 1b and 1c of reference [5], and are listed in table 5.

TABLE 5.—*Reduced moments of inertia for internal rotation* [a] [b]

[Values in units of $10^{-40}$ g cm$^2$]

| | | | |
|---|---|---|---|
| Toluene | 5.32 | ..... | ..... |
| Ethylbenzene | [c] 5.18 | 33.5 | ..... |
| o-Xylene | 5.41 | 5.41 | ..... |
| m-Xylene | 5.41 | 5.41 | ..... |
| p-Xylene | 5.32 | 5.32 | ..... |
| 1,2,3-Trimethylbenzene | 5.44 | 5.46 | 5.44 |
| 1,2,4-Trimethylbenzene | 5.42 | 5.45 | 5.42 |
| 1,3,5-Trimethylbenzene | 5.46 | 5.46 | 5.46 |

[a] The values refer to the groups in the order mentioned in the names for the trimethylbenzenes. The methyl group is given first for ethylbenzene. These values are rounded to three significant figures; hence their product will not agree exactly with that in table 1.

[b] For the moment of inertia 5.32 for the methyl group, unless otherwise indicated.

[c] For the moment of inertia 5.30 for the methyl group.

### (c) Calculation of Potential Barriers from Experimental Entropies

The experimental entropies for these compounds, for the liquids under their saturation pressures, at 298.16° K, are given in the first row of table 6. These values have been taken as the standard entropy of the liquid, at 1-atmosphere pressure and 298.16° K, as the difference is only 0.002 or 0.003 cal/deg mole. The references to the sources of these values are given in the table. The second row gives the standard entropy of vaporization, $\Delta S_v°$, at 298.16° K, as taken from the work of Osborne and Ginnings [10], and reduced to the standard state [14]. The third row (sum of first and second) is the experimental value for the standard entropy of the gas, at 1 atmosphere pressure and 298.16° K. The fourth row gives the sum of the calculated contributions to the standard entropy of the gas for translation, total free (over-all and internal) rotation, and vibration, at 298.16° K. The fifth row (difference of third and fourth) is the decrease in the entropy caused by the restriction of the internal rotations (except for benzene). Finally, the last three rows give respectively the maximum potential barrier consistent with the experimental entropy and its uncertainty, the probable barrier indicated by the experimental entropy value itself, and the minimum barrier consistent with the experimental entropy and its uncertainty.

All contributions of restricted rotation throughout this paper are taken from tables of Pitzer and Gwinn [5].

For ethylbenzene there are two separate potential barriers to be evaluated. The barrier for methyl rotation has been assumed to have the value of 3,400 cal/mole found in propane [12]. On this basis, 1.50 cal/deg mole of the entropy difference, $(S_f°-S°)$, is to be assigned to the methyl rotation, leaving 0.36 cal/deg mole as the contribution of the ethyl rotation, which leads to 1,080 cal/mole as the indicated value of the potential barrier for the ethyl (phenyl) rotation. In this case, the uncertainty in the calculated entropy of vibration and of restricted methyl rotation exceeds that of the experimental value. Hence, calculated maximum and minimum potential barriers would have no meaning.

The experimental value for the entropy of benzene gas at 298.16° K differs from the calculated value by 0.19 $\pm$0.30 cal/deg mole. Even this insignificant difference is in the direction to be explained by the neglected anharmonicity of vibrations.

### (d) Calculation of Potential Barriers from Experimental Heat Capacities

The comparison with the gaseous heat-capacity data of Gwinn, and of Pitzer and Scott [9], is shown in table 7. The experimental values are given in the third column, and the values calculated for the sum of translation, total free rotation (over-all and internal), and vibration are given in the fourth column. The difference of these values, given in the fifth column, is the increase in heat capacity owing to restriction of rotation (except for benzene). The values of the potential barriers ind-

TABLE 6.—*Potential barriers from entropy values at 298.16° K*

[Entropy, cal/degree mole; potential barrier, cal/mole]

| | Benzene | Toluene | Ethylbenzene | o-Xylene | m-Xylene | p-Xylene |
|---|---|---|---|---|---|---|
| Experimental entropy: | | | | | | |
| $S°$ (liquid, 1 atm) [a] | 41.49 | 52.39 | 60.99 | 58.80 | 60.42 | 59.20 |
| Vaporization, $\Delta S_v$ [b] | 23.04 | 23.94 | 25.16 | 25.40 | 25.22 | 25.11 |
| $S°$ (gas, 1 atm) | 64.53± 0.30 | 76.33 ±0.25 | 86.15 ±0.12 | 84.20 ±0.25 | 85.64 ±0.35 | 84.31 ±0.25 |
| Calculated entropy of translation, vibration, and over-all and free internal rotation, $S_f°$ (gas, 1 atm) | 64.34 | 76.56 | 88.01 | 86.15 | 85.80 | 84.51 |
| Difference $(S_f°-S°)$ | | 0.23 | 1.86 | 1.95 | 0.16 | 0.20 |
| Potential barrier: | | | | | | |
| Maximum [d] | | 1,600 | (e) | 2,500 | 1,000 | 900 |
| Most probable | | 1,000 | e 1,080 | 2,200 | 550 | 600 |
| Minimum [d] | | 0 | (e) | 2,000 | 0 | 0 |

[a] References: Benzene [17], toluene [18], ethylbenzene [19, 20], xylenes [9].
[b] Reference [14].
[c] For the ethyl (phenyl) rotation in ethylbenzene assuming a barrier of 3,400 cal/mole for the methyl rotation.
[d] Allowed by the experimental uncertainties.
[e] Uncertain—see text.

cated by the data are shown in the last column. These values are obviously subject to considerable uncertainty, in view of the estimated uncertainties in the experimental heat capacities, and the possible effects of error in vibrational assignment.

Scott and Mellors [11] have reported the value 38.06 ±0.20 cal/deg mole for the gaseous heat capacity ($C_p°$) of ethylbenzene at 373.16° K. This value was obtained by applying a calibration correction to the observed value of 37.71. The calculated value at this temperature for translation, total free rotation, and vibration is 36.56, leaving 1.50 cal/deg mole as the contribution of restricted rotation. Of this, 1.20 is to be assigned to the methyl rotation, assuming, as before, a 3,400 cal/mole barrier. The contribution of the ethyl rotation is therefore 0.30 cal/deg mole, which yields a value of 850 cal/mole for the barrier.

TABLE 7.—*Potential barriers from gaseous heat-capacity data*

| Compound | $T$ | Heat capacity $C°_p$ | | Difference (experimental minus calculated) | Calculated potential barrier ($V$) |
|---|---|---|---|---|---|
| | | Experimental [a] | Calculated ($V$=0) | | |
| | °K | *cal/deg mole* | *cal/deg mole* | | *cal/mole* |
| Benzene | 388 | 26.0±0.3 | 25.96 | 0.04 | |
| | 417 | 28.1±0.3 | 27.85 | .25 | |
| | 481 | 31.4±0.3 | 31.73 | −.33 | |
| Benzene | 393 | 26.4±0.3 | 26.29 | .11 | |
| | 428 | 28.4±0.3 | 28.55 | −.15 | |
| | 463 | 30.3±0.3 | 30.70 | −.40 | |
| Toluene [b] | 393 | 32.8±0.3 | 32.57 | .23 | 1,000 |
| | 428 | 35.7±0.4 | 35.27 | .43 | 1,500 |
| | 463 | 38.0±0.4 | 37.87 | .13 | 750 |
| o-Xylene [b] | 393 | 40.2±0.4 | 38.62 | 1.58 | 1,900 |
| | 428 | 43.5±0.4 | 41.72 | 1.78 | 2,200 |
| | 463 | 46.0±0.5 | 44.72 | 1.28 | 1,800 |
| m-Xylene [b] | 393 | 39.1±0.4 | 39.12 | −0.02 | 0 |
| | 428 | 42.4±0.4 | 42.25 | .15 | 600 |
| | 463 | 45.4±0.4 | 45.24 | .16 | 600 |
| p-Xylene [b] | 393 | 39.0±0.4 | 38.78 | .22 | 650 |
| | 428 | 42.6±0.4 | 41.90 | .70 | 1,300 |
| | 463 | 45.2±0.4 | 44.89 | .31 | 850 |

[a] The first series for benzene is the data of Gwinn [9]; the remaining data are those of Pitzer and Scott [9].
[b] Toluene, m-xylene, and p-xylene calculated for a potential barrier of 6 maxima; o-xylene with a barrier of 3 maxima.

### (e) Selected Values of Potential Barriers

The potential barriers selected on the basis of the entropy and heat-capacity data, and used in the calculation of the final values of the thermodynamic functions, may now be stated. The barriers for the methyl groups in toluene, *p*- and *m*-xylenes were assigned a value of 750 cal/mole, as the best average value indicated by the data on these compounds,[7] and a value of 2,100 cal/mole was assigned to the barriers in *o*-xylene. The differences between these values and the values reported previously [9] are attributable principally to changes in the calculated vibrational contributions resulting from the use of the new values of the fundamental physical constants [1]. The barrier for the ethyl group rotation in ethylbenzene was assigned the value 1,080 cal/mole indicated by the entropy. The entropies calculated with these barriers are compared with the experimental entropies at 298.16° K in table 8.

[7] This value of 750 cal/mole is to be regarded as an empirical parameter for best reproduction of thermodynamic functions. The low-temperature heat-capacity curves of toluene and *m*- and *p*-xylene make it improbable that the real value is this large—see Pitzer and Scott [9], page 826. The thermodynamic data are in reasonable accord with the 500 cal/mole value adopted previously [9].

TABLE 8.—*Comparison of experimental and calculated entropies at 298.16 ° K*

| Compound | Entropy, $S°$ (gas, 1 atm, 298.16° K) | |
|---|---|---|
| | Experimental | Calculated |
| | *cal/deg mole* | *cal/deg mole* |
| Benzene | 64.53±0.30 | 64.34 |
| Toluene | 76.33±0.25 | 76.42 |
| Ethylbenzene | 86.15±0.12 | 86.15 |
| o-Xylene | 84.20±0.25 | 84.31 |
| m-Xylene | 85.64±0.35 | 85.49 |
| p-Xylene | 84.31±0.25 | 84.23 |

The barriers for the trimethylbenzenes were assigned empirically on the basis of the barriers in the xylenes, as follows: (1) 1,2,3-, and 1,2,4-trimethylbenzenes, one 750, and two 2,100 cal/mole barriers, each; (2) 1,3,5-trimethylbenzene, three 750 cal/mole barriers. The derivation of these values is obvious except in the case of the 750 cal/mole barrier assigned to the central methyl group in 1,2,3-trimethylbenzene. It is likely that the interactions of the central methyl group with the adjacent groups on either side increase about equally the maximum and minimum of the potential energy for the rotation, and do not, therefore, alter greatly the potential barrier (variation of potential energy) for the rotation.

## 4. Calculations by the Method of Increments

The thermodynamic functions for the $C_9H_{12}$ alkyl benzenes, aside from the three trimethylbenzenes, were estimated from the functions for appropriate lower alkylbenzene and paraffin hydrocarbons. The formula used for the three methylethylbenzenes was

1-methyl-$x$-ethylbenzene=1,$x$-dimethylbenzene +ethylbenzene−toluene+$R$ ln 2, (8)

where $x$=2,3, and 4 For propylbenzenes,

$n$-propylbenzene=ethylbenzene+$n$-butane −propane, (9)

isopropylbenzene=ethylbenzene+isobutane −propane+$R$ ln (3/2). (10)

The higher normal alkylbenzenes, from $n$-butylbenzene ($C_{10}H_{14}$) to $n$-hexadecylbenzene ($C_{22}H_{38}$), were calculated from the formula

normal alkylbenzene ($C_nH_{2n-6}$)=ethylbenzene ($C_8H_{10}$)+normal paraffin ($C_{n-8}H_{2n-6}$) −propane ($C_3H_8$), ($n \geq 9$). (11)

When $n$ =9 this reduces to the formula for $n$-propylbenzene ($C_9H_{12}$) eq 9. The thermodynamic functions for isobutane were taken from reference [23], and for the normal paraffin hydrocarbons from reference [16]. The logarithmic terms correct for the discrepancies in total symmetry numbers for over-all and internal rotation in the formulas as written. They are to be included in the calculation of the entropy and the negative of the free-energy function, $-(F°-H_0°)/T$, but omitted in the calculation of the heat-content function and the heat capacity.

Some correction may be desirable for the changes in the barriers for rotation of the alkyl groups attached to the benzene ring, especially in 1-methyl-2-ethylbenzene and isopropylbenzene, but it was not considered worthwhile to estimate the corrections in view of the uncertainty of values calculated by the present method.

An indication of the accuracy of the values for $n$-propylbenzene may be obtained by comparing the directly calculated values for ethylbenzene with values calculated from the equation

ethylbenzene=toluene+propane−ethane. (12)

The differences, expressed as the value calculated from eq 12, less the directly calculated value, in cal/deg mole, at 300°, 900°, and 1,500° K, are 1.17, 0.10, and −0.17, for the free-energy function; −1.24, −0.67, and −0.42 for the heat-content function; and −0.92, −0.13, and −0.02 for the heat capacity. However, in this case the difference in the contribution of the methyl rotation in toluene and the ethyl rotation in ethylbenzene is considerable. Correction for the change in this contribution leads to differences of 0.04, −0.32, and −0.42, for the free-energy function; −0.29, −0.28, and −0.18, for the heat-content function; and −0.59, −0.09, and −0.01, for the heat capacity. A correction of this type should be unimportant in eq 9 for $n$-propylbenzene.

## 5. Tables of values of the thermodynamic properties

The resulting values of thermodynamic properties for the 14 alkylbenzenes through $C_9H_{12}$ and for the higher normal monoalkylbenzenes are presented in tables 9 to 18, which give values of the heat-content function, $(H°-H_0°)/T$, the free-energy function, $(F°-H_0°)/T$, the entropy, $S°$, the heat content, $H°-H_0°$, and the heat capacity, $C_p°$, for the gas in the standard state at a pressure of 1 atmosphere.

TABLE 9.—*Values* [a] *of the heat-content function,* $(H°-H_0^\circ)/T$, *for the 14 alkylbenzenes,* $C_6$ *to* $C_{20}$, *for the ideal gaseous state, to 1,500° K*

| Compound (gas) | Formula | Temperature [a] in ° K | | | | | | | | | | | | | | |
|---|---|---|---|---|---|---|---|---|---|---|---|---|---|---|---|---|
| | | 0 | 298.16 | 300 | 400 | 500 | 600 | 700 | 800 | 900 | 1,000 | 1,100 | 1,200 | 1,300 | 1,400 | 1,500 |
| | | Heat-content function, [b] $(H°-H_0^\circ)/T$, in cal/deg mole | | | | | | | | | | | | | | |
| Benzene | $C_6H_6$ | 0 | 11.41 | 11.46 | 14.41 | 17.50 | 20.48 | 23.24 | 25.76 | 28.07 | 30.16 | 32.07 | 33.82 | 35.42 | 36.89 | 38.24 |
| Methylbenzene (toluene) | $C_7H_8$ | 0 | 14.44 | 14.51 | 18.17 | 21.94 | 25.56 | 28.92 | 32.03 | 34.86 | 37.45 | 39.82 | 41.99 | 43.98 | 45.81 | 47.50 |
| Ethylbenzene | $C_8H_{10}$ | 0 | 17.89 | 17.97 | 22.44 | 26.99 | 31.33 | 35.35 | 39.03 | 42.38 | 45.45 | 48.25 | 50.82 | 53.18 | 55.34 | 57.35 |
| 1,2-Dimethylbenzene (o-xylene) | $C_8H_{10}$ | 0 | 18.70 | 18.78 | 23.23 | 27.61 | 31.78 | 35.66 | 39.23 | 42.52 | 45.53 | 48.30 | 50.84 | 53.17 | 55.32 | 57.31 |
| 1,3-Dimethylbenzene (m-xylene) | $C_8H_{10}$ | 0 | 17.86 | 17.94 | 22.31 | 26.72 | 30.94 | 34.88 | 38.52 | 41.86 | 44.93 | 47.74 | 50.32 | 52.69 | 54.87 | 56.88 |
| 1,4-Dimethylbenzene (p-xylene) | $C_8H_{10}$ | 0 | 17.97 | 18.04 | 22.32 | 26.66 | 30.83 | 34.74 | 38.36 | 41.69 | 44.76 | 47.56 | 50.14 | 52.52 | 54.70 | 56.72 |
| n-Propylbenzene | $C_9H_{12}$ | 0 | 21.69 | 21.78 | 27.0 | 32.2 | 37.2 | 41.8 | 46.0 | 49.8 | 53.4 | 56.6 | 59.5 | 62.3 | 64.8 | 67.1 |
| Isopropylbenzene (cumene) | $C_9H_{12}$ | 0 | 20.45 | 20.54 | 26.0 | 31.4 | 36.6 | 41.3 | 45.6 | 49.5 | 53.1 | 56.4 | 59.4 | 62.1 | 64.6 | 67.0 |
| 1-Methyl-2-ethylbenzene | $C_9H_{12}$ | 0 | 22.15 | 22.25 | 27.5 | 32.7 | 37.6 | 42.1 | 46.2 | 50.0 | 53.5 | 56.7 | 59.7 | 62.4 | 64.9 | 67.2 |
| 1-Methyl-3-ethylbenzene | $C_9H_{12}$ | 0 | 21.31 | 21.40 | 26.6 | 31.8 | 36.7 | 41.3 | 45.5 | 49.4 | 52.9 | 56.2 | 59.2 | 61.9 | 64.4 | 66.7 |
| 1-Methyl-4-ethylbenzene | $C_9H_{12}$ | 0 | 21.42 | 21.51 | 26.6 | 31.7 | 36.6 | 41.2 | 45.4 | 49.2 | 52.8 | 56.0 | 59.0 | 61.7 | 64.2 | 66.6 |
| 1,2,3-Trimethylbenzene (hemimellitene) | $C_9H_{12}$ | 0 | 22.10 | 22.19 | 27.0 | 32.0 | 36.6 | 41.1 | 45.2 | 48.9 | 52.4 | 55.6 | 58.6 | 61.3 | 63.9 | 66.2 |
| 1,2,4-Trimethylbenzene (pseudocumene) | $C_9H_{12}$ | 0 | 22.17 | 22.26 | 27.1 | 32.1 | 36.8 | 41.2 | 45.3 | 49.1 | 52.6 | 55.8 | 58.7 | 61.5 | 64.0 | 66.3 |
| 1,3,5-Trimethylbenzene (mesitylene) | $C_9H_{12}$ | 0 | 21.22 | 21.31 | 26.21 | 31.23 | 36.04 | 40.55 | 44.74 | 48.59 | 52.13 | 55.39 | 58.39 | 61.15 | 63.70 | 66.05 |

[a] Interpolation to other temperatures in the interval 298.16° to 1,500° K may be made by appropriate graphical or analytical methods. For temperatures between 200° and 298.16° K, values may be estimated by extrapolating the values for 300°, 400°, 500°, and 600° K. The values in this table are given to more significant figures than are warranted by the absolute accuracy of the individual values in order to retain the internal consistency of the several thermodynamic functions of a single substance, and also to retain the significance of the increment with temperature of a given thermodynamic function.

[b] The heat-content function $(H°-H_0^\circ)/T$, is the heat content at the given temperature less the heat content at 0°K, divided by the absolute temperature (°K) of the given hydrocarbon in the thermodynamic standard gaseous state of unit fugacity (1 atmosphere).

TABLE 10.—*Values* [a] *of the heat-content function,* $(H°-H_0^\circ)/T$, *for the normal alkylbenzenes,* $C_8$ *to* $C_{22}$, *for the ideal gaseous state, to 1,500° K*

| Compound (gas) | Formula | Temperature [a] in ° K | | | | | | | | | | | | | | |
|---|---|---|---|---|---|---|---|---|---|---|---|---|---|---|---|---|
| | | 0 | 298.16 | 300 | 400 | 500 | 600 | 700 | 800 | 900 | 1,000 | 1,100 | 1,200 | 1,300 | 1,400 | 1,500 |
| | | Heat-content function, [b] $(H°-H_0^\circ)/T$, in cal/deg mole | | | | | | | | | | | | | | |
| Benzene | $C_6H_6$ | 0 | 11.41 | 11.46 | 14.41 | 17.50 | 20.48 | 23.24 | 25.76 | 28.07 | 30.16 | 32.07 | 33.82 | 35.42 | 36.89 | 38.24 |
| Methylbenzene (toluene) | $C_7H_8$ | 0 | 14.44 | 14.51 | 18.17 | 21.94 | 25.56 | 28.92 | 32.03 | 34.86 | 37.45 | 39.82 | 41.99 | 43.98 | 45.81 | 47.50 |
| Ethylbenzene | $C_8H_{10}$ | 0 | 17.89 | 17.97 | 22.44 | 26.99 | 31.33 | 35.35 | 39.03 | 42.38 | 45.45 | 48.25 | 50.82 | 53.18 | 55.34 | 57.35 |
| n-Propylbenzene | $C_9H_{12}$ | 0 | 21.69 | 21.78 | 27.0 | 32.2 | 37.2 | 41.8 | 46.0 | 49.8 | 53.4 | 56.6 | 59.5 | 62.3 | 64.8 | 67.1 |
| n-Butylbenzene | $C_{10}H_{14}$ | 0 | 25.12 | 25.23 | 31.2 | 37.1 | 42.8 | 48.0 | 52.8 | 57.1 | 61.1 | 64.8 | 68.2 | 71.3 | 74.1 | 76.8 |
| n-Amylbenzene | $C_{11}H_{16}$ | 0 | 28.55 | 28.67 | 35.4 | 42.0 | 48.3 | 54.2 | 59.5 | 64.4 | 68.9 | 73.0 | 76.8 | 80.3 | 83.5 | 86.4 |
| n-Hexylbenzene | $C_{12}H_{18}$ | 0 | 31.98 | 32.11 | 39.6 | 46.9 | 53.9 | 60.4 | 66.3 | 71.7 | 76.7 | 81.2 | 85.4 | 89.3 | 92.8 | 96.1 |
| n-Heptylbenzene | $C_{13}H_{20}$ | 0 | 35.41 | 35.56 | 43.8 | 51.8 | 59.5 | 66.6 | 73.1 | 79.0 | 84.4 | 89.4 | 94.0 | 98.3 | 102.2 | 105.7 |
| n-Octylbenzene | $C_{14}H_{22}$ | 0 | 38.84 | 39.01 | 48.0 | 56.8 | 65.1 | 72.8 | 79.9 | 86.3 | 92.2 | 97.6 | 102.6 | 107.3 | 111.5 | 115.4 |
| n-Nonylbenzene | $C_{15}H_{24}$ | 0 | 42.27 | 42.46 | 52.2 | 61.7 | 70.7 | 79.0 | 86.6 | 93.6 | 100.0 | 105.8 | 111.2 | 116.3 | 120.8 | 125.1 |
| n-Decylbenzene | $C_{16}H_{26}$ | 0 | 45.70 | 45.90 | 56.4 | 66.6 | 76.3 | 85.3 | 93.4 | 100.9 | 107.8 | 114.1 | 119.9 | 125.3 | 130.2 | 134.7 |
| n-Undecylbenzene | $C_{17}H_{28}$ | 0 | 49.13 | 49.35 | 60.6 | 71.5 | 81.9 | 91.5 | 100.2 | 108.2 | 115.5 | 122.3 | 128.5 | 134.3 | 139.5 | 144.4 |
| n-Dodecylbenzene | $C_{18}H_{30}$ | 0 | 52.56 | 52.80 | 64.8 | 76.4 | 87.4 | 97.7 | 107.0 | 115.4 | 123.3 | 130.5 | 137.1 | 143.3 | 148.9 | 154.0 |
| n-Tridecylbenzene | $C_{19}H_{32}$ | 0 | 55.99 | 56.24 | 69.1 | 81.3 | 93.0 | 103.9 | 113.8 | 122.8 | 131.1 | 138.7 | 145.7 | 152.3 | 158.2 | 163.7 |
| n-Tetradecylbenzene | $C_{20}H_{34}$ | 0 | 59.42 | 59.59 | 73.3 | 86.2 | 98.6 | 110.1 | 120.5 | 130.0 | 138.8 | 146.9 | 154.4 | 161.3 | 167.6 | 173.4 |
| n-Pentadecylbenzene | $C_{21}H_{36}$ | 0 | 62.85 | 63.14 | 77.5 | 91.2 | 104.2 | 116.3 | 127.3 | 137.3 | 146.6 | 155.1 | 163.0 | 170.3 | 176.9 | 183.0 |
| n-Hexadecylbenzene | $C_{22}H_{38}$ | 0 | 66.28 | 66.58 | 81.7 | 96.1 | 109.8 | 122.5 | 134.1 | 144.6 | 154.4 | 163.3 | 171.6 | 179.3 | 186.3 | 192.7 |
| Increment per $CH_2$ group | | 0 | 3.430 | 3.447 | 4.21 | 4.92 | 5.59 | 6.21 | 6.78 | 7.29 | 7.77 | 8.21 | 8.62 | 9.00 | 9.35 | 9.66 |

[a] See footnote "a" of table 9.

[b] The heat-content function, $(H°-H_0^\circ)/T$, is the heat content at the given temperature less the heat content at 0°K, divided by the absolute temperature (°K) of the given hydrocarbon in the thermodynamic standard gaseous state of unit fugacity (1 atmosphere).



702005—46——5

TABLE 11.—*Values* [a] *of the free energy function,* $(F°-H_0^\circ)/T$, *for the 14 alkylbenzenes,* $C_6$ *to* $C_{10}$, *for the ideal gaseous state, 1,500° K*

| Compound (gas) | Formula | Temperature [a] in ° K | | | | | | | | | | | | | | |
|---|---|---|---|---|---|---|---|---|---|---|---|---|---|---|---|---|
| | | 0 | 298.16 | 300 | 400 | 500 | 600 | 700 | 800 | 900 | 1,000 | 1,100 | 1,200 | 1,300 | 1,400 | 1,50 |
| | | Free-energy function,[b] $(F°-H_0^\circ)/T$, in cal/deg mole | | | | | | | | | | | | | | |
| Benzene | $C_6H_6$ | 0 | −52.93 | −53.00 | −56.69 | −60.24 | −63.70 | −67.06 | −70.34 | −73.50 | −76.57 | −79.54 | −82.40 | −85.18 | −87.85 | −90.4 |
| Methylbenzene (toluene) | $C_7H_8$ | 0 | −61.98 | −62.07 | −66.74 | −71.20 | −75.52 | −79.72 | −83.79 | −87.72 | −91.53 | −95.21 | −98.77 | −102.21 | −105.53 | −108.7 |
| Ethylbenzene | $C_8H_{10}$ | 0 | −68.26 | −68.37 | −74.14 | −79.64 | −84.94 | −90.08 | −95.05 | −99.84 | −104.47 | −108.94 | −113.25 | −117.42 | −121.44 | −125.3 |
| 1,2-Dimethylbenzene (*o*-xylene) | $C_8H_{10}$ | 0 | −65.61 | −65.73 | −71.74 | −77.40 | −82.81 | −88.01 | −93.01 | −97.82 | −102.46 | −106.93 | −111.24 | −115.39 | −119.42 | −123.3 |
| 1,3-Dimethylbenzene (*m*-xylene) | $C_8H_{10}$ | 0 | −67.63 | −67.74 | −73.50 | −78.95 | −84.20 | −89.28 | −94.18 | −98.91 | −103.48 | −107.89 | −112.15 | −116.27 | −120.23 | −124.1 |
| 1,4-Dimethylbenzene (*p*-xylene) | $C_8H_{10}$ | 0 | −66.26 | −66.37 | −72.15 | −77.59 | −82.83 | −87.89 | −92.76 | −97.48 | −102.02 | −106.42 | −110.66 | −114.77 | −118.74 | −122.6 |
| *n*-Propylbenzene | $C_9H_{12}$ | 0 | −74.05 | −74.19 | −81.2 | −87.8 | −94.1 | −100.1 | −106.0 | −111.6 | −117.1 | −122.3 | −127.4 | −132.2 | −136.9 | −141.4 |
| Isopropylbenzene (cumene) | $C_9H_{12}$ | 0 | −72.42 | −72.54 | −79.2 | −85.6 | −91.8 | −97.8 | −103.6 | −109.2 | −114.6 | −119.8 | −124.8 | −129.6 | −134.4 | −138.9 |
| 1-Methyl-2-ethylbenzene | $C_9H_{12}$ | 0 | −73.27 | −73.41 | −80.5 | −87.2 | −93.6 | −99.8 | −105.6 | −111.3 | −116.8 | −122.0 | −127.1 | −132.0 | −136.7 | −141.2 |
| 1-Methyl-3-ethylbenzene | $C_9H_{12}$ | 0 | −75.29 | −75.42 | −82.3 | −88.8 | −95.0 | −101.0 | −106.8 | −112.4 | −117.8 | −123.0 | −128.0 | −132.9 | −137.5 | −142.0 |
| 1-Methyl-4-ethylbenzene | $C_9H_{12}$ | 0 | −73.92 | −74.05 | −80.9 | −87.4 | −93.6 | −99.6 | −105.4 | −111.0 | −116.3 | −121.5 | −126.5 | −131.4 | −136.0 | −140.5 |
| 1,2,3-Trimethylbenzene (hemimellitene) | $C_9H_{12}$ | 0 | −71.40 | −71.53 | −78.4 | −84.9 | −91.2 | −97.2 | −102.9 | −108.5 | −113.8 | −119.0 | −123.9 | −128.7 | −133.4 | −137.8 |
| 1,2,4-Trimethylbenzene (pseudocumene) | $C_9H_{12}$ | 0 | −72.57 | −72.70 | −79.6 | −86.2 | −92.4 | −98.4 | −104.2 | −109.8 | −115.1 | −120.3 | −125.3 | −130.1 | −134.7 | −139.1 |
| 1,3,5-Trimethylbenzene (mesitylene) | $C_9H_{12}$ | 0 | −70.93 | −71.06 | −77.66 | −84.04 | −90.18 | −96.08 | −101.77 | −107.26 | −112.56 | −117.68 | −122.62 | −127.40 | −132.03 | −136.5 |

[a] See footnote "a" of table 9.

[b] The free-energy function, $(F°-H_0^\circ)/T$, is the free energy (exclusive of nuclear spin) at the given temperature less the heat content at 0° K, divided by the absolute temperature (° K), of the given hydrocarbon in the thermodynamic standard gaseous state of unit fugacity (1 atmosphere).

TABLE 12.—*Values* [a] *of the free-energy function,* $(F°-H_0^\circ)/T$, *for the normal alkylbenzenes,* $C_6$ *to* $C_{22}$, *for the ideal gaseous state, to 1,500° K*

| Compound (gas) | Formula | Temperature [a] in ° K | | | | | | | | | | | | | | |
|---|---|---|---|---|---|---|---|---|---|---|---|---|---|---|---|---|
| | | 0 | 298.16 | 300 | 400 | 500 | 600 | 700 | 800 | 900 | 1,000 | 1,100 | 1,200 | 1,300 | 1,400 | 1,50 |
| | | Free-energy function [b], $(F°-H_0^\circ)/T$, in cal/deg mole | | | | | | | | | | | | | | |
| Benzene | $C_6H_6$ | 0 | −52.93 | −53.00 | −56.69 | −60.24 | −63.70 | −67.06 | −70.34 | −73.50 | −76.57 | −79.54 | −82.40 | −85.18 | −87.85 | −90.4 |
| Methylbenzene (toluene) | $C_7H_8$ | 0 | −61.98 | −62.07 | −66.74 | −71.20 | −75.52 | −79.72 | −83.79 | −87.72 | −91.53 | −95.21 | −98.77 | −102.21 | −105.53 | −108.7 |
| Ethylbenzene | $C_8H_{10}$ | 0 | −68.26 | −68.37 | −74.14 | −79.64 | −84.94 | −90.08 | −95.05 | −99.84 | −104.47 | −108.94 | −113.25 | −117.42 | −121.44 | −125.3 |
| *n*-Propylbenzene | $C_9H_{12}$ | 0 | −74.05 | −74.19 | −81.2 | −87.8 | −94.1 | −100.1 | −106.0 | −111.6 | −117.1 | −122.3 | −127.4 | −132.2 | −136.9 | −141.4 |
| *n*-Butylbenzene | $C_{10}H_{14}$ | 0 | −79.79 | −79.94 | −88.0 | −95.6 | −102.8 | −109.8 | −116.6 | −123.0 | −129.3 | −135.3 | −141.1 | −146.6 | −152.0 | −157.2 |
| *n*-Amylbenzene | $C_{11}H_{16}$ | 0 | −85.54 | −85.72 | −94.9 | −103.5 | −111.7 | −119.6 | −127.2 | −134.5 | −141.6 | −148.3 | −154.8 | −161.1 | −167.1 | −173.0 |
| *n*-Hexylbenzene | $C_{12}H_{18}$ | 0 | −91.30 | −91.49 | −101.7 | −111.4 | −120.5 | −129.4 | −137.8 | −146.0 | −153.8 | −161.3 | −168.6 | −175.6 | −182.3 | −188.8 |
| *n*-Heptylbenzene | $C_{13}H_{20}$ | 0 | −97.05 | −97.27 | −108.6 | −119.2 | −129.4 | −139.1 | −148.4 | −157.4 | −166.1 | −174.4 | −182.3 | −190.0 | −197.4 | −204.5 |
| *n*-Octylbenzene | $C_{14}H_{22}$ | 0 | −102.80 | −103.05 | −115.5 | −127.1 | −138.2 | −148.9 | −159.1 | −168.9 | −178.3 | −187.4 | −196.1 | −204.5 | −212.5 | −220.3 |
| *n*-Nonylbenzene | $C_{15}H_{24}$ | 0 | −108.56 | −108.82 | −122.3 | −135.0 | −147.1 | −158.6 | −169.7 | −180.4 | −190.6 | −200.4 | −209.9 | −218.9 | −227.7 | −236.1 |
| *n*-Decylbenzene | $C_{16}H_{26}$ | 0 | −114.31 | −114.60 | −129.2 | −142.9 | −155.9 | −168.4 | −180.3 | −191.8 | −202.8 | −213.4 | −223.6 | −233.4 | −242.8 | −251.9 |
| *n*-Undecylbenzene | $C_{17}H_{28}$ | 0 | −120.06 | −120.38 | −136.1 | −150.8 | −164.8 | −178.1 | −191.0 | −203.3 | −215.1 | −226.4 | −237.4 | −247.9 | −257.9 | −267.6 |
| *n*-Dodecylbenzene | $C_{18}H_{30}$ | 0 | −125.81 | −126.16 | −142.9 | −158.7 | −173.6 | −187.9 | −201.6 | −214.7 | −227.4 | −239.5 | −251.1 | −262.3 | −273.1 | −283.6 |
| *n*-Tridecylbenzene | $C_{19}H_{32}$ | 0 | −131.57 | −131.93 | −149.8 | −166.6 | −182.4 | −197.6 | −212.2 | −226.2 | −239.6 | −252.5 | −264.9 | −276.8 | −288.2 | −299.1 |
| *n*-Tetradecylbenzene | $C_{20}H_{34}$ | 0 | −137.32 | −137.71 | −156.7 | −174.5 | −191.3 | −207.4 | −222.8 | −237.6 | −251.9 | −265.5 | −278.6 | −291.3 | −303.3 | −314.9 |
| *n*-Pentadecylbenzene | $C_{21}H_{36}$ | 0 | −143.07 | −143.49 | −163.5 | −182.4 | −200.1 | −217.1 | −233.5 | −249.1 | −264.1 | −278.5 | −292.4 | −305.7 | −318.5 | −330.7 |
| *n*Hexadecylbenzene | $C_{22}H_{38}$ | 0 | −148.83 | −149.26 | −170.4 | −190.2 | −209.0 | −226.9 | −244.1 | −260.6 | −276.4 | −291.6 | −306.2 | −320.2 | −333.6 | −346.6 |
| Increment per $CH_2$ group | ..... | 0 | −5.753 | −5.777 | −6.87 | −7.89 | −8.84 | −9.75 | −10.63 | −11.46 | −12.26 | −13.02 | −13.76 | −14.46 | −15.13 | −15.7 |

[a] See footnote "a" of table 9.

[b] The free-energy function $(F°-H_0^\circ)/T$, is the free energy (exclusive of nuclear spin) at the given temperature less the heat content at 0° K, divided by the absolute temperature (°K), of the given hydrocarbon in the thermodynamic standard gaseous state of unit fugacity (1 atmosphere).

TABLE 13.—*Values* [a] *of the entropy, S°, for the 14 alkylbenzenes, $C_6$ to $C_9$, for the ideal gaseous state, to 1,500° K*

| Compound (gas) | Formula | Temperature [a] in ° K | | | | | | | | | | | | | | |
|---|---|---|---|---|---|---|---|---|---|---|---|---|---|---|---|---|
| | | 0 | 298.16 | 300 | 400 | 500 | 600 | 700 | 800 | 900 | 1,000 | 1,100 | 1,200 | 1,300 | 1,400 | 1,500 |
| | | Entropy,[b] $S°$, in cal/deg mole | | | | | | | | | | | | | | |
| Benzene | $C_6H_6$ | 0 | 64.34 | 64.46 | 71.10 | 77.74 | 84.17 | 90.30 | 96.10 | 101.57 | 106.73 | 111.61 | 116.22 | 120.59 | 124.74 | 128.68 |
| Methylbenzene (toluene) | $C_7H_8$ | 0 | 76.42 | 76.57 | 84.91 | 93.13 | 101.08 | 108.64 | 115.81 | 122.58 | 128.98 | 135.03 | 140.76 | 146.19 | 151.34 | 156.25 |
| Ethylbenzene | $C_8H_{10}$ | 0 | 86.15 | 86.34 | 96.59 | 106.63 | 116.28 | 125.43 | 134.08 | 142.23 | 149.92 | 157.19 | 164.07 | 170.59 | 176.79 | 182.67 |
| 1,2-Dimethylbenzene (o-xylene) | $C_8H_{10}$ | 0 | 84.31 | 84.51 | 94.96 | 105.01 | 114.60 | 123.67 | 132.24 | 140.34 | 147.99 | 155.22 | 162.07 | 168.56 | 174.73 | 180.61 |
| 1,3-Dimethylbenzene (m-xylene) | $C_8H_{10}$ | 0 | 85.49 | 85.68 | 95.81 | 105.67 | 115.14 | 124.16 | 132.70 | 140.78 | 148.41 | 155.63 | 162.47 | 168.96 | 175.12 | 181.00 |
| 1,4-Dimethylbenzene (p-xylene) | $C_8H_{10}$ | 0 | 84.23 | 84.41 | 94.47 | 104.25 | 113.66 | 122.63 | 131.13 | 139.17 | 146.78 | 153.98 | 160.81 | 167.29 | 173.44 | 179.31 |
| Propylbenzene | $C_9H_{12}$ | 0 | 95.74 | 95.97 | 108.1 | 119.9 | 131.2 | 141.9 | 152.0 | 161.5 | 170.5 | 178.9 | 186.9 | 194.5 | 201.7 | 208.6 |
| Isopropylbenzene (cumene) | $C_9H_{12}$ | 0 | 92.87 | 93.08 | 105.2 | 117.0 | 128.3 | 139.0 | 149.2 | 158.7 | 167.6 | 176.1 | 184.2 | 191.8 | 199.0 | 205.9 |
| 1-Methyl-2-ethylbenzene | $C_9H_{12}$ | 0 | 95.42 | 95.66 | 108.0 | 119.9 | 131.2 | 141.8 | 151.9 | 161.4 | 170.3 | 178.8 | 186.8 | 194.3 | 201.6 | 208.4 |
| 1-Methyl-3-ethylbenzene | $C_9H_{12}$ | 0 | 96.60 | 96.83 | 108.9 | 120.5 | 131.7 | 142.3 | 152.3 | 161.8 | 170.7 | 179.2 | 187.2 | 194.7 | 201.9 | 208.8 |
| 1-Methyl-4-ethylbenzene | $C_9H_{12}$ | 0 | 95.34 | 95.56 | 107.5 | 119.1 | 130.2 | 140.8 | 150.8 | 160.2 | 169.1 | 177.5 | 185.5 | 193.1 | 200.3 | 207.1 |
| 1,2,3-Trimethylbenzene (hemimellitene) | $C_9H_{12}$ | 0 | 93.50 | 93.73 | 105.4 | 116.9 | 127.8 | 138.3 | 148.1 | 157.4 | 166.2 | 174.6 | 182.5 | 190.1 | 197.2 | 204.0 |
| 1,2,4-Trimethylbenzene (pseudocumene) | $C_9H_{12}$ | 0 | 94.73 | 94.96 | 106.7 | 118.2 | 129.2 | 139.6 | 149.5 | 158.8 | 167.7 | 176.0 | 184.0 | 191.5 | 198.7 | 205.5 |
| 1,3,5-Trimethylbenzene (mesitylene) | $C_9H_{12}$ | 0 | 92.15 | 92.37 | 103.87 | 115.28 | 126.22 | 136.64 | 146.51 | 155.85 | 164.69 | 173.07 | 181.01 | 188.56 | 195.73 | 202.55 |

[a] See footnote "a" of table 9.

[b] $S°$ is the entropy (exclusive of nuclear spin) of the given hydrocarbon in the thermodynamic standard gaseous state of unit fugacity (1 atmosphere) at the temperature indicated.

TABLE 14.—*Values* [a] *of the entropy, S°, for the normal alkylbenzenes, $C_6$ to $C_{22}$, for the ideal gaseous state, to 1,500° K*

| Compound (gas) | Formula | Temperature [a] in ° K | | | | | | | | | | | | | | |
|---|---|---|---|---|---|---|---|---|---|---|---|---|---|---|---|---|
| | | 0 | 298.16 | 300 | 400 | 500 | 600 | 700 | 800 | 900 | 1,000 | 1,100 | 1,200 | 1,300 | 1,400 | 1,500 |
| | | Entropy,[b] $S°$, in cal/deg mole | | | | | | | | | | | | | | |
| Benzene | $C_6H_6$ | 0 | 64.34 | 64.46 | 71.10 | 77.74 | 84.17 | 90.30 | 96.10 | 101.57 | 106.73 | 111.61 | 116.22 | 120.59 | 124.74 | 128.68 |
| Methylbenzene (toluene) | $C_7H_8$ | 0 | 76.42 | 76.57 | 84.91 | 93.13 | 101.08 | 108.64 | 115.81 | 122.58 | 128.98 | 135.03 | 140.76 | 146.19 | 151.34 | 156.25 |
| Ethylbenzene | $C_8H_{10}$ | 0 | 86.15 | 86.34 | 96.59 | 106.63 | 116.28 | 125.43 | 134.08 | 142.23 | 149.92 | 157.19 | 164.07 | 170.59 | 176.79 | 182.67 |
| n-Propylbenzene | $C_9H_{12}$ | 0 | 95.74 | 95.97 | 108.1 | 119.9 | 131.2 | 141.9 | 152.0 | 161.5 | 170.5 | 178.9 | 186.9 | 194.5 | 201.7 | 208.6 |
| n-Butylbenzene | $C_{10}H_{14}$ | 0 | 104.91 | 105.16 | 119.2 | 132.7 | 145.6 | 157.8 | 169.3 | 180.2 | 190.4 | 200.1 | 209.2 | 217.9 | 226.1 | 234.0 |
| n-Amylbenzene | $C_{11}H_{16}$ | 0 | 114.09 | 114.38 | 130.2 | 145.5 | 160.0 | 173.8 | 186.7 | 198.9 | 210.4 | 221.3 | 231.6 | 241.4 | 250.6 | 259.4 |
| n-Hexylbenzene | $C_{12}H_{18}$ | 0 | 123.28 | 123.61 | 141.3 | 158.3 | 174.5 | 189.8 | 204.1 | 217.7 | 230.5 | 242.5 | 254.0 | 264.8 | 275.1 | 284.8 |
| n-Heptylbenzene | $C_{13}H_{20}$ | 0 | 132.46 | 132.83 | 152.4 | 171.1 | 188.9 | 205.7 | 221.5 | 236.4 | 250.5 | 263.8 | 276.4 | 288.3 | 299.6 | 310.3 |
| n-Octylbenzene | $C_{14}H_{22}$ | 0 | 141.64 | 142.06 | 163.5 | 183.9 | 203.3 | 221.7 | 239.0 | 255.2 | 270.5 | 285.0 | 298.7 | 311.7 | 324.0 | 335.7 |
| n-Nonylbenzene | $C_{15}H_{24}$ | 0 | 150.82 | 151.28 | 174.5 | 196.7 | 217.8 | 237.7 | 256.4 | 273.9 | 290.6 | 306.2 | 321.1 | 335.2 | 348.5 | 361.1 |
| n-Decylbenzene | $C_{16}H_{26}$ | 0 | 160.01 | 160.50 | 185.6 | 209.5 | 232.2 | 253.6 | 273.8 | 292.7 | 310.6 | 327.5 | 343.5 | 358.6 | 373.0 | 386.5 |
| n-Undecylbenzene | $C_{17}H_{28}$ | 0 | 169.19 | 169.73 | 196.7 | 222.3 | 246.6 | 269.6 | 291.2 | 311.4 | 330.6 | 348.7 | 365.9 | 382.1 | 397.5 | 412.0 |
| n-Dodecylbenzene | $C_{18}H_{30}$ | 0 | 178.37 | 178.95 | 207.8 | 235.1 | 261.0 | 285.6 | 308.6 | 330.2 | 350.6 | 370.0 | 388.2 | 405.6 | 422.0 | 437.4 |
| n-Tridecylbenzene | $C_{19}H_{32}$ | 0 | 187.56 | 188.18 | 218.8 | 247.9 | 275.5 | 301.5 | 326.0 | 348.9 | 370.7 | 391.2 | 410.6 | 429.0 | 446.4 | 462.8 |
| n-Tetradecylbenzene | $C_{20}H_{34}$ | 0 | 196.74 | 197.40 | 229.9 | 260.7 | 289.9 | 317.5 | 343.4 | 367.7 | 390.7 | 412.4 | 433.0 | 452.5 | 470.9 | 488.2 |
| n-Pentadecylbenzene | $C_{21}H_{36}$ | 0 | 205.92 | 206.62 | 241.0 | 273.5 | 304.3 | 333.5 | 360.8 | 386.4 | 410.7 | 433.7 | 455.4 | 476.0 | 495.4 | 513.7 |
| n-Hexadecylbenzene | $C_{22}H_{38}$ | 0 | 215.11 | 215.85 | 252.1 | 286.3 | 318.8 | 349.4 | 378.2 | 405.2 | 430.8 | 454.9 | 477.8 | 499.4 | 519.9 | 539.1 |
| Increment per $CH_2$ group | | 0 | 9.183 | 9.224 | 11.08 | 12.80 | 14.43 | 15.97 | 17.40 | 18.75 | 20.03 | 21.24 | 22.38 | 23.46 | 24.48 | 25.43 |

[a] See footnote "a" of table 9.

[b] $S°$ is the entropy (exclusive of nuclear spin) of the given hydrocarbon in the thermodynamic standard gaseous state of unit fugacity (1 atmosphere) at the temperature indicated.

TABLE 15.—*Values* [a] *of the heat content,* $(H^\circ - H^\circ_0)$, *for the 14 alkylbenzenes,* $C_6$ *to* $C_{10}$, *for the ideal gaseous state, to 1,500° K*

| Compound (gas) | Formula | Temperature [a] in ° K | | | | | | | | | | | | | | |
|---|---|---|---|---|---|---|---|---|---|---|---|---|---|---|---|---|
| | | 0 | 298.16 | 300 | 400 | 500 | 600 | 700 | 800 | 900 | 1,000 | 1,100 | 1,200 | 1,300 | 1,400 | 1,5 |
| | | Heat content,[b] $(H^\circ - H^\circ_0)$, in cal/mole | | | | | | | | | | | | | | |
| Benzene | $C_6H_6$ | 0 | 3401 | 3437 | 5762 | 8750 | 12285 | 16267 | 20612 | 25260 | 30163 | 35280 | 40590 | 46040 | 51640 | 57 |
| Methylbenzene (toluene) | $C_7H_8$ | 0 | 4306 | 4352 | 7269 | 10969 | 15334 | 20247 | 25621 | 31373 | 37449 | 43800 | 50390 | 57180 | 64130 | 71 |
| Ethylbenzene | $C_8H_{10}$ | 0 | 5335 | 5391 | 8976 | 13496 | 18799 | 24746 | 31222 | 38144 | 45448 | 53080 | 60980 | 69130 | 77480 | 86 |
| 1,2-Dimethylbenzene (o-xylene) | $C_8H_{10}$ | 0 | 5576 | 5635 | 9291 | 13806 | 19070 | 24962 | 31386 | 38265 | 45531 | 53130 | 61000 | 69120 | 77430 | 85 |
| 1,3-Dimethylbenzene (m-xylene) | $C_8H_{10}$ | 0 | 5325 | 5382 | 8925 | 13359 | 18563 | 24415 | 30817 | 37678 | 44933 | 52520 | 60390 | 68500 | 76820 | 85 |
| 1,4-Dimethylbenzene (p-xylene) | $C_8H_{10}$ | 0 | 5358 | 5414 | 8929 | 13330 | 18499 | 24319 | 30690 | 37525 | 44755 | 52320 | 60170 | 68270 | 76580 | 84 |
| n-Propylbenzene | $C_9H_{12}$ | 0 | 6467 | 6534 | 10790 | 16090 | 22300 | 29250 | 36810 | 44860 | 53360 | 62200 | 71400 | 81000 | 90700 | 100 |
| Isopropylbenzene (cumene) | $C_9H_{12}$ | 0 | 6097 | 6162 | 10380 | 15700 | 21940 | 28900 | 36470 | 44560 | 53090 | 62000 | 71200 | 80800 | 90500 | 100 |
| 1-Methyl-2-ethylbenzene | $C_9H_{12}$ | 0 | 6604 | 6674 | 11000 | 16330 | 22530 | 29460 | 36990 | 45040 | 53530 | 62400 | 71600 | 81100 | 90800 | 100 |
| 1-Methyl-3-ethylbenzene | $C_9H_{12}$ | 0 | 6354 | 6421 | 10630 | 15890 | 22030 | 28910 | 36420 | 44450 | 52930 | 61800 | 71000 | 80500 | 90200 | 100 |
| 1-Methyl-4-ethylbenzene | $C_9H_{12}$ | 0 | 6386 | 6453 | 10640 | 15860 | 21960 | 28820 | 36290 | 44300 | 52750 | 61600 | 70800 | 80200 | 89900 | 99 |
| 1,2,3-Trimethylbenzene (hemimellitene) | $C_9H_{12}$ | 0 | 6590 | 6658 | 10810 | 15980 | 21990 | 28750 | 36130 | 44050 | 52430 | 61200 | 70300 | 79700 | 89400 | 99 |
| 1,2,4-Trimethylbenzene (pseudocumene) | $C_9H_{12}$ | 0 | 6609 | 6677 | 10860 | 16030 | 22060 | 28830 | 36230 | 44160 | 52550 | 61300 | 70500 | 79900 | 89600 | 99 |
| 1,3,5-Trimethylbenzene (mesitylene) | $C_9H_{12}$ | 0 | 6326 | 6392 | 10486 | 15616 | 21623 | 28386 | 35789 | 43728 | 52131 | 60930 | 70070 | 79500 | 89180 | 98 |

[a] See footnote "a" of table 9.

[b] $(H^\circ - H^\circ_0)$ is the heat content at the given temperature less the heat content at 0° K of the given hydrocarbon in the thermodynamic standard gaseous state of unit fugacity (1 atmosphere).

TABLE 16.—*Values* [a] *of the heat content,* $(H^\circ - H^\circ_0)$, *for the normal alkylbenzenes,* $C_6$ *to* $C_{22}$, *for the ideal gaseous state, to 1,500° K*

| Compound (gas) | Formula | Temperature [a] in ° K | | | | | | | | | | | | | | |
|---|---|---|---|---|---|---|---|---|---|---|---|---|---|---|---|---|
| | | 0 | 298.16 | 300 | 400 | 500 | 600 | 700 | 800 | 900 | 1,000 | 1,100 | 1,200 | 1,300 | 1,400 | 1,5 |
| | | Heat content,[b] $(H^\circ - H^\circ_0)$, in cal/mole | | | | | | | | | | | | | | |
| Benzene | $C_6H_6$ | 0 | 3401 | 3437 | 5762 | 8750 | 12285 | 16267 | 20612 | 25260 | 30163 | 35280 | 40590 | 46040 | 51640 | 57 |
| Methylbenzene (toluene) | $C_7H_8$ | 0 | 4306 | 4352 | 7269 | 10969 | 15334 | 20247 | 25621 | 31373 | 37449 | 43800 | 50390 | 57180 | 64130 | 71 |
| Ethylbenzene | $C_8H_{10}$ | 0 | 5335 | 5391 | 8976 | 13496 | 18799 | 24746 | 31222 | 38144 | 45448 | 53080 | 60980 | 69130 | 77480 | 86 |
| n-Propylbenzene | $C_9H_{12}$ | 0 | 6467 | 6534 | 10790 | 16090 | 22300 | 29250 | 36810 | 44860 | 53360 | 62200 | 71400 | 81000 | 90700 | 100 |
| n-Butylbenzene | $C_{10}H_{14}$ | 0 | 7490 | 7566 | 12470 | 18540 | 25650 | 33590 | 42210 | 51400 | 61120 | 71300 | 81800 | 92600 | 103800 | 115 |
| n-Amylbenzene | $C_{11}H_{16}$ | 0 | 8512 | 8600 | 14150 | 21000 | 29000 | 37940 | 47630 | 57960 | 68900 | 80300 | 92100 | 104300 | 116800 | 129 |
| n-Hexylbenzene | $C_{12}H_{18}$ | 0 | 9535 | 9634 | 15840 | 23400 | 32350 | 42280 | 53050 | 64530 | 76670 | 89300 | 102500 | 116000 | 129600 | 143 |
| n-Heptylbenzene | $C_{13}H_{20}$ | 0 | 10558 | 10668 | 17520 | 25920 | 35710 | 46630 | 58470 | 71090 | 84440 | 98400 | 112800 | 127700 | 143000 | 158 |
| n-Octylbenzene | $C_{14}H_{22}$ | 0 | 11581 | 11702 | 19200 | 28380 | 39060 | 50980 | 63890 | 77650 | 92210 | 107400 | 123200 | 139400 | 156100 | 173 |
| n-Nonylbenzene | $C_{15}H_{24}$ | 0 | 12603 | 12736 | 20890 | 30840 | 42410 | 55330 | 69320 | 84220 | 99980 | 116400 | 133500 | 151100 | 169200 | 187 |
| n-Decylbenzene | $C_{16}H_{26}$ | 0 | 13626 | 13771 | 22570 | 33300 | 45760 | 59680 | 74740 | 90780 | 107760 | 125500 | 143800 | 162800 | 182300 | 202 |
| n-Undecylbenzene | $C_{17}H_{28}$ | 0 | 14649 | 14805 | 24260 | 35750 | 49120 | 64030 | 80160 | 97340 | 115530 | 134500 | 154200 | 174500 | 195400 | 216 |
| n-Dodecylbenzene | $C_{18}H_{30}$ | 0 | 15671 | 15839 | 25940 | 38210 | 52470 | 68380 | 85580 | 103910 | 123300 | 143500 | 164500 | 186200 | 208500 | 231 |
| n-Tridecylbenzene | $C_{19}H_{32}$ | 0 | 16694 | 16873 | 27620 | 40670 | 55820 | 72730 | 91000 | 110470 | 131080 | 152600 | 174900 | 197900 | 221600 | 245 |
| n-Tetradecylbenzene | $C_{20}H_{34}$ | 0 | 17717 | 17907 | 29310 | 43130 | 59170 | 77080 | 96420 | 117040 | 138850 | 161600 | 185200 | 209600 | 234700 | 260 |
| n-Pentadecylbenzene | $C_{21}H_{36}$ | 0 | 18740 | 18941 | 30990 | 45590 | 62520 | 81430 | 101850 | 123600 | 146620 | 170600 | 195600 | 221300 | 247700 | 274 |
| n-Hexadecylbenzene | $C_{22}H_{38}$ | 0 | 19762 | 19975 | 32680 | 48050 | 65880 | 85780 | 107270 | 130160 | 154400 | 179700 | 205900 | 233000 | 260800 | 288 |
| Increment per $CH_2$ group | | 0 | 1022.7 | 1034.1 | 1684 | 2458 | 3352 | 4349 | 5422 | 6564 | 7773 | 9030 | 10340 | 11700 | 13090 | 14 |

[a] See footnote "a" of table 9.

[b] $(H^\circ - H_0)$ is the heat content at the given temperature less the heat content at 0° K of the given hydrocarbon in the thermodynamic standard gaseous state of unit fugacity (1 atmosphere).

TABLE 17.—*Values* [a] *of the heat capacity,* $C_p^\circ$, *for the 14 alkylbenzenes,* $C_6$ *to* $C_8$, *for the ideal gaseous state, to 1,500° K*

| Compound (gas) | Formula | Temperature [a] in ° K | | | | | | | | | | | | | | |
|---|---|---|---|---|---|---|---|---|---|---|---|---|---|---|---|---|
| | | 0 | 298.16 | 300 | 400 | 500 | 600 | 700 | 800 | 900 | 1,000 | 1,100 | 1,200 | 1,300 | 1,400 | 1,500 |
| | | Heat capacity,[b] $C_p^\circ$, in cal/deg mole | | | | | | | | | | | | | | |
| Benzene | $C_6H_6$ | 0 | 19.52 | 19.65 | 26.74 | 32.80 | 37.74 | 41.75 | 45.06 | 47.83 | 50.16 | 52.16 | 53.86 | 55.32 | 56.58 | 57.67 |
| Methylbenzene (toluene) | $C_7H_8$ | 0 | 24.80 | 24.95 | 33.25 | 40.54 | 46.58 | 51.57 | 55.72 | 59.22 | 62.19 | 64.73 | 66.90 | 68.77 | 70.38 | 71.78 |
| Ethylbenzene | $C_8H_{10}$ | 0 | 30.69 | 30.88 | 40.76 | 49.35 | 56.44 | 62.28 | 67.15 | 71.27 | 74.77 | 77.77 | 80.35 | 82.57 | 84.49 | 86.16 |
| 1,2-Dimethylbenzene (*o*-xylene) | $C_8H_{10}$ | 0 | 31.85 | 32.02 | 41.03 | 49.11 | 55.98 | 61.76 | 66.64 | 70.80 | 74.35 | 77.40 | 80.02 | 82.28 | 84.24 | 85.93 |
| 1,3-Dimethylbenzene (*m*-xylene) | $C_8H_{10}$ | 0 | 30.49 | 30.66 | 40.03 | 48.43 | 55.51 | 61.43 | 66.41 | 70.63 | 74.23 | 77.31 | 79.95 | 82.22 | 84.19 | 85.89 |
| 1,4-Dimethylbenzene (*p*-xylene) | $C_8H_{10}$ | 0 | 30.32 | 30.49 | 39.70 | 48.06 | 55.16 | 61.12 | 66.14 | 70.39 | 74.02 | 77.13 | 79.80 | 82.09 | 84.07 | 85.79 |
| Propylbenzene | $C_9H_{12}$ | 0 | 36.73 | 36.99 | 48.0 | 57.8 | 66.0 | 72.7 | 78.3 | 83.1 | 87.1 | 90.6 | 93.6 | 96.2 | 98.5 | 100.4 |
| Isopropylbenzene (cumene) | $C_9H_{12}$ | 0 | 36.26 | 36.47 | 48.0 | 57.9 | 66.2 | 72.9 | 78.6 | 83.3 | 87.3 | 90.8 | 93.8 | 96.4 | 98.6 | 100.6 |
| 1-Methyl-2-ethylbenzene | $C_9H_{12}$ | 0 | 37.74 | 37.94 | 48.5 | 57.9 | 65.8 | 72.5 | 78.1 | 82.8 | 86.9 | 90.4 | 93.5 | 96.1 | 98.3 | 100.3 |
| 1-Methyl-3-ethylbenzene | $C_9H_{12}$ | 0 | 36.38 | 36.59 | 47.5 | 57.2 | 65.4 | 72.1 | 77.8 | 82.7 | 86.8 | 90.4 | 93.4 | 96.0 | 98.3 | 100.3 |
| 1-Methyl-4-ethylbenzene | $C_9H_{12}$ | 0 | 36.22 | 36.42 | 47.2 | 56.9 | 65.0 | 71.8 | 77.6 | 82.4 | 86.6 | 90.2 | 93.2 | 95.9 | 98.2 | 100.2 |
| 1,2,3-Trimethylbenzene (hemimellitene) | $C_9H_{12}$ | 0 | 36.85 | 37.04 | 46.9 | 56.1 | 64.0 | 70.9 | 76.7 | 81.6 | 85.9 | 89.5 | 92.7 | 95.4 | 97.8 | 99.8 |
| 1,2,4-Trimethylbenzene (pseudocumene) | $C_9H_{12}$ | 0 | 37.10 | 37.28 | 47.1 | 56.2 | 64.2 | 71.0 | 76.8 | 81.7 | 86.0 | 89.6 | 92.8 | 95.5 | 97.8 | 99.8 |
| 1,3,5-Trimethylbenzene (mesitylene) | $C_9H_{12}$ | 0 | 35.91 | 36.10 | 46.41 | 55.92 | 64.08 | 70.99 | 76.84 | 81.81 | 86.07 | 89.72 | 92.86 | 95.56 | 97.89 | 99.91 |

[a] See footnote "a" of table 9.
[b] $C_p^\circ$ is the heat capacity at constant pressure of the given hydrocarbon in the thermodynamic standard gaseous state of unit fugacity (1 atmosphere) at the temperature indicated.

TABLE 18.—*Values* [a] *of the heat capacity,* $C_p^\circ$, *for the normal alkylbenzenes,* $C_6$ *to* $C_{22}$, *for the ideal gaseous state, to 1,500° K*

| Compound (gas) | Formula | Temperature [a] in ° K | | | | | | | | | | | | | | |
|---|---|---|---|---|---|---|---|---|---|---|---|---|---|---|---|---|
| | | 0 | 298.16 | 300 | 400 | 500 | 600 | 700 | 800 | 900 | 1,000 | 1,100 | 1,200 | 1,300 | 1,400 | 1,500 |
| | | Heat capacity,[b] $C_p^\circ$, in cal/deg mole | | | | | | | | | | | | | | |
| Benzene | $C_6H_6$ | 0 | 19.52 | 19.65 | 26.74 | 32.80 | 37.74 | 41.75 | 45.06 | 47.83 | 50.16 | 52.16 | 53.86 | 55.32 | 56.58 | 57.67 |
| Methylbenzene (toluene) | $C_7H_8$ | 0 | 24.80 | 24.95 | 33.25 | 40.54 | 46.58 | 51.57 | 55.72 | 59.22 | 62.19 | 64.73 | 66.90 | 68.77 | 70.38 | 71.78 |
| Ethylbenzene | $C_8H_{10}$ | 0 | 30.69 | 30.88 | 40.76 | 49.35 | 56.44 | 62.28 | 67.15 | 71.27 | 74.77 | 77.77 | 80.35 | 82.57 | 84.49 | 86.16 |
| Propylbenzene | $C_9H_{12}$ | 0 | 36.73 | 36.99 | 48.0 | 57.8 | 66.0 | 72.7 | 78.3 | 83.1 | 87.1 | 90.6 | 93.6 | 96.2 | 98.5 | 100.4 |
| Butylbenzene | $C_{10}H_{14}$ | 0 | 42.42 | 42.73 | 55.1 | 66.3 | 75.4 | 83.1 | 89.4 | 94.9 | 99.5 | 103.5 | 106.9 | 109.9 | 112.5 | 114.7 |
| Amylbenzene | $C_{11}H_{16}$ | 0 | 48.18 | 48.54 | 62.3 | 74.7 | 84.9 | 93.4 | 100.6 | 106.7 | 111.9 | 116.3 | 120.2 | 123.6 | 126.5 | 128.9 |
| Hexylbenzene | $C_{12}H_{18}$ | 0 | 53.94 | 54.35 | 69.4 | 83.2 | 94.4 | 103.8 | 111.7 | 118.4 | 124.2 | 129.2 | 133.5 | 137.2 | 140.4 | 143.2 |
| Heptylbenzene | $C_{13}H_{20}$ | 0 | 59.70 | 60.16 | 76.5 | 91.6 | 103.8 | 114.2 | 122.9 | 130.2 | 136.6 | 142.1 | 146.8 | 150.9 | 154.4 | 157.4 |
| Octylbenzene | $C_{14}H_{22}$ | 0 | 65.46 | 65.97 | 83.6 | 100.0 | 113.3 | 124.5 | 134.0 | 142.0 | 149.0 | 154.9 | 160.1 | 164.6 | 168.4 | 171.7 |
| Nonylbenzene | $C_{15}H_{24}$ | 0 | 71.22 | 71.78 | 90.8 | 108.5 | 122.8 | 134.9 | 145.1 | 153.8 | 161.4 | 167.8 | 173.4 | 178.2 | 182.4 | 185.9 |
| Decylbenzene | $C_{16}H_{26}$ | 0 | 76.98 | 77.59 | 97.9 | 116.9 | 132.2 | 145.3 | 156.3 | 165.6 | 173.7 | 180.6 | 186.7 | 191.9 | 196.4 | 200.2 |
| Undecylbenzene | $C_{17}H_{28}$ | 0 | 82.74 | 83.40 | 105.1 | 125.3 | 141.7 | 155.6 | 167.4 | 177.4 | 186.1 | 193.5 | 200.0 | 205.6 | 210.4 | 214.4 |
| Dodecylbenzene | $C_{18}H_{30}$ | 0 | 88.50 | 89.21 | 112.2 | 133.8 | 151.2 | 166.0 | 178.6 | 189.2 | 198.5 | 206.4 | 213.3 | 219.3 | 224.4 | 228.7 |
| Tridecylbenzene | $C_{19}H_{32}$ | 0 | 94.26 | 95.02 | 119.3 | 142.2 | 160.6 | 176.4 | 189.7 | 201.0 | 210.8 | 219.2 | 226.6 | 232.9 | 238.4 | 242.9 |
| Tetradecylbenzene | $C_{20}H_{34}$ | 0 | 100.02 | 100.83 | 126.5 | 150.6 | 170.1 | 186.7 | 200.8 | 212.8 | 223.2 | 232.1 | 239.8 | 246.6 | 252.3 | 257.2 |
| Pentadecylbenzene | $C_{21}H_{36}$ | 0 | 105.78 | 106.64 | 133.6 | 159.1 | 179.6 | 197.1 | 212.0 | 224.6 | 235.6 | 244.9 | 253.1 | 260.3 | 266.3 | 271.4 |
| Hexadecylbenzene | $C_{22}H_{38}$ | 0 | 111.54 | 112.45 | 140.7 | 167.5 | 189.0 | 207.5 | 223.1 | 236.4 | 248.0 | 257.8 | 266.4 | 273.9 | 280.3 | 285.7 |
| Increment per $CH_2$ group | | 0 | 5.760 | 5.810 | 7.13 | 8.44 | 9.47 | 10.37 | 11.14 | 11.79 | 12.37 | 12.86 | 13.29 | 13.67 | 13.99 | 14.25 |

[a] See footnote "a" of table 9.
[b] $C_p^\circ$ is the heat capacity at constant pressure of the given hydrocarbon in the thermodynamic standard gaseous state of unit fugacity (1 atmosphere) at the temperature indicated.

# IV. Heat of Formation, Free Energy of Formation, and Equilibrium Constant of Formation

## 1. Method and Data Used in the Calculations

The same method of calculation was used as described in Section IV–1 of reference [1].

For the heats of formation at 25° C of the alkylbenzenes in the gaseous state from the elements, solid carbon (graphite) and gaseous hydrogen, the values given in reference [2] were used.

## 2. Results

The resulting values of the thermodynamic properties for the formation of the 14 alkylbenzenes through $C_9H_{12}$, and of the higher normal monoalkylbenzenes, in the gaseous state, from the elements, solid carbon (graphite) and gaseous hydrogen, all at the given temperature, are presented in tables 19 to 24, which give values of the heat of formation, $\Delta Hf°$, the free energy of formation, $\Delta Ff°$, and the logarithm of the equilibrium constant of formation, $\log_{10} Kf$, to 1,500° $K$.

Figure 1 shows the thermodynamic stability of the normal monoalkylbenzenes in the gaseous state as a function of temperature, in the form of a plot of the standard free energy of formation per carbon atom, divided by the absolute temperature. This plot may be compared with corresponding plots for the normal paraffins [13], the normal 1-alkynes [15], and the normal 1-alkenes [24].

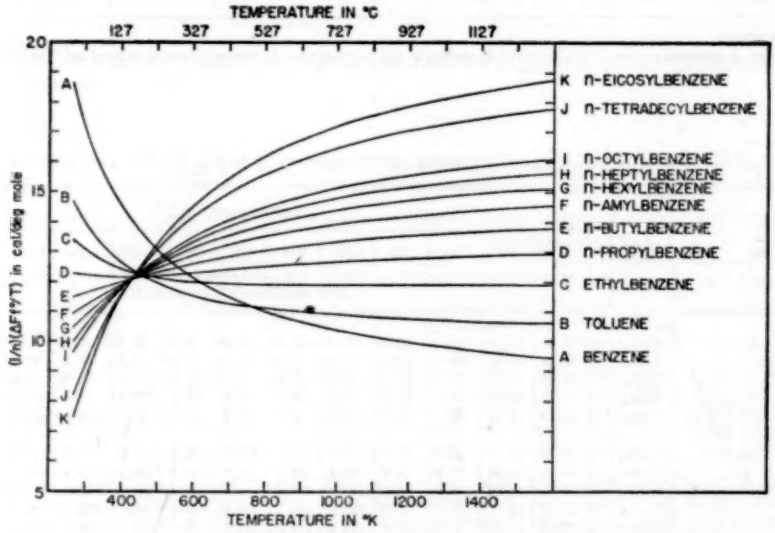


FIGURE 1.—*Thermodynamic stability of the normal monoalkylbenzenes in the gaseous state as a function of temperature.*

The scale of ordinates gives the value of $(1/n)(\Delta Ff°/T)$ in calories per degree mole, where $n$ is the number of carbon atoms per molecule, $T$ is the absolute temperature in degrees Kelvin, and $\Delta Ff°$ is the standard free energy of formation of the hydrocarbon from the elements, solid carbon (graphite) and gaseous hydrogen, all at the given temperature, as given in tables 15 and 16. The scale of abscissas gives the temperature in degrees Kelvin.

TABLE 19.—*Values* [a] *of the heat of formation, $\Delta Hf^\circ$, for the 14 alkylbenzenes, $C_6$ to $C_9$, for the ideal gaseous state, at 1,000 K*

| Compound (gas) | Formula | Temperature[a] in °K | | | | | | | | | | | | | |
|---|---|---|---|---|---|---|---|---|---|---|---|---|---|---|---|
| | | 0 | 298.16 | 300 | 400 | 500 | 600 | 700 | 800 | 900 | 1,000 | 1,100 | 1,200 | 1,300 | 1,400 | 1,500 |
| | | Heat of formation[b], $\Delta Hf^\circ$, in kcal/mole | | | | | | | | | | | | | | |
| Benzene | $C_6H_6$ | 24.000 | 19.820 | 19.796 | 18.554 | 17.536 | 16.711 | 16.040 | 15.510 | 15.100 | 14.818 | 14.63 | 14.52 | 14.45 | 14.41 | 14.39 |
| Methylbenzene (toluene) | $C_7H_8$ | 17.500 | 11.950 | 11.919 | 10.327 | 9.005 | 7.932 | 7.067 | 6.399 | 5.895 | 5.564 | 5.36 | 5.27 | 5.22 | 5.23 | 5.27 |
| Ethylbenzene | $C_8H_{10}$ | 13.917 | 7.120 | 7.083 | 5.218 | 3.699 | 2.488 | 1.529 | 0.798 | 0.266 | −0.061 | −0.28 | −0.28 | −0.26 | −0.18 | −0.05 |
| 1,2-Dimethylbenzene (o-xylene) | $C_8H_{10}$ | 11.096 | 4.540 | 4.506 | 2.711 | 1.189 | −0.062 | −1.076 | −1.858 | −2.434 | −2.799 | −3.01 | −3.08 | −3.09 | −3.04 | −2.92 |
| 1,3-Dimethylbenzene (m-xylene) | $C_8H_{10}$ | 10.926 | 4.120 | 4.083 | 2.175 | 0.571 | −.738 | −1.792 | −2.598 | −3.191 | −3.567 | −3.78 | −3.86 | −3.88 | −3.84 | −3.73 |
| 1,4-Dimethylbenzene (p-xylene) | $C_8H_{10}$ | 11.064 | 4.290 | 4.253 | 2.317 | .680 | −.665 | −1.751 | −2.586 | −3.207 | −3.607 | −3.84 | −3.94 | −3.97 | −3.94 | −3.84 |
| n-Propylbenzene | $C_9H_{12}$ | 9.810 | 1.870 | 1.827 | −0.31 | −2.06 | −3.44 | −4.52 | −5.34 | −5.95 | −6.30 | −6.5 | −6.5 | −6.4 | −6.2 | −6.0 |
| Isopropylbenzene (cumene) | $C_9H_{12}$ | 9.250 | 0.940 | 0.895 | −1.28 | −3.01 | −4.37 | −5.44 | −6.24 | −6.80 | −7.13 | −7.3 | −7.2 | −7.2 | −7.0 | −6.8 |
| 1-Methyl-2-ethylbenzene | $C_9H_{12}$ | 8.092 | .290 | .250 | −1.82 | −3.54 | −4.93 | −6.03 | −6.88 | −7.48 | −7.84 | −8.0 | −8.0 | −8.0 | −7.9 | −7.7 |
| 1-Methyl-3-ethylbenzene | $C_9H_{12}$ | 7.593 | −.460 | −.503 | −2.68 | −4.49 | −5.93 | −7.08 | −7.95 | −8.57 | −8.94 | −9.1 | −9.2 | −9.1 | −9.0 | −8.8 |
| 1-Methyl-4-ethylbenzene | $C_9H_{12}$ | 7.241 | −.780 | −.823 | −3.03 | −4.87 | −6.35 | −7.53 | −8.43 | −9.08 | −9.47 | −9.7 | −9.7 | −9.7 | −9.6 | −9.4 |
| 1, 2, 3-Trimethylbenzene (hemimellitene) | $C_9H_{12}$ | 5.527 | −2.290 | −2.332 | −4.57 | −6.46 | −8.04 | −9.31 | −10.30 | −11.04 | −11.51 | −11.8 | −11.9 | −11.9 | −11.8 | −11.7 |
| 1, 2, 4-Trimethylbenzene (pseudocumene) | $C_9H_{12}$ | 4.468 | −3.330 | −3.372 | −5.59 | −7.46 | −9.02 | −10.28 | −11.26 | −11.98 | −12.45 | −12.7 | −12.8 | −12.8 | −12.7 | −12.6 |
| 1, 3, 5-Trimethylbenzene (Mesitylene) | $C_9H_{12}$ | 4.241 | −3.840 | −3.883 | −6.183 | −8.107 | −9.601 | −10.960 | −11.930 | −12.643 | −13.094 | −13.34 | −13.42 | −13.42 | −13.33 | −13.18 |

[a] See footnote a of table 9.

[b] $\Delta Hf^\circ$ represents the increment in heat content for the reaction of forming the given compound in the gaseous state from the elements carbon (solid graphite) and hydrogen (gaseous), with all the reactants and products in their appropriate standard reference states at the temperature indicated.

TABLE 20.—*Values [a] of the heat of formation, $\Delta Hf°$, for the normal alkylbenzenes, $C_6$ to $C_{22}$, for the ideal gaseous state, to 1,500° K*

| Compound (gas) | Formula | Temperature [a] in °K | | | | | | | | | | | | | |
|---|---|---|---|---|---|---|---|---|---|---|---|---|---|---|---|
| | | 0 | 298.16 | 300 | 400 | 500 | 600 | 700 | 800 | 900 | 1,000 | 1,100 | 1,200 | 1,300 | 1,400 | 1,500 |
| | | Heat of formation, [b] $\Delta Hf°$, in kcal/mole | | | | | | | | | | | | | | |
| Benzene | $C_6H_6$ | 24.000 | 19.820 | 19.796 | 18.554 | 17.536 | 16.711 | 16.040 | 15.510 | 15.100 | 14.818 | 14.63 | 14.52 | 14.45 | 14.41 | 14.39 |
| Methylbenzene (toluene) | $C_7H_8$ | 17.500 | 11.950 | 11.919 | 10.327 | 9.005 | 7.932 | 7.067 | 6.399 | 5.895 | 5.564 | 5.36 | 5.27 | 5.22 | 5.23 | 5.27 |
| Ethylbenzene | $C_8H_{10}$ | 13.917 | 7.120 | 7.083 | 5.218 | 3.699 | 2.488 | 1.529 | 0.798 | 0.266 | −0.061 | −0.23 | −0.28 | −0.26 | −0.18 | −0.05 |
| *n*-Propylbenzene | $C_9H_{12}$ | 9.810 | 1.870 | 1.827 | −0.31 | −2.06 | −3.44 | −4.52 | −5.34 | −5.95 | −6.30 | −6.5 | −6.5 | −6.4 | −6.2 | −6.0 |
| *n*-Butylbenzene | $C_{10}H_{14}$ | 5.89 | −3.30 | −3.35 | −5.78 | −7.78 | −9.34 | −10.56 | −11.48 | −12.14 | −12.49 | −12.6 | −12.6 | −12.5 | −12.3 | −12.0 |
| *n*-Amylbenzene | $C_{11}H_{16}$ | 2.22 | −8.23 | −8.28 | −11.00 | −13.24 | −14.99 | −16.34 | −17.35 | −18.07 | −18.43 | −18.6 | −18.5 | −18.3 | −18.0 | −17.7 |
| *n*-Hexylbenzene | $C_{12}H_{18}$ | −1.46 | −13.15 | −13.21 | −16.23 | −18.71 | −20.64 | −22.12 | −23.22 | −23.99 | −24.37 | −24.5 | −24.4 | −24.1 | −23.8 | −23.4 |
| *n*-Heptylbenzene | $C_{13}H_{20}$ | −5.13 | −18.08 | −18.14 | −21.45 | −24.18 | −26.28 | −27.89 | −29.09 | −29.92 | −30.31 | −30.4 | −30.3 | −30.0 | −29.5 | −29.0 |
| *n*-Octylbenzene | $C_{14}H_{22}$ | −8.80 | −23.00 | −23.07 | −26.67 | −29.64 | −31.93 | −33.67 | −34.96 | −35.85 | −36.25 | −36.4 | −36.2 | −35.8 | −35.3 | −34.7 |
| *n*-Nonylbenzene | $C_{15}H_{24}$ | −12.48 | −27.93 | −28.00 | −31.90 | −35.10 | −37.58 | −39.45 | −40.84 | −41.78 | −42.20 | −42.3 | −42.0 | −41.6 | −41.1 | −40.4 |
| *n*-Decylbenzene | $C_{16}H_{26}$ | −16.15 | −32.86 | −32.94 | −37.12 | −40.57 | −43.23 | −45.23 | −46.71 | −47.70 | −48.14 | −48.2 | −47.9 | −47.5 | −46.8 | −46.1 |
| *n*-Undecylbenzene | $C_{17}H_{28}$ | −19.82 | −37.78 | −37.87 | −42.34 | −46.04 | −48.88 | −51.01 | −52.58 | −53.63 | −54.08 | −54.1 | −53.8 | −53.3 | −52.6 | −51.8 |
| *n*-Dodecylbenzene | $C_{18}H_{30}$ | −23.49 | −42.71 | −42.80 | −47.56 | −51.50 | −54.52 | −56.78 | −58.45 | −59.56 | −60.02 | −60.1 | −59.7 | −59.1 | −58.3 | −57.5 |
| *n*-Tridecylbenzene | $C_{19}H_{32}$ | −27.17 | −47.63 | −47.73 | −52.79 | −56.96 | −60.17 | −62.56 | −64.32 | −65.48 | −65.96 | −66.0 | −65.6 | −65.0 | −64.1 | −63.2 |
| *n*-Tetradecylbenzene | $C_{20}H_{34}$ | −30.84 | −52.56 | −52.66 | −58.01 | −62.43 | −65.82 | −68.34 | −70.19 | −71.41 | −71.90 | −71.9 | −71.5 | −70.8 | −69.8 | −68.9 |
| *n*-Pentadecylbenzene | $C_{21}H_{36}$ | −34.51 | −57.49 | −57.59 | −63.23 | −67.90 | −71.47 | −74.12 | −76.06 | −77.34 | −77.84 | −77.8 | −77.4 | −76.6 | −75.6 | −74.6 |
| *n*-Hexadecylbenzene | $C_{22}H_{38}$ | −38.19 | −62.41 | −62.52 | −68.46 | −73.36 | −77.12 | −79.90 | −81.93 | −83.26 | −83.78 | −83.8 | −83.2 | −82.4 | −81.4 | −80.3 |
| Increment per $CH_2$ group | ..... | −3.673 | −4.926 | −4.931 | −5.223 | −5.465 | −5.648 | −5.778 | −5.871 | −5.927 | −5.941 | −5.93 | −5.89 | −5.83 | −5.76 | −5.69 |

[a] See footnote "a" of table 9.

[b] $\Delta Hf°$ represents the increment in heat content for the reaction of forming the given compound in the gaseous state from the elements carbon (solid, graphite) and hydrogen (gaseous), with all the reactants and products in their appropriate standard reference states at the temperature indicated.

70206—46—6

TABLE 21.—Values of the free energy of formation, $\Delta Ff^\circ$, for the 21 alkylbenzenes, $C_6$ to $C_{12}$, for the ideal gaseous state, to 1,500° K

| Compound (gas) | Formula | Temperature[a] in °K | | | | | | | | | | | | | |
|---|---|---|---|---|---|---|---|---|---|---|---|---|---|---|---|
| | | 0 | 298.16 | 300 | 400 | 500 | 600 | 700 | 800 | 900 | 1,000 | 1,100 | 1,200 | 1,300 | 1,400 | 1,500 |
| | | Free energy of formation,[b] $\Delta Ff^\circ$, in kcal/mole | | | | | | | | | | | | | | |
| Benzene | $C_6H_6$ | 24.000 | 30.989 | 31.058 | 35.008 | 39.242 | 43.663 | 48.211 | 52.838 | 57.537 | 62.270 | 67.02 | 71.79 | 76.57 | 81.34 | 86.11 |
| Methylbenzene (toluene) | $C_7H_8$ | 17.500 | 29.228 | 29.335 | 35.390 | 41.811 | 48.477 | 55.306 | 62.236 | 69.255 | 76.320 | 83.40 | 90.50 | 97.61 | 104.71 | 111.81 |
| Ethylbenzene | $C_8H_{10}$ | 13.917 | 31.208 | 31.357 | 39.741 | 48.554 | 57.646 | 66.921 | 76.302 | 85.779 | 95.303 | 104.84 | 114.39 | 123.95 | 133.48 | 143.02 |
| 1,2-Dimethylbenzene (o-xylene) | $C_8H_{10}$ | 11.096 | 29.177 | 29.329 | 37.883 | 46.852 | 56.103 | 65.548 | 75.110 | 84.777 | 94.494 | 104.23 | 113.99 | 123.76 | 133.50 | 143.24 |
| 1,3-Dimethylbenzene (m-xylene) | $C_8H_{10}$ | 10.926 | 28.405 | 28.554 | 37.008 | 45.906 | 55.099 | 64.492 | 74.006 | 83.630 | 93.307 | 103.00 | 112.72 | 122.45 | 132.15 | 141.85 |
| 1,4-Dimethylbenzene (p-xylene) | $C_8H_{10}$ | 11.064 | 28.952 | 29.104 | 37.688 | 46.724 | 56.060 | 65.604 | 75.275 | 85.058 | 94.897 | 104.76 | 114.64 | 124.54 | 134.40 | 144.27 |
| n-Propylbenzene | $C_9H_{12}$ | 9.810 | 32.810 | 33.000 | 43.73 | 54.94 | 66.48 | 78.22 | 90.09 | 102.07 | 114.08 | 126.1 | 138.2 | 150.3 | 162.3 | 174.3 |
| Isopropylbenzene (cumene) | $C_9H_{12}$ | 9.250 | 32.738 | 32.934 | 43.96 | 55.46 | 67.29 | 79.33 | 91.48 | 103.74 | 116.06 | 128.4 | 140.7 | 153.1 | 165.4 | 177.6 |
| 1-Methyl-2-ethylbenzene | $C_9H_{12}$ | 8.092 | 31.323 | 31.514 | 42.26 | 53.48 | 65.02 | 76.78 | 88.65 | 100.64 | 112.67 | 124.7 | 136.8 | 148.9 | 160.9 | 173.0 |
| 1-Methyl-3-ethylbenzene | $C_9H_{12}$ | 7.593 | 30.217 | 30.406 | 41.05 | 52.20 | 63.68 | 75.38 | 87.20 | 99.14 | 111.14 | 123.2 | 135.2 | 147.2 | 159.2 | 171.2 |
| 1-Methyl-4-ethylbenzene | $C_9H_{12}$ | 7.241 | 30.281 | 30.472 | 41.25 | 52.54 | 64.16 | 76.02 | 88.00 | 100.10 | 112.26 | 124.4 | 136.6 | 148.8 | 161.0 | 173.2 |
| 1,2,3-Trimethylbenzene (hemimellitene) | $C_9H_{12}$ | 5.527 | 29.319 | 29.513 | 40.56 | 52.06 | 63.91 | 76.01 | 88.26 | 100.63 | 113.07 | 125.5 | 138.0 | 150.6 | 163.0 | 175.5 |
| 1,2,4-Trimethylbenzene (pseudocumene) | $C_9H_{12}$ | 4.468 | 27.912 | 28.104 | 39.02 | 50.39 | 62.11 | 74.07 | 86.17 | 98.41 | 110.71 | 123.0 | 135.4 | 147.8 | 160.1 | 172.4 |
| 1,3,5-Trimethylbenzene (mesitylene) | $C_9H_{12}$ | 4.241 | 28.172 | 28.369 | 39.558 | 51.223 | 63.237 | 75.495 | 87.903 | 100.443 | 113.045 | 125.67 | 138.32 | 150.98 | 163.60 | 176.23 |

[a] See footnote "a" of table 9.

[b] $\Delta Ff^\circ$ represents the increment in free energy for the reaction of forming the given compound in the gaseous state from the elements carbon (solid, graphite) and hydrogen (gaseous), with all the reactants and products in their appropriate standard reference states at the temperature indicated.

TABLE 22.—*Values* [a] *of the free energy of formation, $\Delta Ff°$, for the normal alkylbenzenes, $C_6$ to $C_{22}$, for the ideal gaseous state, to 1,500° K*

| Compound (gas) | Formula | Temperature [a] in °K | | | | | | | | | | | | | |
|---|---|---|---|---|---|---|---|---|---|---|---|---|---|---|---|
| | | 0 | 298.16 | 300 | 400 | 500 | 600 | 700 | 800 | 900 | 1,000 | 1,100 | 1,200 | 1,300 | 1,400 | 1,500 |
| | | Free energy of formation, [b] $\Delta Ff°$, in kcal/mole | | | | | | | | | | | | | | |
| Benzene | $C_6H_6$ | 24.000 | 30.989 | 31.058 | 35.008 | 39.242 | 43.663 | 48.211 | 52.838 | 57.537 | 62.270 | 67.02 | 71.79 | 76.57 | 81.34 | 86.11 |
| Methylbenzene (toluene) | $C_7H_8$ | 17.500 | 29.228 | 29.335 | 35.390 | 41.811 | 48.477 | 55.306 | 62.236 | 69.255 | 76.320 | 83.40 | 90.50 | 97.61 | 104.71 | 111.81 |
| Ethylbenzene | $C_8H_{10}$ | 13.917 | 31.208 | 31.357 | 39.741 | 48.554 | 57.646 | 66.921 | 76.302 | 85.779 | 95.303 | 104.84 | 114.39 | 123.95 | 133.48 | 143.02 |
| n-Propylbenzene | $C_9H_{12}$ | 9.810 | 32.810 | 33.000 | 43.73 | 54.94 | 66.48 | 78.22 | 90.09 | 102.07 | 114.08 | 126.1 | 138.2 | 150.3 | 162.3 | 174.3 |
| n-Butylbenzene | $C_{10}H_{14}$ | 5.89 | 34.62 | 34.86 | 47.98 | 61.65 | 75.70 | 89.97 | 104.38 | 118.90 | 133.48 | 148.1 | 162.7 | 177.3 | 191.9 | 206.5 |
| n-Amylbenzene | $C_{11}H_{16}$ | 2.22 | 36.67 | 36.95 | 52.46 | 68.58 | 85.13 | 101.92 | 118.86 | 135.93 | 153.06 | 170.2 | 187.4 | 204.5 | 221.7 | 238.8 |
| n-Hexylbenzene | $C_{12}H_{18}$ | −1.46 | 38.72 | 39.04 | 56.94 | 75.51 | 94.56 | 113.87 | 133.35 | 152.96 | 172.64 | 192.3 | 212.0 | 231.8 | 251.4 | 271.1 |
| n-Heptylbenzene | $C_{13}H_{20}$ | −5.13 | 40.76 | 41.13 | 61.42 | 82.44 | 103.98 | 125.82 | 147.83 | 169.99 | 192.22 | 214.4 | 236.7 | 259.0 | 281.2 | 303.5 |
| n-Octylbenzene | $C_{14}H_{22}$ | −8.80 | 42.81 | 43.22 | 65.90 | 89.37 | 113.41 | 137.77 | 162.32 | 187.02 | 211.80 | 236.5 | 261.4 | 286.2 | 311.0 | 335.8 |
| n-Nonylbenzene | $C_{15}H_{24}$ | −12.48 | 44.86 | 45.31 | 70.38 | 96.30 | 122.84 | 149.72 | 176.80 | 204.04 | 231.38 | 258.7 | 286.0 | 313.4 | 340.7 | 368.1 |
| n-Decylbenzene | $C_{16}H_{26}$ | −16.15 | 46.91 | 47.40 | 74.85 | 103.24 | 132.27 | 161.68 | 191.28 | 221.07 | 250.95 | 280.8 | 310.7 | 340.6 | 370.5 | 400.5 |
| n-Undecylbenzene | $C_{17}H_{28}$ | −19.82 | 48.96 | 49.49 | 79.33 | 110.17 | 141.70 | 173.63 | 205.77 | 238.10 | 270.53 | 302.9 | 335.4 | 367.8 | 400.2 | 432.8 |
| n-Dodecylbenzene | $C_{18}H_{30}$ | 23.49 | 51.00 | 51.58 | 83.81 | 117.10 | 151.12 | 185.58 | 220.25 | 255.13 | 290.11 | 325.0 | 360.0 | 395.0 | 430.0 | 465.1 |
| n-Tridecylbenzene | $C_{19}H_{32}$ | −27.17 | 53.05 | 53.67 | 88.29 | 124.03 | 160.55 | 197.53 | 234.74 | 272.16 | 309.69 | 347.1 | 384.7 | 422.3 | 459.8 | 497.4 |
| n-Tetradecylbenzene | $C_{20}H_{34}$ | −30.84 | 55.10 | 55.76 | 92.77 | 130.96 | 169.98 | 209.48 | 249.22 | 289.19 | 329.27 | 369.2 | 409.4 | 449.5 | 489.5 | 529.8 |
| n-Pentadecylbenzene | $C_{21}H_{36}$ | −34.51 | 57.15 | 57.85 | 97.25 | 137.89 | 179.41 | 221.43 | 263.70 | 306.22 | 348.85 | 391.4 | 434.0 | 476.7 | 519.3 | 562.1 |
| n-Hexadecylbenzene | $C_{22}H_{38}$ | −38.19 | 59.20 | 59.94 | 101.73 | 144.82 | 188.84 | 233.38 | 278.19 | 323.25 | 368.43 | 413.5 | 458.7 | 503.9 | 549.1 | 594.4 |
| Increment per $CH_2$ group | | −3.673 | 2.048 | 2.090 | 4.479 | 6.931 | 9.428 | 11.951 | 14.484 | 17.029 | 19.579 | 22.12 | 24.67 | 27.22 | 29.76 | 32.33 |

[a] See footnote "a" of table 9.

[b] $\Delta Ff°$ represents the increment in free energy for the reaction of forming the given compound in the gaseous state from the elements carbon (solid, graphite) and hydrogen (gaseous), with all the reactants and products in their appropriate standard reference states at the temperature indicated.

TABLE 23.—*Values* [a] *of the logarithm of the equilibrium constant of formation, log 10 Kf, for the 14 alkylbenzenes, $C_6$ to $C_{22}$, for the ideal gaseous state, to 1,500° K*

| Compound (gas) | Formula | Temperature [a] in °K | | | | | | | | | | | | | |
|---|---|---|---|---|---|---|---|---|---|---|---|---|---|---|---|
| | | 0 | 298.16 | 300 | 400 | 500 | 600 | 700 | 800 | 900 | 1,000 | 1,100 | 1,200 | 1,300 | 1,400 | 1,500 |
| | | Logarithm of equilibrium constant of formation, [b] log 10 Kf | | | | | | | | | | | | | | |
| Benzene | $C_6H_6$ | 17.592 | 22.715 | 22.765 | 25.662 | 28.760 | 31.997 | 35.338 | 38.732 | 42.161 | 45.643 | 49.16 | 52.64 | 56.13 | 59.62 | 63.11 |
| Methylbenzene (toluene) | $C_7H_8$ | 12.824 | 21.422 | 21.501 | 25.934 | 30.646 | 35.537 | 40.536 | 45.611 | 50.750 | 55.943 | 61.18 | 66.43 | 71.52 | 76.78 | 81.94 |
| Ethylbenzene | $C_8H_{10}$ | 10.199 | 22.872 | 22.987 | 29.126 | 35.585 | 42.243 | 49.045 | 55.894 | 62.850 | 69.850 | 76.86 | 83.87 | 90.89 | 97.85 | 104.86 |
| n-Propylbenzene | $C_9H_{12}$ | 7.189 | 24.048 | 24.192 | 32.04 | 40.26 | 48.72 | 57.32 | 66.03 | 74.82 | 83.64 | 92.5 | 101.2 | 110.2 | 119.0 | 127.7 |
| n-Butylbenzene | $C_{10}H_{14}$ | 4.317 | 25.220 | 25.549 | 35.16 | 45.18 | 55.46 | 65.93 | 76.49 | 87.14 | 97.87 | 108.6 | 119.3 | 130.0 | 140.7 | 151.4 |
| n-Amylbenzene | $C_{11}H_{16}$ | 1.627 | 26.867 | 27.069 | 38.44 | 50.27 | 62.40 | 74.70 | 87.10 | 99.61 | 112.2 | 124.8 | 137.4 | 150.0 | 162.6 | 175.1 |
| n-Hexylbenzene | $C_{12}H_{18}$ | −1.070 | 28.364 | 28.605 | 41.72 | 55.33 | 69.29 | 83.48 | 97.74 | 112.1 | 126.5 | 140.9 | 155.3 | 169.8 | 184.2 | 198.6 |
| n-Heptylbenzene | $C_{13}H_{20}$ | −3.762 | 29.860 | 30.141 | 45.01 | 60.41 | 76.20 | 92.21 | 108.3 | 124.5 | 140.8 | 157.1 | 173.4 | 189.7 | 206.0 | 222.3 |
| n-Octylbenzene | $C_{14}H_{22}$ | −6.451 | 31.361 | 31.677 | 48.29 | 65.48 | 83.09 | 100.9 | 118.9 | 137.0 | 155.2 | 173.4 | 191.6 | 209.8 | 228.0 | 246.2 |
| n-Nonylbenzene | $C_{15}H_{24}$ | −9.145 | 32.863 | 33.213 | 51.57 | 70.55 | 89.97 | 109.7 | 129.6 | 149.5 | 169.6 | 189.6 | 209.6 | 229.7 | 249.7 | 269.7 |
| n-Decylbenzene | $C_{16}H_{26}$ | −11.84 | 34.369 | 34.749 | 54.85 | 75.62 | 96.85 | 118.4 | 140.1 | 161.9 | 183.8 | 205.7 | 227.6 | 249.5 | 271.4 | 293.3 |
| n-Undecylbenzene | $C_{17}H_{28}$ | −14.53 | 35.868 | 36.285 | 58.13 | 80.70 | 103.7 | 127.2 | 150.7 | 174.4 | 198.1 | 221.9 | 245.6 | 269.4 | 293.2 | 317.0 |
| n-Dodecylbenzene | $C_{18}H_{30}$ | −17.22 | 37.374 | 37.821 | 61.41 | 85.77 | 110.6 | 135.9 | 161.3 | 186.9 | 212.6 | 238.3 | 264.0 | 289.8 | 315.5 | 341.3 |
| n-Tridecylbenzene | $C_{19}H_{32}$ | −19.91 | 38.879 | 39.357 | 64.69 | 90.85 | 117.4 | 144.6 | 171.9 | 199.4 | 227.0 | 254.6 | 282.3 | 310.0 | 337.8 | 365.5 |
| n-Tetradecylbenzene | $C_{20}H_{34}$ | −22.60 | 40.385 | 40.893 | 67.97 | 95.93 | 124.2 | 153.2 | 182.5 | 212.0 | 241.6 | 271.3 | 301.0 | 330.8 | 360.5 | 390.3 |
| n-Pentadecylbenzene | $C_{21}H_{36}$ | −25.29 | 41.890 | 42.429 | 71.25 | 101.0 | 131.0 | 161.8 | 192.8 | 224.0 | 255.2 | 286.5 | 317.8 | 349.1 | 380.4 | 411.7 |
| n-Hexadecylbenzene | $C_{22}H_{38}$ | −27.98 | 43.396 | 43.965 | 74.53 | 106.1 | 137.8 | 170.4 | 203.2 | 236.1 | 269.2 | 302.2 | 335.4 | 368.5 | 401.7 | 434.9 |
| Increment per $CH_2$ group | | −2.692 | 1.500 | 1.532 | 3.282 | 5.078 | 6.907 | 8.759 | 10.61 | 12.47 | 14.34 | 16.20 | 18.07 | 19.94 | 21.80 | 23.68 |

[a] See footnote "a" of table 9.

[b] $\log_{10} Kf$ represents the logarithm of the equilibrium constant for the reaction of forming the given compound in the gaseous state from the elements carbon (solid, graphite) and hydrogen (gaseous), with all the reactants and products in their appropriate standard reference states at the temperature indicated.

TABLE 23.—*Values* [a] *of the logarithm of the equilibrium constant of formation, log* $_{10}$ *Kf, for the 14 alkylbenzenes,* $C_6$ *to* $C_9$, *for the ideal gaseous state, to 1,500° K*

| Compound (gas) | Formula | Temperature [a] in °K | | | | | | | | | | | | | |
|---|---|---|---|---|---|---|---|---|---|---|---|---|---|---|---|
| | | 0 | 298.16 | 300 | 400 | 500 | 600 | 700 | 800 | 900 | 1,000 | 1,100 | 1,200 | 1,300 | 1,400 | 1,500 |
| | | Logarithm of equilibrium constant of formation,[b] $\log_{10} Kf$ | | | | | | | | | | | | | | |
| Benzene | $C_6H_6$ | −∞ | −22.7143 | −22.6252 | −19.1271 | −17.1521 | −15.9040 | −15.0519 | −14.4345 | −13.9716 | −13.6088 | −13.3153 | −13.0738 | −12.8717 | −12.6971 | −12.5461 |
| Methylbenzene (toluene) | $C_7H_8$ | ...do... | −21.4236 | −21.3696 | −19.3356 | −18.2752 | −17.6574 | −17.2671 | −17.0018 | −16.8171 | −16.6794 | −16.5699 | −16.4825 | −16.4102 | −16.3455 | −16.2900 |
| Ethylbenzene | $C_8H_{10}$ | ...do... | −22.8750 | −22.8428 | −21.7132 | −21.2223 | −20.9072 | −20.8934 | −20.8442 | −20.8206 | −20.8281 | −20.8294 | −20.8333 | −20.8358 | −20.8362 | −20.8375 |
| 1, 2-Dimethylbenzene (o-xylene) | $C_8H_{10}$ | ...do... | −21.3860 | −21.3655 | −20.6980 | −20.4786 | −20.4351 | −20.4646 | −20.5188 | −20.5864 | −20.6513 | −20.7081 | −20.7601 | −20.8051 | −20.8399 | −20.8692 |
| 1, 3-Dimethylbenzene (m-xylene) | $C_8H_{10}$ | ...do... | −20.8202 | −20.8014 | −20.2201 | −20.0651 | −20.0693 | −20.1349 | −20.2172 | −20.3077 | −20.3919 | −20.4646 | −20.5296 | −20.5853 | −20.6290 | −20.6670 |
| 1, 4-Dimethylbenzene (p-xylene) | $C_8H_{10}$ | ...do... | −21.2214 | −21.2018 | −20.5912 | −20.4227 | −20.4194 | −20.4821 | −20.5638 | −20.6545 | −20.7393 | −20.8128 | −20.8788 | −20.9358 | −20.9808 | −21.0202 |
| n-Propylbenzene | $C_9H_{12}$ | ...do... | −24.040 | −24.040 | −23.894 | −24.012 | −24.215 | −24.422 | −24.610 | −24.785 | −24.932 | −25.056 | −25.168 | −25.262 | −25.336 | −25.395 |
| Isopropylbenzene (cumene) | $C_9H_{12}$ | ...do... | −23.996 | −23.992 | −24.016 | −24.241 | −24.510 | −24.768 | −24.991 | −25.192 | −25.364 | −25.509 | −25.631 | −25.732 | −25.812 | −25.880 |
| 1-Methyl-2-ethylbenzene | $C_9H_{12}$ | ...do... | −22.960 | −22.958 | −23.090 | −23.377 | −23.684 | −23.970 | −24.218 | −24.437 | −24.624 | −24.780 | −24.914 | −25.027 | −25.119 | −25.199 |
| 1-Methyl-3-ethylbenzene | $C_9H_{12}$ | ...do... | −22.149 | −22.150 | −22.428 | −22.816 | −23.194 | −23.533 | −23.822 | −24.075 | −24.289 | −24.468 | −24.620 | −24.749 | −24.853 | −24.945 |
| 1-Methyl-4-ethylbenzene | $C_9H_{12}$ | ...do... | −22.195 | −22.198 | −22.537 | −22.964 | −23.371 | −23.733 | −24.040 | −24.308 | −24.535 | −24.723 | −24.885 | −25.021 | −25.133 | −25.232 |
| 1, 2, 3-Trimethylbenzene (hemimellitene) | $C_9H_{12}$ | ...do... | −21.490 | −21.500 | −22.159 | −22.754 | −23.279 | −23.731 | −24.110 | −24.436 | −24.712 | −24.942 | −25.140 | −25.310 | −25.450 | −25.571 |
| 1, 2, 4-Trimethylbenzene (pseudocumene) | $C_9H_{12}$ | ...do... | −20.459 | −20.473 | −21.319 | −22.025 | −22.622 | −23.124 | −23.541 | −23.897 | −24.196 | −24.445 | −24.657 | −24.839 | −24.990 | −25.121 |
| 1, 3, 5-Trimethylbenzene (mesitylene) | $C_9H_{12}$ | ...do... | −20.6497 | −20.6666 | −21.6131 | −22.3891 | −23.0336 | −23.5702 | −24.0136 | −24.3904 | −24.7055 | −24.9678 | −25.1916 | −25.3815 | −25.5390 | −25.6761 |

[a] See footnote "a" in table 9.

[b] Log $_{10}$ *Kf* represents the logarithm (to the base 10) of the equilibrium constant for the reaction of forming the given compound in the gaseous state from the elements carbon (solid, graphite) and hydrogen (gaseous), with all the reactants and products in their appropriate standard reference states at the temperature indicated. Log $_{10}$ $Kf = -\Delta Ff^\circ/0.00457566\,T$; $\Delta Ff^\circ$ in kcal/mole, $T$ in °K.

TABLE 24.—*Values* [a] *of the logarithm of the equilibrium constant of formation, $\log_{10} Kf$, for the normal alkylbenzenes, $C_6$ to $C_{22}$, for the ideal gaseous state, to 1,500° K*

| Compound (gas) | Formula | Temperature [a] in °K | | | | | | | | | | | | | | |
|---|---|---|---|---|---|---|---|---|---|---|---|---|---|---|---|---|
| | | 0 | 298.16 | 300 | 400 | 500 | 600 | 700 | 800 | 900 | 1,000 | 1,100 | 1,200 | 1,300 | 1,400 | 1,500 |
| | | Logarithm of equilibrium constant of formation, [b] $\log_{10} Kf$ | | | | | | | | | | | | | | |
| Benzene | $C_6H_6$ | −∞ | −22.7143 | −22.6252 | −19.1271 | −17.1521 | −15.9040 | −15.0519 | −14.4345 | −13.9716 | −13.6088 | −13.3153 | −13.0738 | −12.8717 | −12.6971 | −12.5461 |
| Methylbenzene (toluene) | $C_7H_8$ | do | −21.4236 | −21.3698 | −19.3356 | −18.2752 | −17.6574 | −17.2671 | −17.0018 | −16.8171 | −16.6794 | −16.5699 | −16.4825 | −16.4102 | −16.3455 | −16.2900 |
| Ethylbenzene | $C_8H_{10}$ | do | −22.8750 | −22.8428 | −21.7132 | −21.2223 | −20.9972 | −20.8934 | −20.8442 | −20.8296 | −20.8281 | −20.8294 | −20.8333 | −20.8308 | −20.8362 | −20.8375 |
| *n*-Propylbenzene | $C_9H_{12}$ | do | −24.049 | −24.040 | −23.894 | −24.012 | −24.215 | −24.422 | −24.610 | −24.785 | −24.932 | −25.056 | −25.168 | −25.262 | −25.336 | −25.395 |
| *n*-Butylbenzene | $C_{10}H_{14}$ | do | −25.374 | −25.392 | −26.212 | −26.948 | −27.572 | −28.090 | −28.515 | −28.873 | −29.171 | −29.419 | −29.631 | −29.811 | −29.957 | −30.082 |
| *n*-Amylbenzene | $C_{11}H_{16}$ | do | −26.876 | −26.914 | −28.660 | −29.977 | −31.006 | −31.822 | −32.472 | −33.008 | −33.450 | −33.813 | −34.124 | −34.386 | −34.604 | −34.793 |
| *n*-Hexylbenzene | $C_{12}H_{18}$ | do | −28.377 | −28.437 | −31.107 | −33.007 | −34.440 | −35.553 | −36.429 | −37.144 | −37.729 | −38.208 | −38.616 | −38.961 | −39.250 | −39.504 |
| *n*-Heptylbenzene | $C_{13}H_{20}$ | do | −29.878 | −29.959 | −33.554 | −36.036 | −37.874 | −39.284 | −40.386 | −41.279 | −42.008 | −42.602 | −43.109 | −43.536 | −43.896 | −44.214 |
| *n*-Octylbenzene | $C_{14}H_{22}$ | do | −31.379 | −31.482 | −36.001 | −39.066 | −41.309 | −43.015 | −44.343 | −45.414 | −46.287 | −46.996 | −47.602 | −48.112 | −48.542 | −48.925 |
| *n*-Nonylbenzene | $C_{15}H_{24}$ | do | −32.880 | −33.004 | −38.448 | −42.095 | −44.743 | −46.746 | −48.209 | −49.549 | −50.566 | −51.391 | −52.094 | −52.687 | −53.189 | −53.635 |
| *n*-Decylbenzene | $C_{16}H_{26}$ | do | −34.382 | −34.527 | −40.896 | −45.125 | −48.177 | −50.478 | −52.256 | −53.684 | −54.845 | −55.785 | −56.587 | −57.262 | −57.835 | −58.346 |
| *n*-Undecylbenzene | $C_{17}H_{28}$ | do | −35.883 | −36.050 | −43.343 | −48.154 | −51.611 | −54.209 | −56.213 | −57.820 | −59.124 | −60.180 | −61.080 | −61.837 | −62.481 | −63.057 |
| *n*-Dodecylbenzene | $C_{18}H_{30}$ | do | −37.384 | −37.572 | −45.790 | −51.184 | −55.045 | −57.940 | −60.170 | −61.955 | −63.403 | −64.574 | −65.572 | −66.412 | −67.128 | −67.767 |
| *n*-Tridecylbenzene | $C_{19}H_{32}$ | do | −38.885 | −39.095 | −48.237 | −54.213 | −58.479 | −61.671 | −64.127 | −66.090 | −67.682 | −68.968 | −70.065 | −70.988 | −71.774 | −72.478 |
| *n*-Tetradecylbenzene | $C_{20}H_{34}$ | do | −40.386 | −40.618 | −50.684 | −57.243 | −61.913 | −65.402 | −68.083 | −70.225 | −71.961 | −73.353 | −74.557 | −76.563 | −76.420 | −77.188 |
| *n*-Pentadecylbenzene | $C_{21}H_{36}$ | do | −41.888 | −42.140 | −53.132 | −60.272 | −65.347 | −69.134 | −72.040 | −74.360 | −76.240 | −77.757 | −79.050 | −80.138 | −81.066 | −81.899 |
| *n*-Hexadecylbenzene | $C_{22}H_{38}$ | do | −43.389 | −43.663 | −55.579 | −63.302 | −68.781 | −72.865 | −75.997 | −78.496 | −80.519 | −82.152 | −83.542 | −84.713 | −85.713 | −86.610 |
| Increment per $CH_2$ group | | do | −1.5012 | −1.5226 | −2.4472 | −3.0295 | −3.4341 | −3.7312 | −3.9568 | −4.1352 | −4.2790 | −4.3944 | −4.4926 | −4.5782 | −4.6463 | −4.7106 |

[a] See footnote "a" of table 9.

[b] Log $_{10}$ $Kf$ represents the logarithm (to the base 10) of the equilibrium constant for the reaction of forming the given compound in the gaseous state from the elements carbon (solid, graphite) and hydrogen (gaseous), with all the reactants and products in their appropriate standard reference states at the temperature indicated. Log $_{10}$ $Kf = -\Delta Ff°/0.00457566\,T$; $\Delta Ff°$ in kcal/mole, $T$ in °K.

# V. Free Energies and Equilibria of Isomerization

From the values in table 21 and 23, calculations are made of the values of the free energies and equilibrium constants for the isomerization of the $C_8H_{10}$ and the $C_9H_{12}$ alkylbenzenes, according to the reactions

$C_8H_{10}$ (ethylbenzene, gas)$=C_8H_{10}$ (isomeric alkylbenzene, gas) (13)

$C_9H_{12}$ (*n*-propylbenzene, gas)$=C_9H_{12}$ (isomeric alkylbenzene, gas). (14)

The resulting values are given in tables 25 and 26, under the following headings, for the isomerization reaction as written: $\Delta F°/T$, the standard free-energy change divided by the absolute temperature; and $K$, the equilibrium constant. In tables 27 and 28 are given values of $N$, the mole fraction of the given isomer present at equilibrium with its other isomers. For any two isomers, the ratio of the corresponding values of $K$ (or of $N$) in tables 25 and 27 gives the ratio of the amounts of those two isomers present at equilibrium with one another in the gas phase at the given temperature. For the purpose of retaining the significance of their change with temperature, the values in tables 25 to 28 are written with more figures than are warranted by the absolute uncertainty.

TABLE 25.—*Values of the free energies and equilibrium constants for the isomerization of ethylbenzene to the isomeric $C_8$ alkyl benzenes in the ideal gaseous state to 1,500° K*

| Temperature | Ethylbenzene=o-xylene | | Ethylbenzene=m-xylene | | Ethylbenzene=p-xylene | |
|---|---|---|---|---|---|---|
| | $\Delta F°/T$ | $K$ | $\Delta F°/T$ | $K$ | $\Delta F°/T$ | $K$ |
| °K | | | | | | |
| 298.16 | −6.813 | 30.83 | −9.402 | 113.45 | −7.566 | 45.03 |
| 300 | −6.760 | 30.02 | −9.341 | 110.00 | −7.509 | 43.76 |
| 400 | −4.645 | 10.35 | −6.832 | 31.12 | −5.134 | 13.24 |
| 500 | −3.403 | 5.54 | −5.295 | 14.36 | −3.659 | 6.30 |
| 600 | −2.572 | 3.65 | −4.246 | 8.47 | −2.644 | 3.78 |
| 700 | −1.962 | 2.68 | −3.471 | 5.74 | −1.882 | 2.58 |
| 800 | −1.489 | 2.12 | −2.869 | 4.24 | −1.283 | 1.91 |
| 900 | −1.113 | 1.75 | −2.388 | 3.33 | −0.801 | 1.50 |
| 1,000 | −0.809 | 1.50 | −1.998 | 2.73 | −.406 | 1.23 |
| 1,100 | −.555 | 1.32 | −1.669 | 2.32 | −.076 | 1.04 |
| 1,200 | −.335 | 1.18 | −1.390 | 2.01 | +.208 | 0.90 |
| 1,300 | −.145 | 1.08 | −1.151 | 1.78 | .453 | .80 |
| 1,400 | +.017 | 0.99 | −0.948 | 1.61 | .662 | .72 |
| 1,500 | .145 | .93 | −.780 | 1.48 | .836 | .66 |

TABLE 26.—*Values of the free energies and equilibrium constants for the isomerization of propylbenzene to the isomeric $C_9$ alkyl benzenes in the ideal gaseous state to 1,500° K*

| Temperature | n-Propylbenzene=isopropylbenzene | | n-Propylbenzene=1-methyl-2-ethylbenzene | | n-Propylbenzene=1-methyl-3-ethylbenzene | | n-Propylbenzene=1-methyl-4-ethylbenzene | | n-Propylbenzene=1,2,3-trimethylbenzene | | n-Propylbenzene=1,2,4-trimethylbenzene | | n-Propylbenzene=1,3,5-trimethylbenzene | |
|---|---|---|---|---|---|---|---|---|---|---|---|---|---|---|
| | $\Delta F°/T$ | $K$ | $\Delta F°/T$ | $K$ | $\Delta F°/T$ | $K$ | $\Delta F°/T$ | $K$ | $\Delta F°/T$ | $K$ | $\Delta F°/T$ | $K$ | $\Delta F°/T$ | $K$ |
| °K | | | | | | | | | | | | | | |
| 298.16 | −0.24 | 1.13 | −4.98 | 12.26 | −8.69 | 79.28 | −8.48 | 71.33 | −11.71 | 362.4 | −16.43 | 3897 | −15.55 | 2503 |
| 300 | −.22 | 1.12 | −4.95 | 12.07 | −8.65 | 77.70 | −8.43 | 69.56 | −11.62 | 346.3 | −16.32 | 3687 | −15.44 | 2368 |
| 400 | +.56 | 0.75 | −3.68 | 6.37 | −6.70 | 29.1 | −6.21 | 22.8 | −7.94 | 54.4 | −11.78 | 375 | −10.43 | 190 |
| 500 | 1.05 | .59 | −2.91 | 4.32 | −5.47 | 15.7 | −4.79 | 11.1 | −5.75 | 18.1 | −9.09 | 97.0 | −7.42 | 41.8 |
| 600 | 1.35 | .51 | −2.43 | 3.40 | −4.67 | 10.5 | −3.86 | 6.98 | −4.28 | 8.62 | −7.29 | 39.2 | −5.40 | 15.1 |
| 700 | 1.58 | .45 | −2.07 | 2.83 | −4.07 | 7.75 | −3.16 | 4.90 | −3.17 | 4.93 | −5.94 | 19.9 | −3.90 | 7.12 |
| 800 | 1.74 | .42 | −1.80 | 2.47 | −3.61 | 6.15 | −2.61 | 3.72 | −2.29 | 3.17 | −4.89 | 11.7 | −2.73 | 3.95 |
| 900 | 1.86 | .39 | −1.59 | 2.24 | −3.25 | 5.13 | −2.19 | 3.01 | −1.60 | 2.24 | −4.06 | 7.71 | −1.81 | 2.49 |
| 1,000 | 1.98 | .37 | −1.41 | 2.03 | −2.94 | 4.39 | −1.82 | 2.50 | −1.01 | 1.66 | −3.37 | 5.45 | −1.04 | 1.69 |
| 1,100 | 2.07 | .35 | −1.26 | 1.88 | −2.69 | 3.87 | −1.52 | 2.15 | −0.52 | 1.30 | −2.80 | 4.09 | −0.41 | 1.23 |
| 1,200 | 2.12 | .34 | −1.16 | 1.79 | −2.51 | 3.54 | −1.30 | 1.92 | −.13 | 1.07 | −2.34 | 3.25 | +.11 | 0.95 |
| 1,300 | 2.15 | .34 | −1.07 | 1.71 | −2.35 | 3.26 | −1.10 | 1.74 | +.22 | 0.90 | −1.93 | 2.64 | .55 | .76 |
| 1,400 | 2.18 | .33 | −0.99 | 1.65 | −2.21 | 3.04 | −0.93 | 1.60 | .52 | .77 | −1.58 | 2.22 | .93 | .63 |
| 1,500 | 2.22 | .33 | −.90 | 1.57 | −2.06 | 2.82 | −.75 | 1.46 | .80 | .67 | −1.25 | 1.88 | 1.29 | .52 |

TABLE 27.—*Values of the equilibrium concentrations for the isomerization of the $C_8$ alkylbenzenes in the ideal gaseous state to 1,500° K*

| Temperature | Composition, in mole fraction, of equilibrium mixture of isomers | | | |
|---|---|---|---|---|
| | Ethylbenzene | o-Xylene | m-Xylene | p-Xylene |
| °K | | | | |
| 298.16 | 0.0052 | 0.162 | 0.596 | 0.237 |
| 300 | .0054 | .163 | .595 | .237 |
| 400 | .018 | .186 | .558 | .238 |
| 500 | .037 | .204 | .528 | .232 |
| 600 | .059 | .216 | .501 | .224 |
| 700 | .083 | .224 | .478 | .215 |
| 800 | .108 | .228 | .458 | .206 |
| 900 | .132 | .231 | .439 | .198 |
| 1,000 | .155 | .232 | .423 | .190 |
| 1,100 | .176 | .233 | .408 | .183 |
| 1,200 | .196 | .232 | .395 | .177 |
| 1,300 | .215 | .231 | .383 | .171 |
| 1,400 | .232 | .230 | .372 | .166 |
| 1,500 | .246 | .229 | .364 | .161 |

TABLE 28.—*Values of the equilibrium concentration for the isomerization of the $C_9$ alkylbenzenes in the ideal gaseous state to 1,500° K*

| Temperature | Composition, in mole fraction, of equilibrium mixture of isomers | | | | | | | |
|---|---|---|---|---|---|---|---|---|
| | n-Propylbenzene | Isopropylbenzene | 1-Methyl-2-ethylbenzene | 1-Methyl-3-ethylbenzene | 1-Methyl-4-ethylbenzene | 1,2,3-Trimethylbenzene | 1,2,4-Trimethylbenzene | 1,3,5-Trimethylbenzene |
| °K | | | | | | | | |
| 298.16 | 0.00014 | 0.00016 | 0.0018 | 0.011 | 0.010 | 0.052 | 0.564 | 0.361 |
| 300 | .00015 | .00017 | .0018 | .012 | .011 | .053 | .561 | .361 |
| 400 | .0015 | .0011 | .009 | .043 | .033 | .080 | .553 | .280 |
| 500 | .005 | .003 | .023 | .083 | .059 | .095 | .511 | .221 |
| 600 | .012 | .006 | .040 | .123 | .082 | .101 | .459 | .177 |
| 700 | .020 | .009 | .058 | .159 | .100 | .101 | .407 | .146 |
| 800 | .031 | .013 | .076 | .189 | .114 | .097 | .359 | .121 |
| 900 | .041 | .016 | .092 | .212 | .124 | .092 | .320 | .103 |
| 1,000 | .052 | .019 | .106 | .230 | .131 | .087 | .287 | .088 |
| 1,100 | .063 | .022 | .119 | .244 | .135 | .082 | .258 | .077 |
| 1,200 | .072 | .025 | .129 | .255 | .139 | .077 | .235 | .068 |
| 1,300 | .081 | .027 | .139 | .264 | .141 | .073 | .214 | .061 |
| 1,400 | .089 | .030 | .147 | .270 | .142 | .069 | .197 | .056 |
| 1,500 | .098 | .032 | .154 | .275 | .142 | .065 | .183 | .051 |

In figures 2 and 3 are plotted, as a function of the temperature, the values of $\Delta F°/T$ given in tables 25 and 26 for the isomerization of the $C_8H_{10}$ and the $C_9H_{12}$ alkybenzenes. These plots may be compared with corresponding plots for the paraffins [21, 22], the acetylenes [15], and the monoolefins [24]. From these charts, one may see at a glance, for any temperature in the given range, and within the limits of uncertainty of the calculations, which of the isomers is thermodynamically most stable (lowest value of $\Delta F°/T$) and which is the least stable (highest value of $\Delta F°/T$).

In figures 4 and 5 are plotted, as a function of temperature, for the $C_8H_{10}$ and the $C_9H_{12}$ alkylbenzenes, respectively, the amounts, in mole fraction of each of the isomers present at equilibrium with its other isomers in the gas phase, as given in tables 27 and 28. The vertical width of each band gives the mole fraction for that isomer at the selected temperature. The mole fractions of the several isomers are plotted additively, so that their sum is unity at all temperatures.

In table 29 the directly measured equilibrium compositions for several reactions [9, 25] are compared with those calculated in this paper. The values agree within the combined limits of uncertainty of the experimental and calculated values.

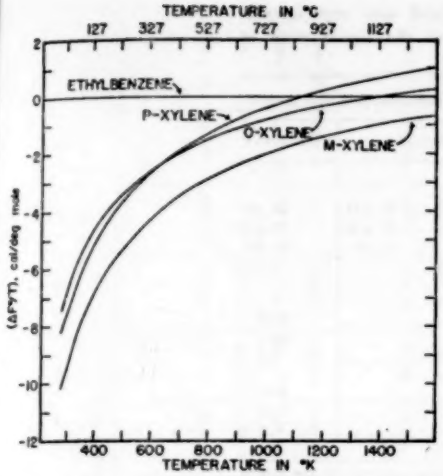


FIGURE 2.—*Free energy of isomerization of the* $C_8H_{10}$ *alkylbenzenes.*

The scale of ordinates gives the value of $\Delta F^\circ/T$, in calories per degree mole, for the isomerization of ethylbenzene into the other isomers, in the gaseous state, as indicated. The scale of abscissas gives the temperature in degrees Kelvin.

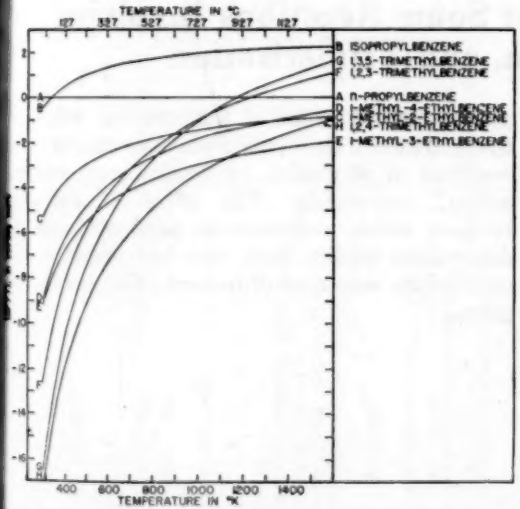


FIGURE 3.—*Free energy of isomerization of the* $C_9H_{12}$ *alkylbenzenes.*

The scale of ordinates gives the value of $\Delta F^\circ/T$, in calories per degree mole, for the isomerization of *n*-propylbenzene into the other isomers, in the gaseous state, as indicated. The scale of abscissas gives the temperature in degrees Kelvin.

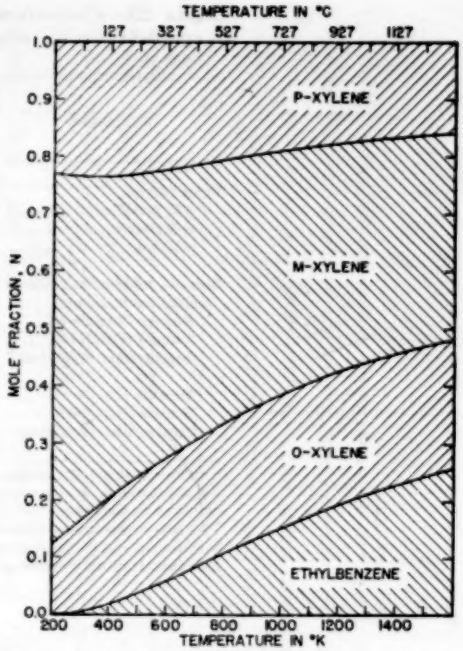


FIGURE 4.—*Equilibrium concentrations of the* $C_8H_{10}$ *alkylbenzenes.*

The scale of ordinates measures the amount in mole fraction, and the scale of abscissas gives the temperature in degrees Kelvin and degrees centigrade. The vertical width of a band at a given temperature measures the mole fraction of the given isomer present when at equilibrium with all of its other isomers, in the gas phase.

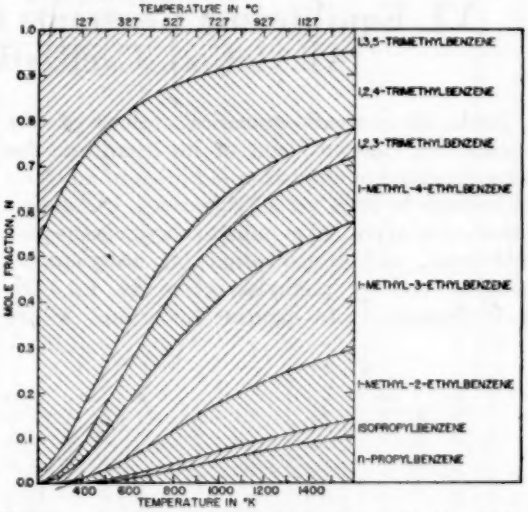


FIGURE 5.—*Equilibrium concentrations of the* $C_9H_{12}$ *alkylbenzenes.*

The scale of ordinates measures the amount in mole fraction, and the scale of abscissas gives the temperature in degrees Kelvin and degrees centigrade. The vertical width of a band at a given temperature measures the mole fraction of the given isomer present when at equilibrium with all of its other isomers, in the gas phase.

TABLE 29.—*Comparison of calculated and experimental equilibria for the alkylbenzenes in the liquid state at 323° K*

| Component | Equilibrium composition in mole percent | | |
|---|---|---|---|
| | Experimental [a] | | Calculated [b] |
| Three xylenes: | | | |
| *o*-Xylene (liquid) | 12 ±3 | 16 ±10 | 20 ±6 |
| *m*-Xylene (liquid) | 71 ±5 | 65 ±10 | 58 ±10 |
| *p*-Xylene (liquid) | 17 ±2 | 19 ±5 | 22 ±8 |
| Benzene, toluene, and xylenes (initial composition): | | | |
| Benzene (liquid)=50 | 54 | | 57.5 |
| Toluene (liquid)=50 | 41 | | 35.0 |
| Total xylenes (liquid)=0 | 4.7 | | 7.5 |
| Benzene (liquid)=55 | 58.5 | | 54.5 |
| Toluene (liquid)=36 | 36.5 | | 37.0 |
| Total xylenes (liquid)=9 | 5.0 | | 8.5 |

[a] The data in the first column are those of Pitzer and Scott [9]; the data in the second column are those of Norris and Vaala [25], with the uncertainties estimated by the present authors.

[b] These values are calculated from the thermodynamic functions given in this report and the vapor pressure data given in the tables of the American Petroleum Institute Research Project 44 [26].

# VI. Equilibrium Constants for Some Reactions Involving Alkylation, Cyclization, and Trimerization

Table 30 presents numerical values of the equilibrium constant, and of its logarithm, for some reactions of alkylation (addition of an olefin to benzene to form an alkylbenzene), cyclization (conversion of normal paraffin to alkylbenzene plus hydrogen), and trimerization (of acetylene to benzene and of methylacetylene to 1,3,5-trimethylbenzene). In figures 6, 7, and 8 are plotted, as a function of temperature, values of the logarithm of the equilibrium constant for these reactions of alkylation, cyclization, and trimerization, respectively. The effect of changing isomers, either reactants or products, can be determined readily from the free energies and equilibrium constants of isomerization previously given.

TABLE 30.—Values of equilibrium constants for reactions of alkylation, cyclization, and trimerization, at 1,000° K

| Reaction | Temperature in °K | | | | | | | | | | | | | |
|---|---|---|---|---|---|---|---|---|---|---|---|---|---|---|
| | 298.16 | 300 | 400 | 500 | 600 | 700 | 800 | 900 | 1,000 | 1,100 | 1,200 | 1,300 | 1,400 | 1,500 |
| | Logarithm of the equilibrium constant, $\log_{10} K$ | | | | | | | | | | | | | |
| **ALKYLATION** | | | | | | | | | | | | | | |
| $C_6H_6$ (benzene, gas)+$C_2H_4$ (ethylene, gas)=$C_8H_{10}$ (ethylbenzene, gas) | 11.7738 | 11.6605 | 7.0710 | 4.3417 | 2.5261 | 1.2382 | 0.2806 | −0.4584 | −1.0455 | −1.5223 | −1.9155 | −2.2445 | −2.5240 | −2.7665 |
| $C_6H_6$ (benzene, gas)+$C_3H_6$ (propylene, gas)=$C_9H_{12}$ (*n*-propylbenzene, gas) | 9.634 | 9.531 | 5.380 | 2.928 | 1.295 | 0.145 | −.707 | −1.365 | −1.881 | −2.302 | −2.654 | −2.947 | −3.196 | −3.403 |
| $C_6H_6$ (benzene, gas)=$C_3H_6$ (propylene, gas)=$C_9H_{12}$ (isopropylbenzene, gas) | 9.686 | 9.579 | 5.257 | 2.698 | 1.000 | −0.200 | −1.088 | −1.771 | −2.314 | −2.754 | −3.117 | −3.417 | −3.672 | −3.889 |
| $C_6H_6$ (benzene, gas)+$C_nH_{2n}$ (1-alkene, gas)=$C_nH_{2n+1}C_6H_5$ (*n*-alkylbenzene, gas); $n>3$ | 9.960 | 9.851 | 5.593 | 3.068 | 1.390 | 0.202 | −0.680 | −1.357 | −1.895 | −2.333 | −2.698 | −3.003 | −3.262 | −3.483 |
| **CYCLIZATION** | | | | | | | | | | | | | | |
| $C_6H_{14}$ (*n*-hexane, gas)=$C_6H_6$ (benzene, gas)+$4H_2$ (gas) | −22.677 | −22.406 | −11.418 | −4.712 | −0.176 | +3.097 | 5.566 | 7.494 | 9.041 | 10.308 | 11.365 | 12.258 | 13.021 | 13.686 |
| $C_7H_{16}$ (*n*-heptane, gas)=$C_7H_8$ (toluene, gas)+$4H_2$ (gas) | −19.892 | −19.636 | −9.184 | −2.806 | +1.502 | 4.613 | 6.956 | 8.785 | 10.251 | 11.448 | 12.448 | 13.294 | 14.018 | 14.654 |
| $C_8H_{18}$ (*n*-octane, gas)=$C_8H_{10}$ (ethylbenzene, gas)+$4H_2$ (gas) | −19.840 | −19.587 | −9.144 | −2.724 | +1.597 | 4.718 | 7.067 | 8.905 | 10.378 | 11.584 | 12.588 | 13.441 | 14.172 | 14.817 |
| $C_9H_{20}$ (*n*-nonane, gas)=$C_9H_{12}$ (*n*-propylbenzene, gas)+$4H_2$ (gas) | −19.516 | −19.263 | −8.849 | −2.487 | +1.813 | 4.918 | 7.259 | 9.085 | 10.553 | 11.751 | 12.746 | 13.591 | 14.318 | 14.968 |
| $C_nH_{2n+2}$ (*n*-paraffin, gas)=$C_nH_{2n-6}$ (*n*-alkylbenzene, gas)+$4H_2$ (gas); $n>9$ | −19.341 | −19.092 | −8.721 | −2.393 | +1.890 | 4.981 | 7.310 | 9.133 | 10.593 | 11.784 | 12.776 | 13.618 | 14.344 | 14.992 |
| **TRIMERIZATION** | | | | | | | | | | | | | | |
| $3C_2H_2$ (acetylene, gas)=$C_6H_6$ (benzene, gas) | 87.2327 | 86.5922 | 60.4947 | 44.7349 | 34.1816 | 26.6256 | 20.9559 | 16.5390 | 13.0126 | 10.1321 | 7.7369 | 5.7151 | 3.9862 | 2.4941 |
| $3C_3H_4$ (methylacetylene, gas)=$C_9H_{12}$ (1,3,5-trimethylbenzene, gas) | 81.191 | 80.916 | 55.895 | 40.845 | 30.789 | 23.598 | 18.205 | 14.012 | 10.664 | 7.930 | 5.657 | 3.740 | 2.102 | 0.688 |
| **ALKYLATION** | Equilibrium constant, °K | | | | | | | | | | | | | |
| $C_6H_6$ (benzene, gas)+$C_2H_4$ (ethylene, gas)=$C_8H_{10}$ (ethylbenzene, gas) | $5.940\times10^{11}$ | $4.576\times10^{11}$ | $1.178\times10^{7}$ | $2.196\times10^{4}$ | $3.358\times10^{2}$ | 17.31 | 1.908 | 0.3480 | $9.005\times10^{-1}$ | $3.004\times10^{-1}$ | $1.215\times10^{-1}$ | $5.695\times10^{-2}$ | $2.992\times10^{-1}$ | $1.712\times10^{-2}$ |
| $C_6H_6$ (benzene, gas)+$C_3H_6$ (propylene, gas)=$C_9H_{12}$ (*n*-propylbenzene, gas) | $4.30\times10^{9}$ | $3.40\times10^{9}$ | $2.40\times10^{4}$ | $8.47\times10^{3}$ | 19.72 | 1.397 | $1.96\times10^{-1}$ | $4.32\times10^{-2}$ | $1.31\times10^{-2}$ | $4.99\times10^{-3}$ | $2.22\times10^{-3}$ | $1.13\times10^{-3}$ | $6.37\times10^{-4}$ | $3.95\times10^{-4}$ |
| $C_6H_6$ (benzene, gas)+$C_3H_6$ (propylene, gas)=$C_9H_{12}$ (isopropylbenzene, gas) | $4.85\times10^{9}$ | $3.79\times10^{9}$ | $1.81\times10^{4}$ | $4.99\times10^{3}$ | 10.00 | 0.631 | $8.16\times10^{-2}$ | $1.69\times10^{-2}$ | $4.85\times10^{-3}$ | $1.76\times10^{-3}$ | $7.64\times10^{-4}$ | $3.83\times10^{-4}$ | $2.13\times10^{-4}$ | $1.29\times10^{-4}$ |
| $C_6H_6$ (benzene, gas)+$C_nH_{2n}$ (1-alkene, gas)=$C_nH_{2n+1}C_6H_5$ (*n*-alkylbenzene, gas); $n>3$ | $9.12\times10^{9}$ | $7.10\times10^{9}$ | $3.92\times10^{4}$ | $1.17\times10^{4}$ | 24.55 | 1.592 | 0.209 | $4.40\times10^{-2}$ | $1.27\times10^{-2}$ | $4.64\times10^{-3}$ | $2.00\times10^{-3}$ | $9.93\times10^{-4}$ | $5.47\times10^{-4}$ | $3.29\times10^{-4}$ |
| **CYCLIZATION** | | | | | | | | | | | | | | |
| $C_6H_{14}$ (*n*-hexane, gas)=$C_6H_6$ (benzene, gas)+$4H_2$ (gas) | $2.10\times10^{-22}$ | $3.93\times10^{-22}$ | $3.82\times10^{-12}$ | $1.94\times10^{-4}$ | 0.667 | $1.25\times10^{3}$ | $3.68\times10^{5}$ | $3.12\times10^{7}$ | $1.10\times10^{9}$ | $2.03\times10^{11}$ | $2.32\times10^{11}$ | $1.81\times10^{13}$ | $1.05\times10^{13}$ | $4.85\times10^{13}$ |
| $C_7H_{16}$ (*n*-heptane, gas)=$C_7H_8$ (toluene, gas)+$4H_2$ (gas) | $1.28\times10^{-20}$ | $2.31\times10^{-20}$ | $6.54\times10^{-10}$ | $1.56\times10^{-2}$ | 31.77 | $4.10\times10^{4}$ | $9.03\times10^{6}$ | $6.10\times10^{8}$ | $1.78\times10^{10}$ | $2.80\times10^{11}$ | $2.80\times10^{12}$ | $1.97\times10^{13}$ | $1.04\times10^{14}$ | $4.51\times10^{14}$ |

TABLE 30.—*Values of equilibrium constants for reactions of alkylation, cyclization, and trimerization, to 1,500° K—Continued*

| Reaction | Temperature in °K | | | | | | | | | | | | | |
|---|---|---|---|---|---|---|---|---|---|---|---|---|---|---|
| | 298.16 | 300 | 400 | 500 | 600 | 700 | 800 | 900 | 1,000 | 1,100 | 1,200 | 1,300 | 1,400 | 1,500 |
| | Logarithm of the equilibrium constant, log *a* K | | | | | | | | | | | | | |
| CYCLIZATION—continued | | | | | | | | | | | | | | |
| $C_8H_{18}$ (*n*-octane, gas) = $C_6H_{10}$ (ethylbenzene, gas) + $4H_2$ (gas) | $1.45\times10^{+20}$ | $2.59\times10^{+20}$ | $7.18\times10^{+16}$ | $1.80\times10^{+14}$ | 30. 54 | $5.22\times10^{+4}$ | $1.17\times10^{+7}$ | $8.03\times10^{+8}$ | $2.30\times10^{+10}$ | $3.84\times10^{+11}$ | $3.87\times10^{+12}$ | $2.76\times10^{+13}$ | $1.49\times10^{+14}$ | $6.56\times10^{+14}$ |
| $C_9H_{20}$ (*n*-nonane, gas) = $C_9H_{12}$ (*n*-propylbenzene, gas) + $4H_2$ (gas) | $3.05\times10^{+20}$ | $5.46\times10^{+20}$ | $1.42\times10^{+17}$ | $3.26\times10^{+14}$ | 65. 02 | $8.28\times10^{+4}$ | $1.81\times10^{+7}$ | $1.22\times10^{+9}$ | $3.57\times10^{+10}$ | $5.64\times10^{+11}$ | $5.57\times10^{+12}$ | $3.90\times10^{+13}$ | $2.08\times10^{+14}$ | $9.29\times10^{+14}$ |
| $C_nH_{2n+2}$ (*n*-paraffin, gas) = $C_nH_{2n-6}$ (*n*-alkylbenzene, gas) + $4H_2$ (gas); $n>9$ | $4.56\times10^{+20}$ | $8.00\times10^{+20}$ | $1.90\times10^{+17}$ | $4.04\times10^{+14}$ | 77. 70 | $9.57\times10^{+4}$ | $2.04\times10^{+7}$ | $1.36\times10^{+9}$ | $3.92\times10^{+10}$ | $6.08\times10^{+11}$ | $5.97\times10^{+12}$ | $4.15\times10^{+13}$ | $2.21\times10^{+14}$ | $9.82\times10^{+14}$ |
| TRIMERIZATION | | | | | | | | | | | | | | |
| $3C_2H_2$ (acetylene, gas) = $C_6H_6$ (benzene, gas) | $1.709\times10^{+57}$ | $3.910\times10^{+56}$ | $3.124\times10^{+42}$ | $5.431\times10^{+32}$ | $1.519\times10^{+26}$ | $4.223\times10^{+21}$ | $9.097\times10^{+18}$ | $3.460\times10^{+16}$ | $1.030\times10^{+15}$ | $1.358\times10^{+14}$ | $5.490\times10^{+13}$ | $5.190\times10^{+13}$ | $6.087\times10^{+13}$ | $3.120\times10^{+13}$ |
| $3C_2H_4$ (methylacetylene, gas) = $C_9H_{12}$ (1,3,5-trimethylbenzene, gas) | $1.55\times10^{+61}$ | $8.24\times10^{+60}$ | $7.85\times10^{+44}$ | $7.00\times10^{+34}$ | $6.15\times10^{+28}$ | $3.06\times10^{+23}$ | $1.60\times10^{+20}$ | $1.03\times10^{+18}$ | $4.61\times10^{+16}$ | $8.51\times10^{+15}$ | $4.54\times10^{+15}$ | $5.50\times10^{+15}$ | $1.26\times10^{+16}$ | $4.83$ |




FIGURE 6.—*Logarithm of the equilibrium constant for some reactions of alkylation.*

The scale of ordinates gives the value of the logarithm (to the base 10) of the equilibrium constant for some reactions of alkylation (addition of an olefin to benzene to form an alkylbenzene), in the gaseous state. The scale of abscissas gives the temperature in degrees Kelvin and degrees centigrade. The corresponding numerical values are given in table 30.

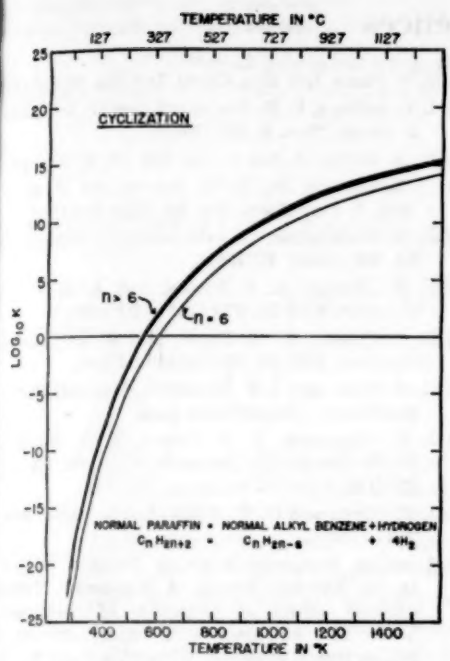


FIGURE 7.—*Logarithm of the equilibrium constant for some reactions of cyclization*

The scale of ordinates gives the value of the logarithm (to the base 10) of the equilibrium constant for the reaction of cyclization of a normal paraffin to form a normal alkylbenzene, in the gaseous state. The scale of abscissas gives the temperature in degrees Kelvin and degrees centigrade. The values calculated for n-heptane and higher paraffins fall within the width of the heavy line indicated. The corresponding numerical values are given in table 30.

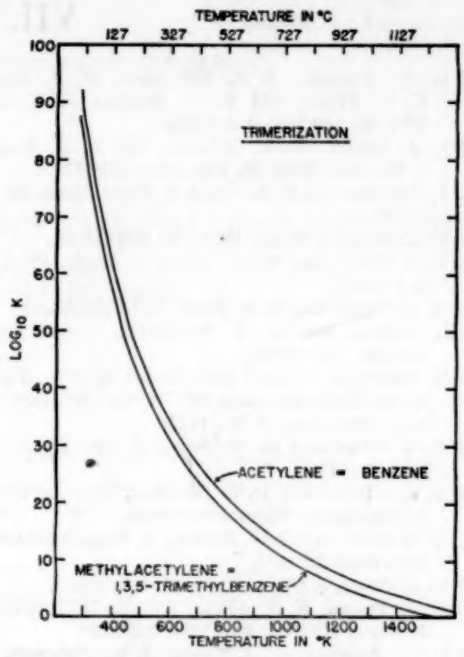


FIGURE 8.—*Logarithm of the equilibrium constant for some reactions of trimerization*

The scale of ordinates gives the value of the logarithm (to the base 10) of the equilibrium constant for some reactions of trimerization of alkynes to alkylbenzenes, in the gaseous state. The scale of abscissas gives the temperature in degrees Kelvin and degrees centigrade. The corresponding numerical values are given in table 30.

# VII. References


[1] D. D. Wagman, J. E. Kilpatrick, W. J. Taylor, K. S. Pitzer, and F. D. Rossini, J. Research NBS **34**, 143 (1945) RP1634.

[2] E. J. Prosen, W. H. Johnson, and F. D. Rossini, J. Research NBS **36**, 455 (1946) RP1714.

[3] J. Sherman and R. B. Ewell, J. Phys. Chem. **46**, 641 (1942).

[4] K. S. Pitzer, J. Chem. Phys. **14**, 239 (1946).

[5] K. S. Pitzer, and W. D. Gwinn, J. Chem. Phys. **10**, 428 (1942).

[6] W. J. Taylor and K. S. Pitzer, to be published.

[7] L. Pauling and L. O. Brockway, J. Am. Chem. Soc. **59**, 1223 (1937).

[8] G. Herzberg, Infrared and Raman spectra of polyatomic molecules, page 437 (D. Van Nostrand Co., Inc., New York, N. Y., 1945).

[9] K. S. Pitzer and D. W. Scott, J. Am. Chem. Soc. **65**, 803 (1943).

[10] N. S. Osborne and D. C. Ginnings, National Bureau of Standards. Unpublished data.

[11] R. B. Scott and J. W. Mellors, J. Research NBS **34**, 243 (1945) RP1640.

[12] K. S. Pitzer, J. Chem. Phys. **12**, 310 (1944).

[13] E. J. Prosen, K. S. Pitzer, and F. D. Rossini, J. Research NBS **34**, 403 (1945) RP1650.

[14] D. D. Wagman, W. J. Taylor, J. M. Pignocco, and F. D. Rossini, National Bureau of Standards. Unpublished data.

[15] D. D. Wagman, J. E. Kilpatrick, K. S. Pitzer, and F. D. Rossini, J. Research NBS **35**, 467 (1945) RP1682.

[16] K. S. Pitzer, Ind. Eng. Chem. Ind. Ed. **36**, 829 (194

[17] J. E. Ahlberg, E. R. Blanchard, and W. O. Lundb J. Chem. Phys. **5**, 539 (1937).

[18] K. K. Kelley, J. Am. Chem. Soc. **51**, 2738 (1929).

[19] G. B. Guthrie, Jr., R. W. Spitzer, and H. M. Hu man, J. Am. Chem. Soc. **66**, 2120 (1944).

[20] R. B. Scott and F. G. Brickwedde, J. Research NB **35**, 501 (1945) RP1684.

[21] F. D. Rossini, E. J. Prosen, and K. S. Pitzer, Research NBS **27**, 529 (1941) RP1440.

[22] E. J. Prosen, K. S. Pitzer, and F. D. Rossini, Research NBS **34**, 255 (1945) RP1641.

[23] K. S. Pitzer and J. E. Kilpatrick, National Bureau Standards. Unpublished data.

[24] J. E. Kilpatrick, E. J. Prosen, K. S. Pitzer, a F. D. Rossini, J. Research NBS **36**, 559 (19 RP1722.

[25] J. F. Norris and G. T. Vaala, J. Am. Chem. Soc. 2131 (1939).

[26] American Petroleum Institute Research Project at the National Bureau of Standards. Tables selected values of properties of hydrocarbon Table No. 5k (part 1). Vapor pressures a boiling points, at 10 to 1,500 mm Hg (June 30, 194

[27] N. Herzfeld, C. K. Ingold, and H. G. Poole, J. Che Soc. (London) **1946**, 316.


WASHINGTON, February 11, 1946.

S. Department of Commerce
tional Bureau of Standards

Research Paper RP1733
Volume 37, August 1946

Part of Journal of Research of the National Bureau of Standards

# Study of the Damaging Effect of Fatigue Stressing on SAE X4130 Steel

*By John A. Bennett*

The damaging effect of fatigue stressing above the endurance limit was investigated with notched specimens of SAE X4130 steel. The damage was measured by the decrease in endurance at another stress. A deflection method for detecting the formation of a fatigue crack permitted the damage measurement to be limited chiefly to the precrack stage. The results showed that the apparent rate of damage depends on the stress history. If the prestress is higher than the test stress, the damage occurs rapidly at first, then more slowly. The reverse is true if the damaging stress is lower than that used to measure the damage.

Tests also were made with smooth specimens in an effort to determine the cumulative damage caused by fatigue at more than one stress. Two methods were developed for extrapolating to determine the point at which fatigue cracking starts, so the damaging cycle ratios could be based on the life of the specimens prior to cracking. Complete *S-N* curves were determined for specimens after each of eight different damaging treatments. With these curves a method of expressing damage was developed that permitted the direct addition of damage occurring at different stresses. The reliability of this method was checked by testing specimens after fatigue loading at two or more different stresses and comparing the results with predictions based on the addition of the indicated damage. The agreement was within the experimental error.

## Contents

| | Page |
|---|---|
| I. Introduction | 124 |
| II. Materials and specimens | 124 |
| III. Testing machines and special apparatus | 125 |
| 1. Deflection measuring micrometer | 125 |
| 2. Stroboscopic viewing device | 126 |
| 3. Apparatus for counting and measuring fatigue cracks | 126 |
| IV. Test results with notched specimens | 126 |
| V. Test results with smooth specimens | 131 |
| 1. Methods of estimating the start of cracking | 131 |
| 2. Damage tests, including strength loss line hypothesis | 133 |
| 3. Multiple prestress tests | 136 |
| 4. Repair of damage | 137 |
| VI. Discussion | 138 |
| VII. Conclusions | 138 |
| VIII. References | 139 |

# I. Introduction

Most ferrous metals exhibit a fatigue limit. If a sample of the metal is subjected to a pulsating stress greater than the fatigue limit, a crack will form that eventually will lead to fracture. Prior to formation of the first crack a change is taking place in the metal that is detectable only by means of a fatigue test. For example, if a specimen is subjected to an overstress for one-half the number of cycles required to cause fracture, the mechanical properties of the material, other than fatigue, appear to be unchanged. However, the fatigue properties, both the endurance at stresses above the fatigue limit and the fatigue limit itself, will be lowered.

The purpose of the work described in this report was to study some of the phenomena associated with this damaging process, particularly with a view to making the information more readily applicable to steel structures against failure under alternating loads.

Previous investigations of fatigue damage have dealt largely with smooth specimens, although the majority of fatigue failures in service propagate from points of stress concentration. Therefore, it was thought worthwhile to make a thorough study with notched specimens for comparison with the results with smooth specimens. This study comprised the first part of the present investigation, and the results are discussed in sec IV of this report. The work was done under auspices of and with financial assistance from National Advisory Committee for Aeronaut and has been described in a publication of committee [1].[1]

A large proportion of the highly stressed mach elements in service probably are stressed abo their fatigue limit, occasionally during their l It is important, therefore, to know how m damage is done by this overstressing. As the n of damage in a simple test is known [2] to b complicated function of the stress history, it h not been possible to predict systematically i performance of material in service where the str variation follows a random schedule. The seco part of this investigation dealt with the study the damage caused by combinations of differ ranges of stress. It was hoped that the laborato tests could be made to conform more closely the random fluctuation of stress usually encou tered in service by making the loading sched more and more complicated. The results of th part of the investigation are described in section of this report.

[1] Figures in brackets indicate the literature references at the end of paper.

# II. Materials and Specimens

All the fatigue tests included in this report were made on R. R. Moore machines. The specimens were of normalized SAE X 4130 steel. A different heat was used for each part of the investigation. The mechanical properties of the steels are listed in table 1.

TABLE 1.—*Mechanical properties of the steels*

| | M 390 used for notched specimens | M 357 used for smooth specimens |
|---|---|---|
| Yield strength, 0.2-percent offset, lb/in.$^2$ | 62,500 | 63,000 |
| Ultimate tensile strength, lb/in.$^2$ | 104,200 | 98,000 |
| Elongation in 1 in., percent | 27 | 29 |
| Reduction of area, percent | 57 | 60 |
| Rockwell hardness, B scale | 99 | 89 |

The notched specimens used in the tests d scribed in section IV had a cylindrical test secti 0.35 in. in diameter, into which was cut a sm circular circumferential notch 0.05 in. deep a 0.05 in. in radius. The stresses listed for th specimens were calculated for the smallest secti 0.25 in. in diameter, without regard to str concentration. The notches were finished with copper wire, slightly smaller in diameter than t notch, charged with a slurry of No. 302 emery water. The specimens were rotated slowly in lathe while the wire, held at right angles to t axis of the specimen, was rotated rapidly. Th the fine polishing scratches at the bottom of t groove were substantially parallel to the axis of t specimen.

The smooth specimens used in the tests described in section V had a minimum section 0.25 in. in diameter, with a contour radius of 9¾ in. They were polished with Aloxite polishing paper belts mounted on a rubber drum 5½ in. in diameter. The specimens were mechanically rotated

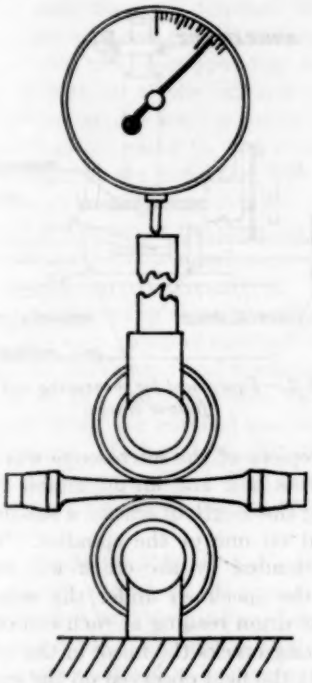

FIGURE 1.—*Specimen comparator.*

about 15 rpm while being held lightly against the rotating drum, the axis of the specimen being at right angles to the axis of the drum. The drum speed was 1,750 rpm, and the specimens usually could be polished satisfactorily in less than 1 minute. The only precaution necessary was to avoid heavy pressure of the specimen against the abrasive. This polishing method has proved economical in preparing standard R. R. Moore specimens. Although the resulting surface is not highly polished, the results obtained with these specimens are as consistent as those with a higher polish. All the specimens were examined with a low-power microscope to make sure that none with circumferential scratches were tested.

The minimum diameter of the specimens was measured, with a probable error of about 0.0001 in. For the notched specimens this was done with the aid of calibrated gage wires slightly less than 0.1 in. in diameter placed in the groove, the distance between the outsides of the wires being measured with micrometer calipers. The smooth specimens were measured with a vertical comparator using a $\frac{1}{10,000}$-in. dial gage. A sketch of this instrument is shown in figure 1. In place of the usual anvils, contact with the specimen was made with two ball bearings about 1¾-in. outside diameter. The specimen was placed between the bearings with the axis of the specimen at right angles to those of the bearings. In this way the specimen could be moved back and forth parallel to its length to locate the minimum section without danger of scratching the surface.

For some of the work described in section V it was necessary to have a reference mark at the minimum section of the specimens. To locate this point, a light source was set up so that an edge of the projected beam coincided with the line between the centers of the comparator bearings. Thus when a minimum reading was obtained on the dial, the edge of the beam passed across the minimum section of the specimen. A reference mark was made at this position with a very small drop of rubber cement placed on the specimen with a fine wire.

## III. Testing Machines and Special Apparatus

The R. R. Moore machines used in this investigation were equipped with ball-bearing spindles, and all tests were run at 3,600 rpm. A variable autotransformer was used to reduce the speed of the 10,000-rpm motors with which some of the machines were equipped.

### 1. Deflection Measuring Micrometer

This has been described in detail in a previous publication [3]. Briefly, the upper one of a pair of contacts was fastened to the specimen end of a bearing housing on the R. R. Moore machine, the lower contact being carried on a micrometer screw mounted on the bed of the machine. The contacts operated a signalling device through a tube circuit, so the position of the upper contact could be determined by raising the lower contact and noting the reading of the micrometer drum when the circuit closed. The contacts were set slightly apart so that any increase in the deflec-

tion of the specimen during test would close the circuit, operating the signal. The best results with this apparatus were obtained by mounting the fatigue-testing machine on springs to minimize vibrations from extraneous sources. No specimen was used that caused excessive vibration when the machine was running. With these precautions, it was possible to detect a deflection of 0.001 to 0.002 mm.

### 2. Stroboscopic Viewing Device

One of a pair of contacts was mounted in a Bakelite disk and fitted to the shaft of the R. R. Moore machine, the other (stationary) contact being mounted so as to be rotatable about the center line of the machine. These contacts were used to flash a stroboscope, and by adjusting the stationary contact circumferentially the flash could be made to occur at any position in the revolution of the specimen. The flashing light was directed, by means of a condenser and mirror, onto the bottom surface of the specimen, and a low-power microscope fitted with a prism in front of of the objective was used to view the illuminated area. Because this area was stressed in tension, the fatigue cracks were opened and made readily visible.

### 3. Apparatus for Counting and Measuring Fatigue Cracks

A traveling microscope was used for this work, figure 2. The specimen was removed from the fatigue machine and mounted in spindles on the stage so that it was parallel to the traversing screw of the microscope. Weights hung on the ends of the spindles produced a bending moment which stressed the upper surface in tension. The area being examined was illuminated by an intense beam incident at a grazing angle in the plane of the axes of the specimen and microscope. As t scratches seen under the microscope were also this plane, little light was reflected into the mic scope. A fatigue crack, being at right angles the incident beam, showed up brightly against t generally dark background.

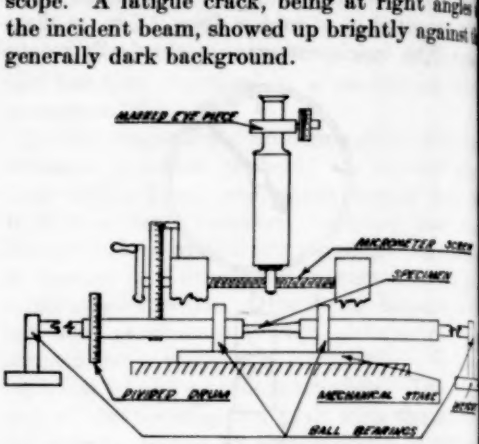


FIGURE 2.—*Equipment for measuring and counting fatigue cracks.*

The eyepiece of the microscope was fitted wi both a cross hair and an adjustable mask. F measuring the length of cracks, a subdivided dru was fitted on one of the spindles. The centr angle subtended by the crack was obtained b rotating the specimen under the cross hair a noting the drum reading at each end of the cra For counting cracks the mask in the eyepiece w set so that the field observed on the specimen w just one millimeter wide (the edges of the ma were at right angles to the length of the specimen The surface could then be scanned in 1 mm wi bands, starting from the reference mark at th minimum section, by traversing the microsco 1 mm after each revolution of the specimen. ratchet was set to give a click to indicate th completion of each revolution.

## IV. Test Results with Notched Specimens

Previous work, both at this Bureau and elsewhere, revealed two significant factors for satisfactorily evaluating fatigue damage. First, the dispersion of the experimental results necessitates an average of about eight specimens to give a sufficiently precise result for any one condition. Second, the evaluation of damage by running tests to complete fracture is limited to cycle ratios [2]

[2] "Cycle ratio" is defined as the ratio of the number of cycles run at a given overstress to the number necessary to cause failure at that stress.

sufficiently small so that the chance of crack form tion during prestressing is negligible; otherwi the damage in some cases would be depende only on the size of an initial fatigue crack rath than on the effect of prestressing.

The methods followed in the study of fatig damage with notched specimens were chosen the basis of these considerations. In order guard against crack formation it was necessary have a means of detecting fatigue cracks at s

y stage without stopping the test. Such a hod was developed based on the fact that the lection of a rotating beam specimen under stant load increases when a crack forms. The aratus and technic used to detect and measure deflection are described in section III of this ort. The deflection is a function of the size rack, and the criterion of failure chosen was a lection of 0.005 mm, corresponding to a crack about 12-percent of the original cross sec- n [3]. The specimens were actually run until deflection had increased to 0.01 mm in order make certain that the deflection was due to a ck, but the data in this section are based on number of cycles run at the time the specimen lected 0.005 mm. This number is referred to $N_c$.

Tests were conducted in the conventional man- (to fracture) on a group of notched specimens determine the $S$–$N$ curve and the fatigue limit. ur stresses in the range between the fatigue it ($\pm$39,000 lb/in.$^2$ for notched specimens) and yield strength of the steel (62,500 lb/in.$^2$) e used in the investigation. The four stresses sen were $\pm$42,000, $\pm$48,000, $\pm$54,000, and 0,000 lb/in.$^2$

Tests were made to determine $N_e$ at each of se four stresses. At least 10 specimens were ted at each stress, and the median of each group s used as the value of endurance at that stress. e median was considered to be more representa- e of a group of endurance values than the rage, as it is less affected by an occasional exces- ly divergent value. Also the median can be ermined in cases where some elements of the up cannot be expressed numerically but are wn to lie in a certain range. For example, in ermining the endurance at a given stress, if y one specimen of the group did not fail, the rage endurance of the group would be infinite, ereas the median value would be finite.

As the scatter of the results was not uniform the four groups, it was necessary to test more cimens in some cases than in others in order to ain approximately the same precision for each ue of $N_e$. The number of tests in each group ged from 11 to 17.

The values of $N_e$ (the number of cycles to form rack of definite size) for each selected stress are ed in table 2.

In the next stage of the investigation each specimen was first stressed for a predetermined number of cycles at one of the four chosen stresses, then the stress was changed as given in table 3 and the number of cycles to failure determined. The difference between this value and the median (see footnote 3) value of endurance for the original material at the same stress (table 2) gave a measure of the damage caused by the prestressing. This difference was expressed as a percentage of the undamaged endurance.

For each of the combinations in table 3, tests were made with the prestressing carried to 10, 25, 50, 75, and 90 percent of the median value of $N_e$. The number of tests made for each prestress condition was between 6 and 10, depending on the scatter of the individual values. The median values for each group are listed in table 4.[3] The variation of damage with percentage of prestress is shown graphically in figures 3 and 4 for a test stress of $\pm$48,000 lb/in.$^2$, and in figures 5 and 6 for a test stress of $\pm$54,000 lb/in.$^2$ In the graphs the broken lines join the upper and lower quartile points of each group of values and thus give an indication of the scatter of the data. The curves from figures 3 to 6 are combined in figure 7 for comparison.

In the test groups in which prestressing was carried to 75 and 90 percent of the endurance, some specimens failed before the prestressing was completed, that is, the damage was greater than 100-percent. The inclusion of these results caused no difficulty in determining the median, although it did make the comparison of precision between the groups more uncertain.

While the results of the damage tests as shown in figure 7 are not directly comparable with those obtained with smooth specimens [1, 2], there are certain similarities. The tendency with both types of specimen was for the curve representing a prestress above the test stress to lie above the 45° line. The opposite tendency was noted when the magnitude of the prestress was below that of the test stress. (The 45° line may be considered as the damage curve for a prestress equal to the test stress.)

---

[3] The middle number of a series arranged in order of magnitude is the median. The middle one of the numbers that lie below the median is the lower quartile, the middle one of those above is the upper quartile. Half the difference between the upper and lower quartiles is the semi-interquartile (SIQ) range. This is a measure of the dispersion of the individual values which expresses the same limits relative to the median as the probable error expresses relative to the average.

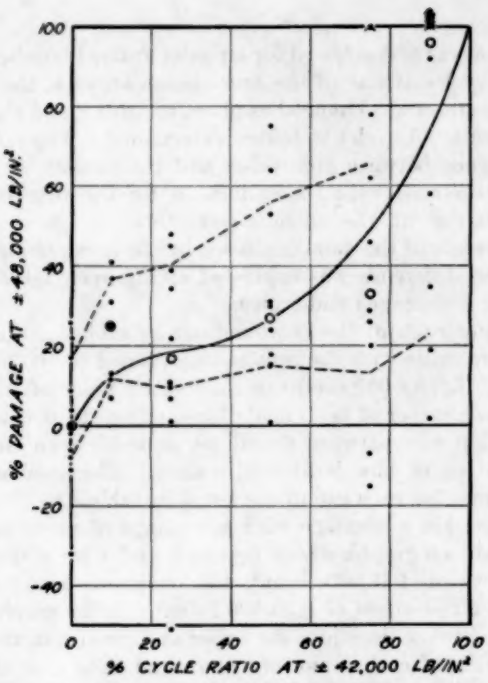


FIGURE 3.—*Damage at ±48,000 lb/in.² due to stressing at ±42,000 lb/in.²*

Notched specimens. Cycle ratios and damage based on $N_r$.

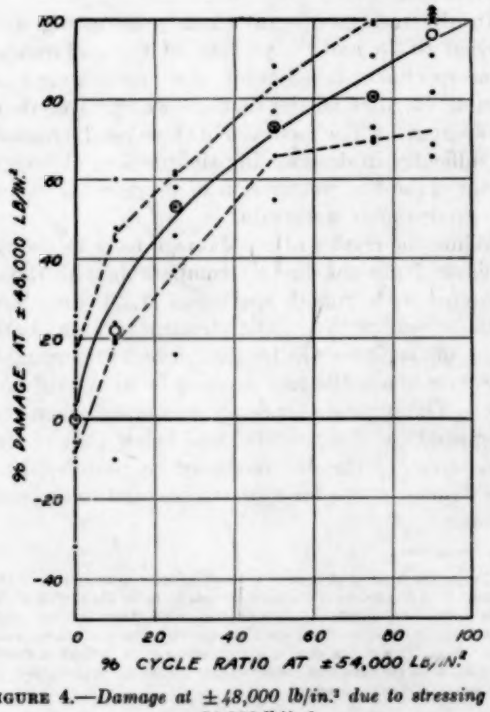


FIGURE 4.—*Damage at ±48,000 lb/in.² due to stressing at ±54,000 lb/in.²*

Notched specimens. Cycle ratios and damage based on $N_r$.

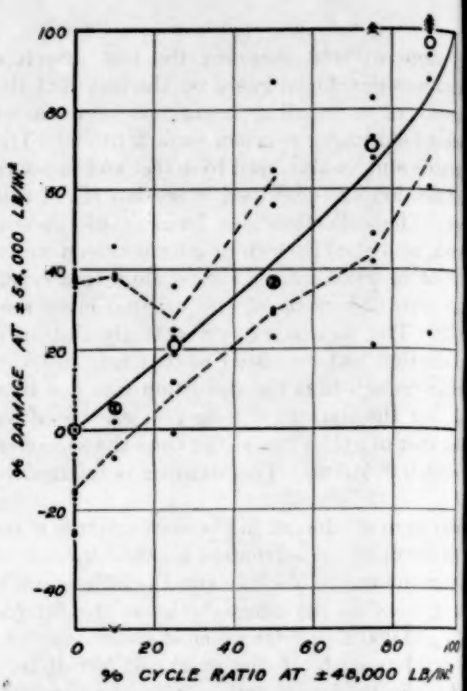


FIGURE 5.—*Damage at ±54,000 lb/in.² due to stressing at ±48,000 lb/in.²*

Notched specimens. Cycle ratios and damage based on $N_r$.

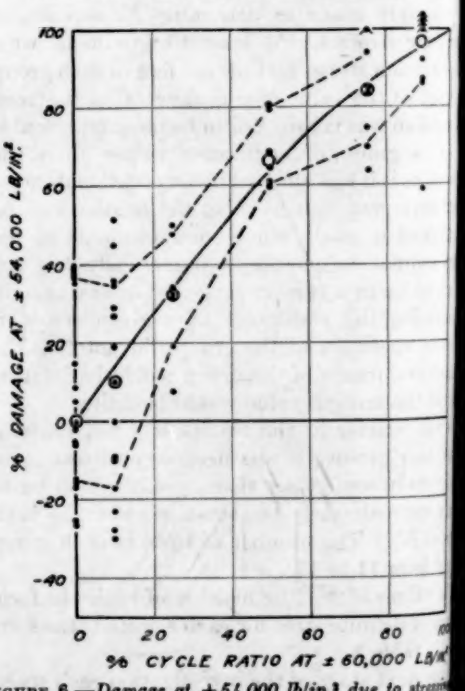


FIGURE 6.—*Damage at ±54,000 lb/in.² due to stressing at ±60,000 lb/in.²*

Notched specimens. Cycle ratios and damage based on $N_r$.

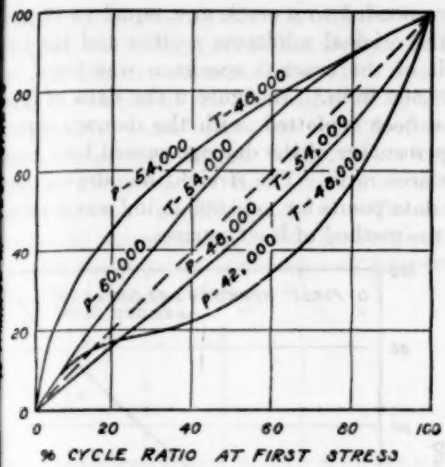


RE 7.—*Damage as measured by loss of endurance ($N_e$).*

from figures 3 to 6, notched specimens. *P*=Prestress in pounds per square inch. *T*=Test stress in pounds per square inch.

TABLE 2.—*Endurance of notched specimens*

| Stress, lb/in.² | Number of cycles to crack |
|---|---|
| ±42,000 | 963,000 |
| ±48,000 | 264,000 |
| ±54,000 | 93,000 |
| ±60,000 | 44,000 |

TABLE 3.—*Damage test conditions*

| Prestress, lb/in.² | Test stress lb/in.² |
|---|---|
| ±42,000 | ±48,000 |
| ±54,000 | |
| ±48,000 | ±54,000 |
| ±60,000 | |

order to provide a basis of comparison with results of fatigue damage reported by others ally based on the fatigue limit), some tests of type were conducted with two values of pre-s, ±42,000 and ±60,000 lb/in.². The effect arious amounts of prestressing on the fatigue subsequently determined by fracture tests is n in table 5 and figure 8. The number of s of prestress used for the 75-percent and 90-nt cycle ratios was the same as the number in the previous phase of the investigation, correction was made in determining the cycle s represented by these amounts of prestress-ing. The method of making this correction will be shown for the case of the highest cycle ratio at ±42,000 lb/in.²

TABLE 4.—*Effect of prestress on endurance of notched specimens of SAE X4130 steel stressed as rotating beams*

| Number of specimens | Test stress | Prestress | Cycle ratio, percent of $N_e$ value | Endurance, $10^3$ cycles | Damage | SIQ [1] |
|---|---|---|---|---|---|---|
| | lb/in.² | lb/in.² | | | % | % |
| 17 | ±42,000 | ..... | 0 | 963 | 0 | 25 |
| 11 | ±48,000 | ..... | 0 | 264 | 0 | 13 |
| 7 | ±48,000 | ±42,000 | 10 | 198 | 25 | 12.5 |
| 10 | ±48,000 | ±42,000 | 25 | 220 | 16.7 | 18 |
| 10 | ±48,000 | ±42,000 | 50 | 192 | 27.3 | 20 |
| 10 | ±48,000 | ±42,000 | 75 | 177 | 32.9 | 26 |
| 10 | ±48,000 | ±42,000 | 90 | 11 | 95.8 | ---- |
| 8 | ±48,000 | ±54,000 | 10 | 205 | 22.3 | 14 |
| 7 | ±48,000 | ±54,000 | 25 | 125 | 52.6 | 12 |
| 7 | ±48,000 | ±54,000 | 50 | 72 | 72.7 | 9 |
| 7 | ±48,000 | ±54,000 | 75 | 50 | 81.1 | 15 |
| 8 | ±48,000 | ±54,000 | 90 | 12 | 95.5 | ---- |
| 17 | ±54,000 | ..... | 0 | 93 | 0 | 26 |
| 8 | ±54,000 | ±48,000 | 10 | 87 | 6.4 | 23 |
| 6 | ±54,000 | ±48,000 | 25 | 73 | 21.5 | 10 |
| 8 | ±54,000 | ±48,000 | 50 | 59 | 36.6 | 16 |
| 8 | ±54,000 | ±48,000 | 75 | 27 | 71 | ---- |
| 8 | ±54,000 | ±48,000 | 90 | 3 | 96.8 | ---- |
| 15 | ±54,000 | ±60,000 | 10 | 84 | 9.7 | 21 |
| 7 | ±54,000 | ±60,000 | 25 | 63 | 32.2 | 14 |
| 6 | ±54,000 | ±60,000 | 50 | 31 | 66.7 | 10 |
| 8 | ±54,000 | ±60,000 | 75 | 15 | 83.9 | 12 |
| 8 | ±54,000 | ±60,000 | 90 | 3 | 96.8 | ---- |
| 15 | ±60,000 | ..... | 0 | 44 | 0 | 23 |

[1] SIQ=Semi-interquartile range.

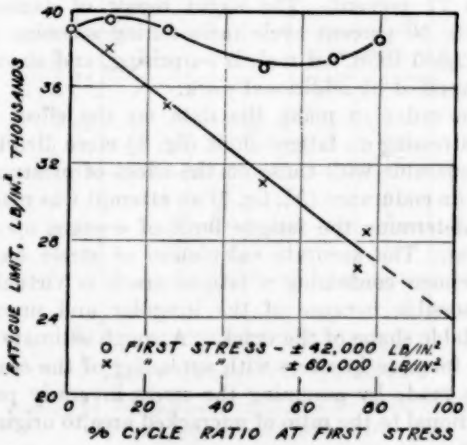


FIGURE 8.—*Effect of prestress on fatigue limit.*

Notched specimens.

TABLE 5.—*Effect of prestress on fatigue limit of notched specimens of SAE X4130 steel stressed as rotating beams*

| Prestress ±42,000 lb/in.² | | | Prestress ±60,000 lb/in.² | | |
|---|---|---|---|---|---|
| Cycle ratio | Fatigue limit | Damage, percentage of maximum | Cycle ratio | Fatigue limit | Damage, percentage of maximum |
| % | *lb/in.²* | | % | *lb/in.²* | |
| 10 | ±39,500 | −3 | 10 | ±38,000 | 6 |
| 25 | ±39,000 | 0 | 25 | ±35,000 | 26 |
| 50 | ±37,000 | 13 | 50 | ±31,000 | 52 |
| 68 | ±37,500 | 10 | 75 | ±26,500 | 81 |
| 80 | ±38,500 | 3 | 77 | ±28,500 | 68 |

The median $N_e$ for this stress was $963\times10^3$. When it was desired to prestress a group of specimens to 90 percent of this value, or $867\times10^3$ cycles, some of the specimens failed before prestressing was completed. Only those which did not fail in prestressing could be used for the determination of fatigue limit, so this determination was not truly representative. Therefore, in the original series of values of $N_e$, the median of all values greater than $867\times10^3$ was taken as being representative of the specimens which were used to determine the fatigue limit after prestressing. The cycle ratio as plotted in figure 8 is based on this second median ($1{,}057\times10^3$ cycles), and is consequently less than 90 percent. A similar correction was made for the 75 percent prestress at ±42,000 lb/in.², and for the 90 percent value at ±60,000 lb/in.² The corrected values of cycle ratio at ±42,000 lb/in.² were 68 percent and 80 percent; at ±60,000 lb/in.² the highest value was 77 percent. The slight repair of damage above 50 percent cycle ratio during stressing at ±42,000 lb/in.², if real, is surprising, and should be verified by additional work.

In order to make the data on the effect of prestressing on fatigue limit (fig. 8) more directly comparable with those on the effect of prestressing on endurance ($N_e$, fig. 7) an attempt was made to determine the fatigue limit of cracked specimens. The accurate calculation of stress on a specimen containing a fatigue crack is virtually impossible because of the irregular and unpredictable shape of the crack. A rough estimate of the increase in stress with spreading of the crack was made by assuming the stress inversely proportional to the ratio of uncracked area to original area.

The specimens used for this determination had deflected 0.010 mm in the fatigue test. This corresponded to a crack area equal to 17 percent of the original minimum section and the fatigue limit of the cracked specimen was found to be ±23,500 lb/in.² In figure 9 the data of figure 8 have been replotted, with the damage expressed as percentage of the damage caused by a crack of this area ratio. The straight line drawn through the data points for ±60,000 lb/in.² was determined by the method of least squares.

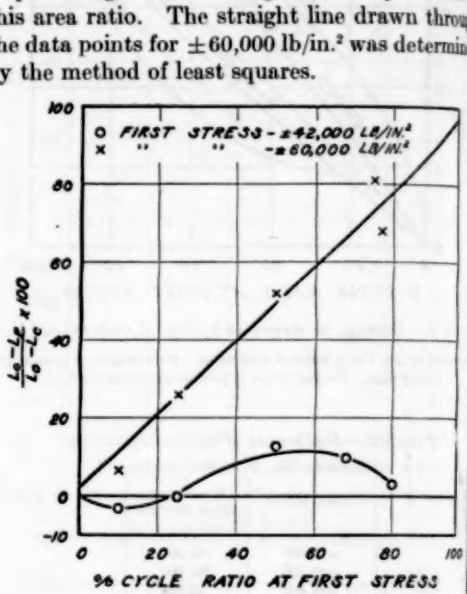


FIGURE 9.—*Damage as measured by loss of fatigue limit of notched specimens.*

$L_o$=fatigue limit of original specimen. $L_p$=Fatigue limit of prestressed specimen. $L_c$=fatigue limit of cracked specimen.

Figure 10 shows the *S-N* curves for specimens with three types of stress concentration: smooth (zero concentration), notched, and cracked (maximum concentration). The points marked *X* or + in figure 10 are the results from cracked specimens having crack areas other than 17 percent. It will be noted that the value for a specimen having an area ratio of 50 percent lies very far above the 17 percent ratio curves, while the values for specimens having a 12 percent ratio are in the same range or lower. This suggests that the stress concentration at high stresses is less for large than for small cracks. More experimental work would be required before any general statement could be made with certainty.

In table 6 are shown the values of stress concentration factors given by the ratios of the fatigue limits of the specimens under three conditions of stress concentration. Almen [4] has shown that the slope of the falling part of the *S-N* curve

creases with increasing stress concentration. If e slope of the falling part of the *S-N* curve is a easure of effective stress concentration, then the tios of the slopes of the three lines of figure 10 ould give the same values for these factors as tained from the fatigue limits. There was bstantial agreement of these factors as deter-ined by the two methods (table 6). The value theoretical stress concentration factor given in ble 6 for the notched specimen was calculated om a table given in reference [5].

BLE 6.—*Stress concentration factors in specimens of SAE X4130 steel stressed as rotating beams*

| Type of specimen | Fatigue limit | SCF [1] from fatigue limit | Slope of *S-N* curve | SCF from slope | Theoretical SCF |
|---|---|---|---|---|---|
| | *lb/in.²* | | | | |
| ooth | ±50,000 | 1.0 | −0.767 | 1.0 | 1.0 |
| tched | ±39,000 | 1.28 | −.983 | 1.28 | 1.59 |
| cked (17%) | ±23,500 | 2.13 | −1.46 | 1.91 | |

[1] SCF=Stress-concentration factor.

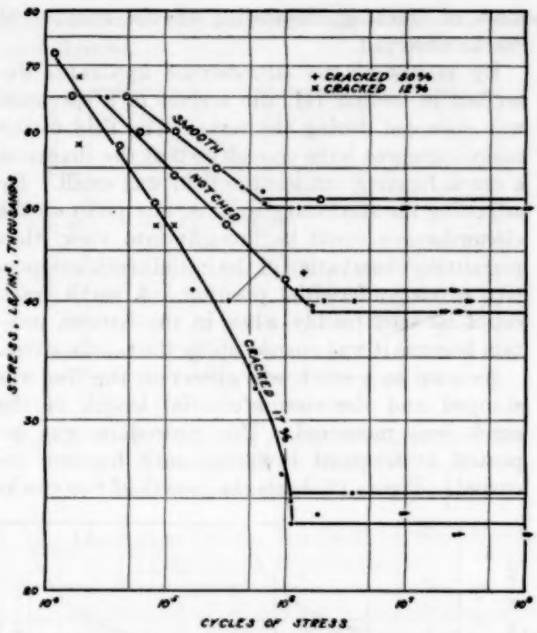


FIGURE 10.—*S-N curves for SAE X4130 steel under three conditions of stress concentration.*

Large open points represent the median values from a group of specimens tested at the same stress. Small closed points are the results of individual tests.

# V. Test Results With Smooth Specimens

## l. Methods of Estimating the Start of Cracking

The preceding experiments showed that fatigue mage results are more reproducible when based the number of cycles to form a small crack an when based on the number of cycles to frac-re. It was considered that even greater repro-cibility might be obtained if it were possible to termine the number of cycles at which a crack st starts. Then the damaging cycle ratios could based on the precrack stage only. This was ne in the experiments described below, all tests ng made on smooth (9¾-in. contour radius) cimens.

In the discussion of methods for estimating the rt of cracking, the relationship shown in figure should be kept in mind. This shows a semi-arithmic plot of test stress against the number cracks formed prior to fracture. The points tted are based only on cracks lying in a band m wide at the center of the specimen. The number of cracks increased rapidly as the stress was raised above the fatigue limit. Because of

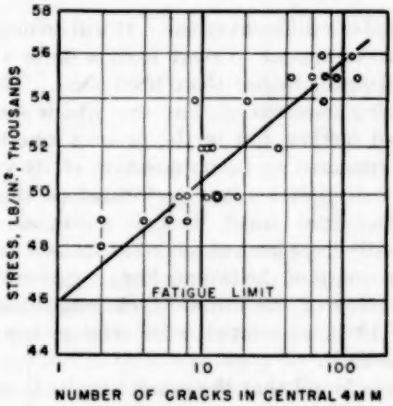


FIGURE 11.—*Influence of applied stress on the number of cracks formed prior to fracture.*

the large variation in the number of cracks formed, two different methods were used for estimating the

start of cracking, depending on the number of cracks observed.

By means of the stroboscopic apparatus described in section III, the surface of a specimen was observed during the tests. The field of the microscope was large enough so that the chance of a crack forming outside the field was small. By adjusting the stationary contact, any point on the circumference could be brought into view, thus permitting observation of the initial crack irrespective of circumferential position. A small crack could be seen readily when in the bottom position because it was opened up by the tensile stress.

As soon as a crack was observed, the test was stopped and the circumferential length of the crack was measured. This procedure was repeated at frequent intervals until fracture occurred. Figure 12 shows the growth of two cracks

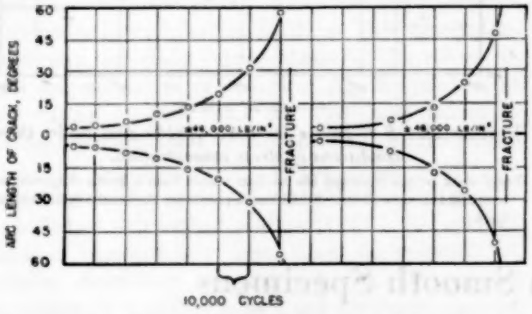


FIGURE 12.—*Curves showing change of crack length at each of two different stresses.*

The midpoint of the crack when first measured is taken as zero.

each under a different stress. It will be noted that the curves appear to start from a finite value of crack length, rather than from zero. This is a surprising observation, and one which should be checked further, but in the present investigation there appeared to be no question of its validity, so all extrapolation was performed on this basis. The fact that small, though numerous cracks frequently have been observed at stresses considerably in excess of the fatigue limit suggests that the large value of the initial crack length shown in figure 12 is associated with stresses nearer the fatigue limit.

It was found that the crack length, $L$, could be expressed by the equation

$$\log (L-C)=\alpha N, \qquad (1)$$

where $C$ and $\alpha$ are constants, the latter dependent on stress; $N$ is the number of cycles, and $A$ the logarithmic base. This is shown graphically in figure 13 where $(L-C)$ is plotted logarithmically against $N$ for one of the curves shown in figure 12. When curves similar to figure 13 were plotted for various nominal stress values, it was found that the slope was a simple function of the stress, as shown in figure 14.

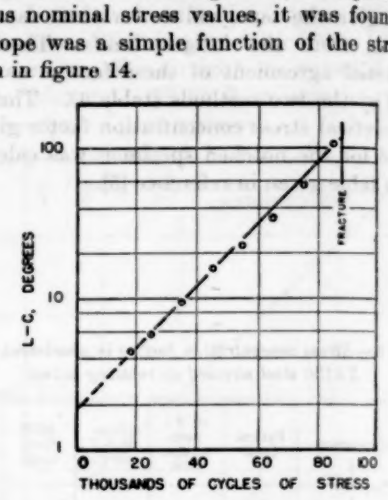


FIGURE 13.—*Semilogarithmic plot of crack growth curve*

The ordinate is the arc length ($L$) of the crack minus a constant ($C$)

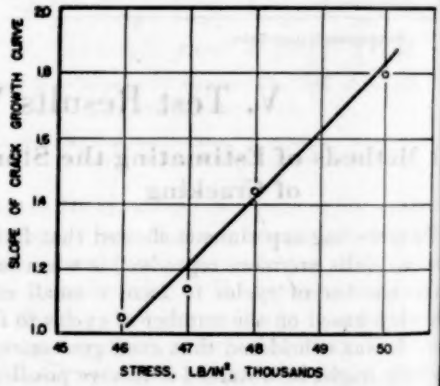


FIGURE 14.—*Influence of stress on the rate of crack growth*

Curves of the type shown in figure 13 were used to determine by extrapolation the point at which cracking starts, assuming that the cracks grew exponentially from an original arc length of about 6°, as indicated in figure 12. The deflectometer measuring apparatus described in section III of this report was used to indicate the presence of a crack, but this did not operate until the crack reached 50° or 60° in the circumferential length, the growth curves (fig. 13) being used to extrapolate back to the start of the crack.

The above method was used only in cases where he total number of cracks was not more than five, nce more numerous cracks might change the rface stress sufficiently to invalidate the extra- olation. For specimens which had numerous acks the extrapolation was performed as follows: y means of the masked eyepiece described in ction III, the cracks were counted in circum- rential bands 1 mm wide. Practically all the acks occurred within 6 mm of the center of the ecimen and for the purpose of totaling the mber of cracks this area was divided into three nes. The first extended 2 mm each side of e center, the second from 2 to 4 mm on each de and the third 4 to 6 mm. The average stress each zone was calculated from the geometry the specimen and found to be 99.8, 98.8, and .0 percent of the stress at the center for the st, second, and third zones, respectively. The uare root of the number of cracks in a band otted against the average stress in that band, ve a nearly linear relationship which could be trapolated back to the stress at which no cracks ould be formed. Curves of this type are shown figure 15.

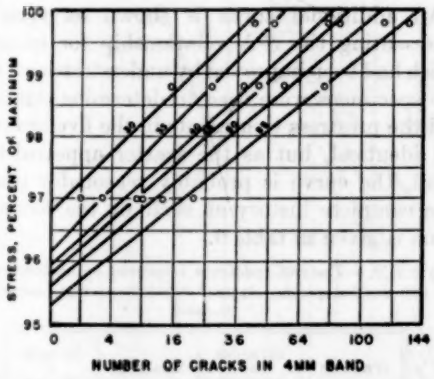


GURE 15.—*Results of crack counts on one smooth specimen at various stages between the beginning of cracking and fracture.*

mbers on curves represent thousands of cycles of stress which the specimen d run when the cracks were counted. Total fracture occured at 89,000 cles.

Points obtained for the start of cracking by these o methods of extrapolation (figs. 13 and 15) e shown on figure 16, both the stress and number cycles being plotted logarithmically. The aight line through the points was determined the method of least squares. A similar graph sed on the points representing fracture is also included in this figure (the points for this curve are not shown).

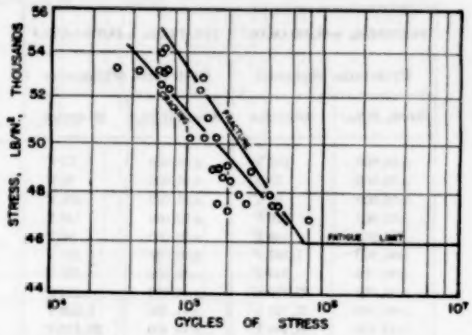


FIGURE 16.—*S-N curves for start of cracking and for fracture in normalized SAE X4130 steel.*

The experimental points are for cracking only.

## 2. Damage Tests, Including Strength-Loss Line Hypothesis

In the next phase of the work, two stresses were chosen between the fatigue limit and the yield strength of the material, and specimens were stressed for various cycle ratios at these stresses. The stresses chosen were ±48,000 and ±54,000 lb/in.², and the cycle ratios were based on the number of cycles to the start of cracking.[4] Eight prestress conditions were used, as shown in table 7.

TABLE 7.—*Prestress conditions*

| Stress | Cycle ratio, percentage of $N_s$ |
|---|---|
| *lb/in.²* | |
| ±48,000 | 10 |
| | 33⅓ |
| | 66⅔ |
| | 90 |
| ±54,000 | 10 |
| | 33⅓ |
| | 66⅔ |
| | 90 |

The prestressed specimens were used to determine a complete *S-N* curve for each condition, a typical curve of this type being shown in figure 17. This method has been used recently by Kommers [2] to measure fatigue damage. These curves were determined in the usual manner, that is by tests to fracture. The experimental data are

[4] The term $N_s$ will be used to designate the number of cycles to the start of cracking. This value is determined from the cracking curve of figure 16.

TABLE 8.—*Results of damage tests*

[Cycle ratios are based on $N_s$. "F" indicates that specimen fractured, "U" indicates that the specimen did not break.]

| PRESTRESS, ±48,000 LB/IN.² | | PRESTRESS, ±48,000 LB/IN.² | |
|---|---|---|---|
| Cycle ratio, 10 percent | | Cycle ratio, 66⅔ percent | |
| Stress, lb/in.² | $10^3$ cycles | Stress, lb/in.² | $10^3$ cycles |
| ±54,000 | 102 F | ±54,000 | 73 F |
| ±54,000 | 70 F | ±54,000 | 63 F |
| ±54,000 | 96 F | ±54,000 | 131 F |
| ±52,000 | 225 F | ±52,000 | 129 F |
| ±50,000 | 146 F | ±50,000 | 96 F |
| ±46,200 | 1,187 F | ±46,000 | 1,131 F |
| ±46,200 | 514 F | ±46,000 | 516 F |
| ±46,000 | 22,339 U | ±44,600 | 240 F |
| ±46,000 | 27,721 U | ±44,400 | 1,038 F |
| ±45,800 | 44,988 U | ±44,400 | 20,635 U |
| | | ±44,200 | 36,233 U |
| Cycle ratio, 33⅓ percent | | Cycle ratio, 90 percent | |
| ±54,000 | 61 F | ±54,000 | 99 F |
| ±54,000 | 81 F | ±54,000 | 24 F |
| ±54,000 | 142 F | ±54,000 | 58 F |
| ±52,000 | 86 F | ±52,000 | 112 F |
| ±50,000 | 141 F | ±50,000 | 111 F |
| ±47,000 | 313 F | ±46,000 | 622 F |
| ±46,000 | 743 F | ±44,000 | 132 F |
| ±45,300 | 1,608 F | ±42,600 | 410 F |
| ±45,100 | 22,711 U | ±42,400 | 416 F |
| ±45,000 | 831 F | ±42,200 | 34,516 U |
| ±44,900 | 40,787 U | ±42,000 | 17,709 U |
| ±44,800 | 21,942 U | | |
| ±44,500 | 20,027 U | | |

| PRESTRESS, ±54,000 LB/IN.² | | PRESTRESS, ±48,000 LB/IN.² | |
|---|---|---|---|
| Cycle ratio, 10 percent | | Cycle ratio, 66⅔ percent | |
| Stress, lb/in.² | $10^3$ cycles | Stress, lb/in.² | $10^3$ cycles |
| ±52,000 | 110 F | ±52,000 | 69 F |
| ±50,000 | 318 F | ±50,000 | 186 F |
| ±48,000 | 720 F | ±48,000 | 132 F |
| ±45,800 | 2,033 F | ±48,000 | 86 F |
| ±45,800 | 834 F | ±46,000 | 454 F |
| ±45,600 | 33,016 U | ±44,000 | 19,227 U |
| ±45,600 | 428 F | ±44,000 | 19,133 U |
| ±45,400 | 21,033 U | ±43,000 | 18,986 U |
| | | ±42,000 | 459 F |
| | | ±40,400 | 16,101 U |
| Cycle ratio, 33⅓ percent | | Cycle ratio, 90 percent | |
| ±52,000 | 79 F | ±59,000 | 12 F |
| ±50,000 | 109 F | ±52,000 | 54 F |
| ±48,000 | 267 F | ±50,000 | 91 F |
| ±46,000 | 1,276 F | ±48,000 | 128 F |
| ±45,600 | 327 F | ±45,000 | 641 F |
| ±44,000 | 853 F | ±44,000 | 162 F |
| ±43,800 | 23,882 U | ±43,000 | 25,304 U |
| ±43,800 | 19,229 U | ±42,000 | 144 F |
| ±43,600 | 21,451 U | ±42,000 | 16,009 U |
| | | ±41,000 | 575 F |
| | | ±40,400 | 176 F |
| | | ±40,200 | 249 F |
| | | ±40,000 | 21,338 U |
| | | ±40,000 | 11,643 U |

shown in table 8. The curves for the eight pr
stress conditions are shown in figures 18 and 1
The cycle ratio for the largest number of cycl
should be less than 90 percent because of th
specimens which cracked before reaching th
predetermined number of cycles. However, u
like the tests described in section IV, these resul
could not be accurately corrected for the prem
ture failures, so no attempt was made to do so.

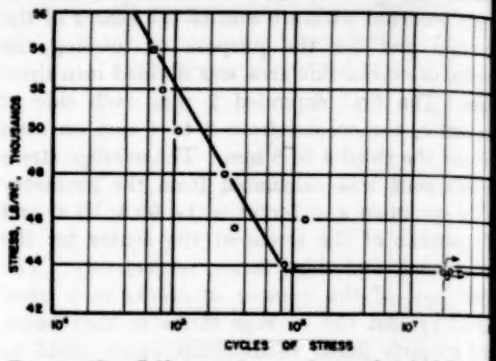


FIGURE 17.—*S-N curve for specimens that had been su
jected to 33⅓ percent cycle ratio at ±54,000 lb/in.²*

The square point is at the stress used for prestressing and the numbe
cycles obtained by subtracting the prestress cycles from expected life at t
stress.

An additional curve is shown on figure 1
representing the *S-N* relationship for specime
which had been improved by understressing. On
five specimens were used to determine this curv
and the prestress treatments in the five cases wa
not identical, but as the scatter appeared to
small, the curve is probably reasonably reliab
The complete history of each of the five spe
mens is given in table 9.

TABLE 9.—*Tests of specimen improved by understressi*

["F" indicates that specimen fractured, "U" indicates that specimen did
fracture]

| Prestress | $10^3$ cycles at prestress | Test stress | $10^3$ cycles at test stress |
|---|---|---|---|
| *lb/in.²* | | *lb/in.²* | |
| ±45,000 | 21,700 | ±56,000 | 80 F |
| ±46,000 | 24,239 | ±58,000 | 79 F |
| ±45,900 | 18,567 | ±54,000 | 144 F |
| ±45,900 | 26,700 | ±52,000 | 438 F |
| ±45,800 | 31,578 | ±50,000 | 3,933 U |

In figure 19, a dashed line represents the *S*
relationship for specimens which had been damag
100 percent, that is, specimens which were j
ready to crack. This curve was obtained
follows: Points were obtained at ±48,000 a
±54,000 lb/in.² by subtracting the number

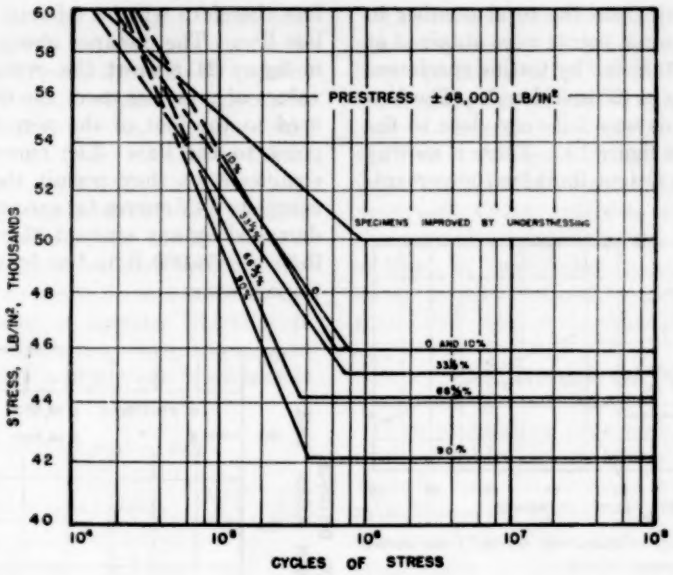


FIGURE 18.—*S-N curves for specimens overstressed at ±48,000 lb/in.² and for specimens improved by understressing.*

The figures on the curves represent the cycle ratio (based on $N_s$) to which the specimens were run in prestress.

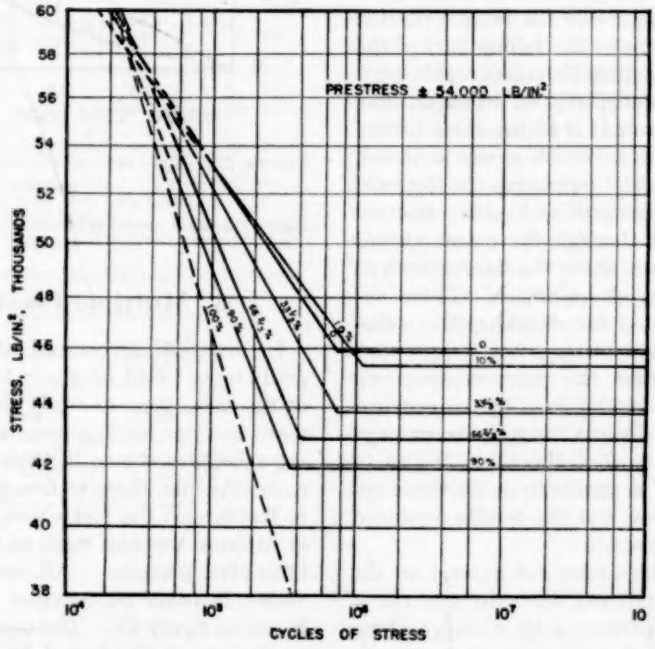


FIGURE 19.—*S-N curves for specimens overstressed at ±54,000 lb/in.²*

The figures on the curves represent the cycle ratios (based on $N_s$) to which the specimens were run in prestress.

cycles to form a crack from the total number to fracture. Two additional points were obtained at $\pm 42{,}000$ and $\pm 38{,}000$ lb/in.$^2$ by testing specimens having very small cracks (2° to 3° long). The four points obtained in this way fell very close to the straight line shown in figure 19. There is no way to obtain directly the fatigue limit for 100-percent-damaged specimens.

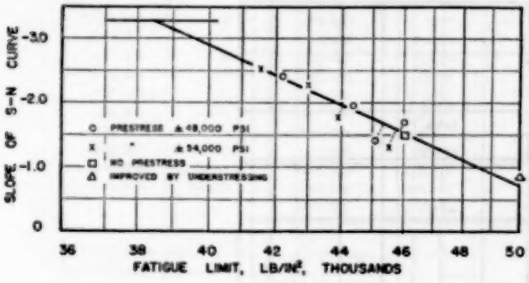


FIGURE 20.—*Strength loss relationship derived from curves of figures 18 and 19.*

It will be noted in figures 18 and 19 that the curves appear to radiate from approximately the same point. This suggests that the damage could be measured by a simple geometrical property of the *S-N* curves. In figure 20 the fatigue limit is plotted against the slope of the falling part of the *S-N* curve. Although there is considerable scatter, the points lie approximately on a straight line, indicating that the damage is of the same nature regardless of the stress at which it was inflicted. The horizontal line at 3.27 represents the slopes of the 100-percent-damage curve and the intersection of this line with that through the points should serve as a means of estimating the fatigue limit of the 100-percent-damaged specimens. There appears to be no method for checking the value obtained.

It will be noted that the point representing specimens that had been improved by understressing lies near the straight line through the damage points. This indicates that the changes due to understressing are of a similar type to those occurring on overstressing, but the results produced are in the opposite direction.

If the type of damage does not depend on the stress at which it is inflicted, then the amount of damage should be represented by distance along the curve of figure 20, being expressed as percent of the distance from the value for the original material to that for 100-percent damage. This line therefore will be referred to as the strength loss line. The distance along this line is plotted in figure 21 against the cycle ratio for the two values of prestress used, the distance being measured to the foot of the perpendicular from each point to the line. The curves of figure 21 are significant as they permit the prediction of the complete *S-N* curves for specimens that have been damaged by any amount of prestress at $\pm 48{,}000$ lb/in.$^2$, $\pm 54{,}000$ lb/in.$^2$ or by any combintion of these stresses.

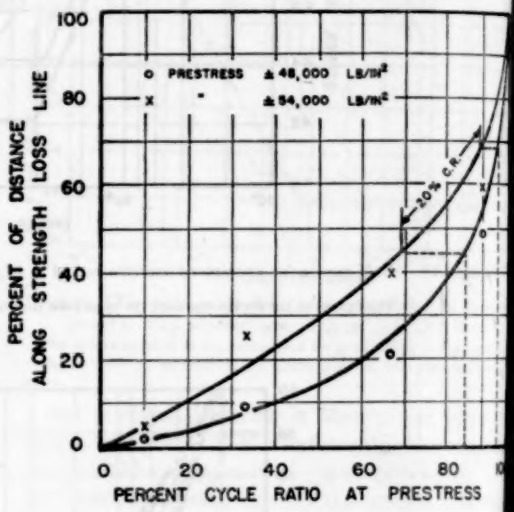


FIGURE 21.—*Cycle ratio versus damage relationship for two stresses.*

Dashed lines show method of predicting results for one complex loading schedule.

## 3. Multiple Prestress Tests

In order to investigate the reliability of the predictions based on the curves of figure 21, and at the same time to study the damage caused by more complex loading programs, the six prestressing schedules shown in table 10 were used. For each schedule, three to five specimens were tested to fracture at the test stress, and for schedule V an attempt was also made to determine the fatigue limit after prestress. All results of these tests are shown in table 10, together with the predictions based on figure 21. The method of making the predictions is illustrated by the dotted lines on the figure, showing the steps involved in schedule V. A cycle ratio of 85 percent at $\pm 48{,}000$

in.² results in 44 percent damage. A 44 percent damage corresponds to 69 percent cycle tio at ±54,000 lb/in.², and 69+20=89 percent cle ratio at 54,000 lb/in.², which corresponds to percent damage. A 69 percent damage would caused by 96 percent cycle ratio at ±48,000 in.², so a 4 percent cycle ratio should remain er the prestressing is complete. The number cycles to the start of cracking at this stress is 3,000, and 0.04×333,000=13,000, which repreits the number of cycles to form a crack at the t stress. In addition, it requires 78,000 cycle this stress for the crack to grow to fracture, so total predicted life under these conditions is 000 cycles.

TABLE 10.—*Multiple prestress tests*

| Prestress schedule [a] | Test results, $10^3$ cycles to fracture | | | | | Median $10^3$ cycles | Prediction $10^3$ cycles |
|---|---|---|---|---|---|---|---|
| ..... | 126 | 304 | 163 | 147 | 207 | 163 | 177 |
| ..... | 65 | 81 | 57 | 37 | 21 | 57 | 56 |
| ..... | 7 | 28 | 5 | ..... | ..... | 7 | 34 |
| ..... | 174 | 80 | 101 | ..... | ..... | 101 | 148 |
| ..... | <0 | 98 | <0 | 102 | 86 | 86 | 91 |
| ..... | 106 | 266 | 75 | ..... | ..... | 106 | 137 |

[a]—33⅓ percent cycle ratio at ±48,000 lb/in.² + 33⅓ percent cycle ratio at 000 lb/in.², test ±48,000 lb/in.²
—33⅓ percent cycle ratio at ±54,000 lb/in.² + 33⅓ percent cycle ratio at 000 lb/in.², test ±54,000 lb/in ².
—75 percent cycle ratio at ±54,000 lb/in.² + 15 percent cycle ratio at 000 lb/in.², test ±54,000 lb/in ².
—50 percent cycle ratio at ±48,000 lb/in.² + 33⅓ percent cycle ratio at 000 lb/in.², test ±48,000 lb/in ².
—85 percent cycle ratio at ±48,000 lb/in.² + 20 percent cycle ratio at 000 lb/in.², test ±48,000 lb/in ².
—15 percent cycle ratio at ±48,000 lb/in.², + 10 percent cycle ratio at 000 lb/in.², then repeat twice more. Test ±48,000 lb/in.².
Determination of fatigue limit for schedule IV.
" indicates that specimen fractured. "U" indicates that specimen did reak.
ddition to those listed, three specimens cracked before the prestressing ompleted.

| Stress, lb./in.² | $10^3$ cycles | Fatigue-limit prediction, lb./in.² |
|---|---|---|
| ±42,000 | 4,898 U | ±43,200 |
| ±42,200 | 22,715 U | ----------- |
| ±42,800 | 5,459 U | ----------- |
| ±43,000 | 399 F | ----------- |

The results listed in table 10 show reasonable agreement with the predictions, considering the large probable error of the tests involved. A small change in the rate of damage from one specimen to the next, particularly in the region where the curves of figure 21 are steep, may cause a large variation in the damage due to a certain prestress. Other methods tried for predicting these results, including the simple cumulative addition of cycle ratios suggested by Miner [6], failed to give reasonably close values for more than one or two of the schedules.

## 4. Repair of Damage

Two exploratory tests were made to verify the work of others on the repair of fatigue damage. In each case the prestress was 90 percent cycle ratio (based on $N_c$) at ±48,000 lb/in ². The first specimen was then stressed at ±42,200 lb/in.² (just under the new fatigue limit) for $34\times10^6$ cycles. When tested at ±48,000 lb/in.² this specimen did not fail in $40\times10^6$ cycles. The understressing had not only repaired the prior damage but raised the fatigue limit above that of the material in its original condition. As a matter of interest, this same specimen was subsequently "coaxed" by stressing 20 to 30 million cycles at each of seven successively higher stresses. At a stress of ±62,000 lb/in.² the specimen endured $21\times10^6$ cycles, then failed after 2,500,000 cycles at ±64,000 lb/in ². Thus a specimen damaged to the extent where the fatigue limit was less than ±42,500 lb/in.² was improved by suitable stress treatment, bringing its fatigue limit above ±62,000 lb/in ².

The second damaged specimen was normalized in a vacuum, reproducing as closely as possible the temperature cycle of the original heat treatment. When tested at ±48,000 lb/in.² the specimen fractured in 126,000 cycles. The normal expectancy for specimens after this prestress would be 143,000 cycles, indicating that the heat treatment resulted in no repair of the fatigue damage.

# VI. Discussion

The life of a specimen under fatigue stressing consists of two distinct phases. During the first, part of the material is progressively damaged until a small crack is formed, and during the second this crack grows until fracture occurs. In this report the term "fatigue damage" is used to designate only the change occurring during the first stage, material being considered 100 percent damaged at the time the first crack forms. If one wishes to study the first-stage damage, some method of determining the start of cracking is required. Lacking this, the effects of the second stage will confuse the results. Within the stress range used in this study, the proportion of the total life represented by the second stage varies from as much as 50 percent to as little as 10 percent, so it can be seen that a large error would be involved if the two stages were not separated.

With the *SAE* X4130 steel used in this investigation, the ratio of the second stage to the total life of the specimen was larger at stresses considerably above the fatigue limit than at stresses close to the fatigue limit. This is contrary to what certain other investigators have reported, but such a discrepancy may be expected, since the ratio depends on many factors such as the slope of the *S-N* curve for the original material, the ra of crack propagation in the metal, and the size the specimen.

The damage resulting from a particular numb of cycles of overstress depends on the past histo of the specimen. Thus, the performance cann be predicted accurately for metals in service whi are subjected to various ranges of stress, unless t complete loading schedule is known. Since th generally is not possible, the best that can be do for increasing the safety of a given steel struct is to apply a large number of cycles of stress bel the fatigue limit after each period of overstre This usually is taken care of by the nature of t service, but in some applications involving e ceptionally high stresses it might be worthwhi to apply low stresses purposely to counteract t effect of unusually long periods of high stress.

The results of the limited number of te made with specimens improved by understressi suggest that this improvement can be measur by distance along a strength loss line in a mann similar to that used for measuring damage (fig. 2 If this can be done, then the results of any loadi schedule can be predicted, regardless of wheth the stresses are above or below the fatigue lim

# VII. Conclusions

The results given in this paper lead to several important conclusions regarding fatigue damage occurring *prior* to the start of cracking.

1. If the damage occurring at one stress was determined by measurement at another, the apparent rate of damage depended on the value of both stresses. When the first was larger than the second, the damage occurred rapidly at first, then more slowly: the reverse was true when the first stress was the smaller.

2. The *S-N* curves for specimens after various damaging treatments showed that with increasing damage, the absolute value of the slope of the falling part of the curves increased and the fatigue limit decreased.

3. These differences in the *S-N* curves provided a measure of damage by which the damage occurring at different stresses could be directly added. The performance of specimens tested under co plex loading schedules could be ascertained the use of cycle-ratio versus damage curves the stresses involved.

4. The improvement due to understressi apparently can be measured in the same wa damage due to overstress.

5. Fatigue damage prior to the start of crack was repaired by understressing but not by h treatment.

Certain other conclusions regarding fatigue p nomena in general may be drawn from the resu obtained.

6. The slopes of the falling part of the *S* curves for the same material in smooth, notch and cracked specimens showed approximately t same (stress concentration) ratios as the fati limits.

7. The number of cracks formed in a specimen fore fracture increased rapidly as the test stress s raised above the fatigue limit.

8. The length, $L$, of fatigue cracks may be presented by the equation

$$\log (L-C)=\alpha N$$

here $C$ and $\alpha$ are constants, and $N$ is number of cles.

9. In specimens stressed considerably above e fatigue limit, the number of cracks, $M$, in a narrow circumferential band of the specimen can be expressed by the equation

$$\sqrt{M}=KS,$$

where $K$ is a constant, and $S$ is the average stress in the band.

10. The development of a small crack in a specimen resulted in a large decrease in the value of the fatigue limit as compared with specimens which had been stressed just short of cracking.

# VIII. References


J. A. Bennett, Effect of fatigue stressing short of failure on some typical aircraft metals, NACA Technical Note 992 (Oct. 1945).

J. B. Kommers, The effect of overstress in fatigue on the endurance life of steel, ASTM preprint No. 23 (1945).

J. A. Bennett, The early detection of cracks resulting from fatigue stressing, NACA Restricted Bulletin 4I15 (Sept. 1944).

[4] J. O. Almen, The useful data to be derived from fatigue tests, Metal Progress **44,** 254 (1943).

[5] R. J. Roark, Formulas for stress and strain (McGraw-Hill Book Co., Inc., New York, N. Y., 1943).

[6] M. A. Miner, Cumulative damage in fatigue, J. Applied Mech. **12,** A 159 (Sept. 1945).



WASHINGTON, February 6, 1946.

U. S. Department of Commerce
National Bureau of Standards

Research Pap RP1734
Volume 37, August 1946

Part of Journal of Research of the National Bureau of Standards

# Purification, Purity, and Freezing Points of 31 Hydrocarbons of the API-NBS Series[1]

*By Augustus R. Glasgow, Jr., Evelyn T. Murphy,[2] Charles B. Willingham, and Frederick D. Rossini*

**This report describes the purification and determination of freezing points and purity of 31 hydrocarbons of the API-NBS series, including 2 pentanes, 5 hexanes, 2 heptanes, 1 octane, 3 alkylcyclopentanes, 3 alkylcyclohexanes, and 15 alkylbenzenes.**

## I. Introduction

In May 1943, the Advisory Committee for the American Petroleum Institute Hydrocarbon Research Committee, operating the API Hydrocarbon Research Project[3] at the Ohio State University, requested the American Petroleum Institute Research Project 6 at the National Bureau of Standards to begin purification of a series of hydrocarbon compounds of the highest practicable purity, under the label API–NBS hydrocarbons. This work was begun July 1, 1943, with a large number of compounds of relatively high purity being supplied by the API Hydrocarbon Research Project for further purification. During the first year of operation, the purification of 31 compounds of the API-NBS series was completed. This report describes the purification and determination of freezing points and purity of these hydrocarbons, which are being made available on loan to qualified investigators for the measurement of needed properties.[4]

[1] This investigation was performed at the National Bureau of Standards as part of the work of the American Petroleum Institute Research Project 6 on the Analysis, Purification, and Properties of Hydrocarbons.

[2] Research Associate on the American Petroleum Institute Research Project at the National Bureau of Standards.

[3] On September 1, 1944, this project became the American Petroleum Research Project 45 on the "Synthesis and Properties of Hydrocarbons of Low-Molecular Weight", with Cecil E. Boord continuing as Supervisor and Robert F. Marschner becoming chairman of the Advisory Committee. D. P. Barnard was chairman of the former API Hydrocarbon Research Committee, which was merged on September 1, 1944, with the API Advisory Committee on Fundamental Research on the Composition and Properties of Petroleum, of which J. Bennett Hill was chairman.

[4] The allocation of these samples, by loan to qualified investigators for the measurement of needed properties, is handled by the Advisory Committee for the API Research Project 44 at the National Bureau of Standards on the "Collection, Analysis, and Calculation of Data on the Properties of Hydrocarbons" (W. E. Kuhn, chairman, Otto Beeck, Gustav Egloff, and S. Kurtz, Jr., with F. D. Rossini as Supervisor of the Project).

### Contents

| | Page |
|---|---|
| I. Introduction | 141 |
| II. Materials and purification | 142 |
| III. Freezing points and purity | 144 |
| IV. References | 145 |

# II. Materials and Purification

The starting materials were supplied as follows:[5]

By the API Hydrocarbon Research Project, now the API Research Project 45 on the "Synthesis and Properties of Hydrocarbons of Low-Molecular Weight", at the Ohio State University, under the supervision of Cecil E. Boord: Cyclopentane, ethylcyclopentane (A), methylcyclohexane (approximately half), ethylcyclohexane, *m*-xylene (A), *p*-xylene (A), 1,3,5-trimethylbenzene, *n*-butylbenzene (A), isobutylbenzene (A), *sec*-butylbenzene (A), and *tert*-butylbenzene (A).

By the Barrett Division of the Allied Chemical and Dye Corporation: Cyclohexane, methylcyclohexane (approximately half).

By the Standard Oil Co. (Indiana) and the M. W. Kellogg Co.: 2,3-Dimethylbutane.

By the General Motors Corporation: 2,2,3-Trimethylbutane.

By the Houdry Process Corporation: Methylcyclopentane.

By the Humble Oil & Refining Co.: Toluene.

By the Monsanto Chemical Co.: Ethylbenzene, isopropylbenzene.

By the Standard Oil Development Co.: *o*-Xylene (A).

By the Dow Chemical Co.: *n*-Propylbenzene (A).

By the API Research Project 6: *n*-Pentane, isopentane, *n*-hexane, 2-methylpentane, 3-methylpentane, 2,2-dimethylbutane, *n*-heptane, 2,2,4-trimethylpentane, benzene, 1,2,3-trimethylbenzene (A), 1,2,4-trimethylbenzene (A). In this group, the stocks of the following compounds were obtained by purchase of commercially available materials: *n*-Pentane, isopentane, and 2,2-dimethylbutane from the Phillips Petroleum Co.; *n*-heptane from the Westvaco Chlorine Products Co.; 2,2,4-trimethylpentane from the Rohm & Hass Co.; benzene, from the Koppers Co.

Information regarding the volume of the starting material, details of the purification by distillation, and volume of the selected "best" lot, is given in table 1. Additional details of the distilling columns are given in preceding reports [1, 2].[6] In addition to the purification by distillation, the benzene, *m*-xylene, and *p*-xylene were subjected to a purification by crystallization with centrifuging by B. J. Mair and A. J. Streiff of this laboratory [7].

For this group of 31 compounds, time was not available for the detailed examination of the purity, by measurement of freezing points, of the distillate as a function of its volume,[6] and the best sample was taken as an appropriately selected "heart" cut (not necessarily the middle part of the distillate) having the volume given in the last column of table 1. This volume may be compared for each compound with the volume of the starting material given in the third column. The heart cut was selected largely on the basis of refractive index and boiling point, although, as will be shown in the next report on the purification of API–NBS hydrocarbons [3], this is a procedure which frequently results in the discarding of the best material. Each final lot was filtered through silica gel [4] to remove water and nonhydrocarbon impurities.

[5] A letter A following the name of a compound indicates that subsequently a new and usually slightly purer sample (B) has been or is being prepared, the description of which will appear in a later report.

[*] Figures in brackets indicate the literature references at the end of this paper.

[6] In the next report on the purification of API–NBS and API-Standard hydrocarbons, in connection with the cooperative program of the National Bureau of Standards and the American Petroleum Institute on Standard Samples of hydrocarbons, a procedure will be described wherein enough freezing points are measured to determine the purity of the distillate as a function of its volume [3].

TABLE 1.—*Information on the starting materials and purification*

| Compound [a] | Starting material provided by laboratory [b] | Distillation [c] | | | | | | Volume of selected sample |
|---|---|---|---|---|---|---|---|---|
| | | Volume | Kind | Azeotrope-forming substance if used [f] | Still No. | Number of theoretical plates at total reflux (approx.) | Reflux ratio (approx.) | |
| **PARAFFINS** | | *Liters* | | | | | | *ml* |
| n-Pentane | APIRP 6 | 2.8 | Regular | | D | 100 | 100/1 | 370 |
| 2-Methylbutane (isopentane) | APIRP 6 | 2.8 | do | | D | 100 | 100/1 | 370 |
| n-Hexane | APIRP 6 | 1.2<br>1.2 | Azeotropic | Methanol | E<br>M | 100<br>100 | 100/1<br>100/1 | 375 |
| 2-Methylpentane | APIRP 6 | 1.9 | do | do | E | 100 | 100/1 | 325 |
| 3-Methylpentane | APIRP 6 | 0.50<br>1.4 | do | do | Q<br>H | 100<br>110 | 120/1<br>120/1 | 255 |
| 2,3-Dimethylbutane | APIRP 6 | 2.8 | Regular | | F | 100 | 100/1 | 290 |
| 2,3-Dimethylbutane | Std. (Ind.); Kellogg | 1.9 | Azeotropic | Methanol | M | 100 | 100/1 | 275 |
| n-Heptane | APIRP 6 | 1.0 | do | Ethanol | 8 | 130 | 145/1 | 380 |
| 2,2,3-Trimethylbutane | General Motors | 1.3 | do | Methanol | 9 | 135 | 165/1 | 360 |
| 2,2,4-Trimethylpentane | APIRP 6 | 2.4 | do | Ethanol | 10 | 135 | 165/1 | 350 |
| **ALKYLCYCLOPENTANES** | | | | | | | | |
| Cyclopentane | APIRP 45 | 0.80 | do | Methanol | 2 | 100 | 135/1 | 415 |
| Methylcyclopentane | Houdry | 1.8<br>0.45 | do | do | D<br>J | 100<br>125 | 100/1<br>100/1 | 380 |
| Ethylcyclopentane (A) | APIRP 45 | .40 | do | do | P | 100 | 120/1 | 200 |
| **ALKYLCYCLOHEXANES** | | | | | | | | |
| Cyclohexane | Barrett | 2.7 | Regular | | D | 100 | 100/1 | 400 |
| Methylcyclohexane | Barrett, APIRP 45 | 1.1 | Azeotropic | Ethanol | 8 | 130 | 145/1 | 400 |
| Ethylcyclohexane | APIRP 45 | 0.92 | do | Cellosolve | 9 | 135 | 165/1 | 450 |
| **ALKYLBENZENES** | | | | | | | | |
| Benzene | APIRP 6 | .59 | Regular [e] | | I | 125 | 100/1 | 450 |
| Toluene | Humble | .47 | do | | J | 125 | 100/1 | 330 |
| Ethylbenzene | Monsanto | .82 | Azeotropic | Methyl Cellosolve | E | 100 | 100/1 | 330 |
| o-Xylene (A) | Std. Oil Dev. | .60 | Regular | | J | 125 | 100/1 | 280 |
| m-Xylene (A) | APIRP 45 | .34 | Regular [e] | | I | 125 | 100/1 | 240 |
| p-Xylene (A) | APIRP 45 | .60 [d] | do.[e] | | I | 125 | 100/1 | 350 |
| n-Propylbenzene (A) | Dow | .48 | do | | J | 125 | 100/1 | 220 |
| Isopropylbenzene | Monsanto | .80 | Azeotropic | Cellosolve | M | 100 | 100/1 | 350 |
| 1,2,3-Trimethylbenzene (A) | APIRP 6 | .45 | do | Methyl Carbitol | 9 | 135 | 165/1 | 100 |
| 1,2,4-Trimethylbenzene (A) | APIRP 6 | .89 | do | do | 10 | 135 | 165/1 | 400 |
| 1,3,5-Trimethylbenzene | APIRP 45 | 1.2 | do | do | 8 | 130 | 145/1 | 260 |
| n-Butylbenzene (A) | APIRP 45 | 0.94 | do | do | 8 | 130 | 145/1 | 260 |
| sec-Butylbenzene (A) | APIRP 45 | 1.1 | do | do | 7 | 130 | 145/1 | 240 |
| tert-Butylbenzene (A) | APIRP 45 | 1.1 | do | do | 7 | 130 | 145/1 | 300 |
| | | 1.1 | do | do | 8 | 130 | 145/1 | 360 |

[a] A letter A following the name of a compound indicates that subsequently new and usually slightly purer sample (B) has been or is being prepared, the description of which will appear in a later report.

[b] The abbreviations represent the following laboratories:
APIRP 45; American Petroleum Institute Research Project 45 (formerly the American Petroleum Institute Hydrocarbon Research Project) on the "Synthesis and Properties of Hydrocarbons of Low Molecular Weight," at the Ohio State University, Columbus, Ohio; C. E. Boord, Supervisor.
APIRP 6; American Petroleum Institute Research Project 6 on the "Analysis, purification, and properties of hydrocarbons", at the National Bureau of Standards, Washington, D. C.; F. D. Rossini, Supervisor.
Barrett; Barrett Division of the Allied Chemical & Dye Corporation, New York, N. Y.
Dow; Dow Chemical Co., Midland, Mich.
General Motors; General Motors Corporation, Detroit, Mich.
Houdry; Houdry Process Corporation, Marcus Hook, Pa.
Humble; Humble Oil & Refining Co., Houston, Texas.
Kellogg; M. W. Kellogg Co., New York, N. Y.
Monsanto; Monsanto Chemical Co., Dayton, Ohio.
Std. Oil Dev.; Standard Oil Development Co., Elizabeth, N. J.
Std. (Ind.); Standard Oil Co. (Indiana), Whiting, Ind.

[c] See references [1] and [2] for further details.

[d] Three separate distillations of this volume were made.

[e] See text regarding additional purification by crystallization.

[f] Methyl Cellosolve is ethylene glycol monomethyl ether; Cellosolve is ethylene glycol monoethyl ether; methyl Carbitol is diethylene glycol monomethyl ether.

# III. Freezing Points and Purity

For each of the compounds except 3-methylpentane, which failed to yield crystals, the freezing point of the actual sample was determined from time-temperature freezing or melting curves obtained with the apparatus and procedure recently described [5]. From these data, the freezing point for zero impurity was determined according to the procedure described in reference [5].

For benzene and *p*-xylene, in which the solubility of water is quite appreciable, and for which the freezing points are above that of water, the sample was introduced, by filtration through a small tube containing silica gel, directly into the freezing tube with substantially no contact with the air of the room after water in the sample was removed by the silica gel. Dry air was kept flowing into the top of the freezing tube during the experiment.

The purity of the actual sample was calculated according to the method described in section VII of reference [5], using the values of the freezing point of the actual sample and the freezing point for zero impurity determined in this investigation (except as otherwise indicated), together with values of the cryoscopic constants obtained from the "*z*" tables of the American Petroleum Institute Research Project 44 [6] or from unpublished data from references [3] and [8]. For each of the compounds except 3-methylpentane, table 2 indicates whether freezing or melting experiments were used, and gives the values of the freezing point of the actual sample, the freezing point for zero impurity where determined in this investigation, and the calculated amount of impurity. The amount of impurity in the 3-methylpentane was estimated by analogy with 2-methylpentane. From the manner of preparation and purification of these compounds, it is believed that the impurities in most cases are substantially all close-boiling isomers.

TABLE 2.—*Freezing points and purity of 31 API-NBS hydrocarbons*

| Compound | Kind of time-temperature observations used to determine the freezing point [a] | Freezing point of the actual sample, in air at 1 atm. [b] | Freezing point for zero impurity in air at 1 atm. | Calculated amount of impurity in the actual sample [c] |
|---|---|---|---|---|
| **PARAFFINS** | | °C | °C | *Mole percent* |
| *n*-Pentane | F | −129.753 | −129.723±.015 | 0.15 ±.07 |
| 2-Methylbutane (isopentane) | F | −159.922 | −159.890±.012 | .15 ±.06 |
| *n*-Hexane | F | −95.342 | −95.320±.010 | .11 ±.05 |
| 2-Methylpentane | F | −153.685 | −153.680±.010 | .03 ±.02 |
| 3-Methylpentane | | | | [d](.10 ±.08) |
| 2,2-Dimethylbutane | F | −99.97 | −99.73 ±.13 | .05 ±.03 |
| 2,3-Dimethylbutane | F | −128.57 | −128.41 ±.06 | .07 ±.03 |
| *n*-Heptane | F and M | −90.607 | −90.595±.010 | .06 ±.05 |
| 2, 2,3-Trimethylbutane | F | −25.037 | −24.96 ±.05 | .03 ±.02 |
| 2, 2,4-Trimethylpentane | M | −107.396 | −107.365±.013 | .12 ±.05 |
| **ALKYLCYCLOPENTANES** | | | | |
| Cyclopentane | F | −93.90 | −93.80 ±.04 | .023±.010 |
| Methylcyclopentane | F | −142.474 | −142.445±.012 | .16 ±.06 |
| Ethylcyclopentane (A) | M | −138.460 | | .08 ±.04 |
| **ALKYLCYCLOHEXANES** | | | | |
| Cyclohexane | F and M | +6.547 | +6.554±.005 | .003±.002 |
| Methylcyclohexane | M | −126.596 | | .10 ±.08 |
| Ethylcyclohexane | M | −111.325 | | .10 ±.08 |
| **ALKYLBENZENES** | | | | |
| Benzene | F | +5.509 | +5.533±.010 | .037±.020 |
| Toluene | F and M | −95.011 | −94.991±.012 | .05 ±.03 |
| Ethylbenzene | M | −94.995 | −94.950±.025 | .16 ±.09 |
| *o*-Xylene (A) | M | −25.187 | −25.175±.010 | .032±.027 |
| *m*-Xylene (A) | F and M | −47.928 | −47.872±.020 | .15 ±.05 |
| *p*-Xylene (A) | F | +13.239 | +13.263±.012 | .06 ±.03 |
| *n*-Propylbenzene (A) | M | −99.585(I) | | .29 ±.08 |
| *Iso*-Propylbenzene | M | −96.043 | −96.028±.010 | .04 ±.03 |
| 1, 2, 3-Trimethylbenzene (A) | F | −25.494 | | .20 ±.04 |
| 1, 2, 4-Trimethylbenzene (A) | M | −43.913(I) | | .32 ±.20 |
| 1, 3,5-Trimethylbenzene | M | −44.738(I) | | .04 ±.02 |
| *n*-Butylbenzene (A) | M | −87.904 | | .09 ±.08 |
| *iso*-Butylbenzene (A) | M | −51.527 | | .14 ±.09 |
| *sec*-Butylbenzene (A) | M | −75.572 | | .31 ±.06 |
| *tert*-Butylbenzene (A) | M | −57.872 | | .05 ±.03 |

[a] F indicates freezing and M indicates melting. See reference [5] for details.

[b] A roman numeral I indicates that the value is for that crystalline form having the highest freezing point.

[c] The values in this column were calculated as described in reference [5], using the values of the cryoscopic constants and freezing points for zero impurity given in the "*z*" tables of the American Petroleum Institute Research Project 44, reference [6]. For the 19 compounds for which values of the freezing point for zero impurity are reported in this paper, the values given in reference [6] are, at the time of this writing, identical to those in this table.

[d] The amount of impurity in the 3-methylpentane was estimated by analogy with 2-methylpentane.

Grateful acknowledgment is made to the following persons and laboratories for supplying the materials for purification listed in table 1: C. E. Boord, Supervisor of the American Petroleum Institute Research Project 45 (formerly the API Hydrocarbon Research Project) at the Ohio State University, Columbus, Ohio; W. J. Sweeney, Standard Oil Development Co., New York, N. Y.; T. A. Boyd and W. G. Lovell, General Motors Corporation, Detroit, Mich.; E. A. Smith, Houdry Process Corporation, Marcus Hook, Pa.; R. E. Dreisbach, Dow Chemical Co., Midland, Mich.

rrett Division of the Allied Chemical & Dye rporation, New York, N. Y.; Standard Oil Co. diana), Whiting, Ind.; M. W. Kellogg Co., w York, N. Y.; Monsanto Chemical Co., yton, Ohio; Humble Oil & Refining Co., Hous-, Tex.

Especial acknowledgment is due George Calingaert, formerly chairman of the subcommittee on purification and properties under the API Hydrocarbon Research Project, who made the arrangements for starting the series of API–NBS hydrocarbons.

## IV. References

C. B. Willingham and F. D. Rossini, J. Research NBS **37**, 15, (1946) RP 1724.

A. F. Forziati, A. R. Glasgow, Jr., C. B. Willingham, and F. D. Rossini, J. Research NBS **36**, 129 (1946) RP 1695.

A. J. Streiff, E. T. Murphy, C. B. Willingham, V. A. Sedlak, and F. D. Rossini, National Bureau of Standards. American Petroleum Institute Research Project 6. Unpublished.

B. J. Mair and A. F. Forziati, J. Research NBS **32**, 151 (1944) RP 1582.

A. R. Glasgow, Jr., A. J. Streiff, and F. D. Rossini, J. Research NBS **35**, 355 (1945) RP 1676.

[6] American Petroleum Institute Research Project 44 at the National Bureau of Standards. Tables 1*z*, 2*z*, 3*z*, and 5*z*. Heat and entropy of fusion, freezing points, and cryoscopic constants. Dec. 31, 1944, to Aug. 31, 1945.

[7] B. J. Mair and A. J. Streiff, J. Research NBS **27**, 343 (1941) RP 1423.

[8] A. J. Streiff, E. T. Murphy, J. C. Cahill, H. F. Flanagan, V. A. Sedlak, C. B. Willingham, and F. D. Rossini, National Bureau of Standards. American Petroleum Institute Research Project 6. Unpublished.

WASHINGTON, April 3, 1946.

S. Department of Commerce
tional Bureau of Standards

Research Paper RP1735
Volume 37, August 1946

Part of Journal of Research of the National Bureau of Standards

# bsorption Measurements for Broad Beams of 1- and 2-Million-Volt X-Rays

*By George Singer, Carl B. Braestrup*, and Harold O. Wyckoff*

Experimentally determined concrete-absorption curves are given for wide-angle X-ray beams produced by a 1- and 2-million-volt resonance generator. Data on the variation of X-ray intensity with the distance from a concrete barrier are included. With this information as a basis, the thickness of a concrete barrier necessary for protection against a broad X-ray beam has been computed for 1- and 2-million-volt X-rays and for various tube currents and barrier-to-target distances.

## I. Introduction

One- and two-million-volt X-radiation is now d routinely for industrial radiography. In s application the cone of radiation used is much ader than is common in other applications. is is so for two reasons. The first is that the of a large field effects a saving in the time uired to radiograph a large object or a number small objects in one lot. The second is that massive cones needed to restrict the field very penetrating radiation must necessarily it the mobility of the X-ray generator; their is therefore commonly avoided, although irable for other reasons.

Concrete, being structurally self-supporting, tively inexpensive, and easily fabricated, has come the standard material for the construction barriers for protection against very penetrating iation. Theoretical absorption curves appli- le to such barriers are not currently available wide-angle beams. In the calculations for h absorption curves a correction must be made scattering which retains the scattered photons hin the confines of the primary beam, a process ding to reduce the attenuation for wide-angle ms in comparison with that for narrow beams he same radiation.

This problem has been recognized in several papers relating to X-ray protection.[1] [2] [3] [4] However, there are considerable technical difficulties involved in obtaining such data experimentally. For this reason all discussion in the literature relating to the increase in barrier thickness needed for wide-angle beams over that for narrow beams is of a general and indirect nature, and is not sufficiently detailed for specific application in the development of protection specifications.

In the design of protective barriers, information is also needed on the variation of X-ray-dosage rate with distance from the protective barrier to the position at which personnel will be stationed. Because of scattering from the barrier it is to be expected that for very penetrating radia-

nior Physicist, Department of Hospitals, City of New York.

[1] R. Jaeger and A. Trost, Elektrotech. Z. **61**, 1,025 (1940).
[2] T. R. Folson and E. F. Focht, Am. J. Roentgenol. Radium Therapy **51**, 76 (1944).
[3] G. Singer and George C. Laurence, Ind. Radiology **40**, Fall (1945); Radiology **46**, 69 (1946).
[4] G. Failla, Am. J. Roentgenol. **54**, 553 (1945).

Contents

| | | Page |
|---|---|---|
| I. | Introduction | 147 |
| II. | Method | 148 |
| III. | Results | 149 |
| IV. | Conclusions | 150 |

tion this variation will not follow the inverse-square law for the distance measured from the tube target. It is to be expected that this variation will be more rapid than indicated by this law because both the X-ray-tube target and the irradiated volume of concrete act as sources of radiation.

It is the purpose of this paper to present (1) experimental data on absorption of X-ray concrete for wide-angle beams generated by ages of 1 and 2 million volts, (2) prelimi data on the variation of the dosage rate with distance from a protective barrier, and (3) on concrete protection requirements for 1- 2-million-volt radiation under certain condit which obtain in industry.

## II. Method

The experimental arrangement used in obtaining the basic data given below is indicated in figure 1. The concrete wall, *C*, is the main wall of the building housing the generator and is 41 inches [5] thick; *D*, is the covered maze within which the ionization measurements were made.

Dosage measurements were made by calibrated dosage instruments designed by Braestrup.[6] Three sizes of ionization chambers were used; their characteristics are listed in table 1. The ionization chamber potentials were measured before and after irradiation by means of a string electrometer which is an integral part of the dosage meter. All ionization chambers were calibrated with both 175-kv X-rays and gamma-rays f radium. Both calibrations agreed very with the theoretical values based upon the volume and capacitance. At the National reau of Standards the small thimble cha and the electrometer head were checked ag a similar instrument combination with 1-mil volt radiation and were found to be in agree therewith to within 2 percent.

[5] Because the thickness of protective barriers is often of practical interest to persons unfamiliar with metric units, we have specified the dimensions of all barriers in feet and inches.

[6] C. B. Braestrup, Radiology **38**, 22, 207 (1942).

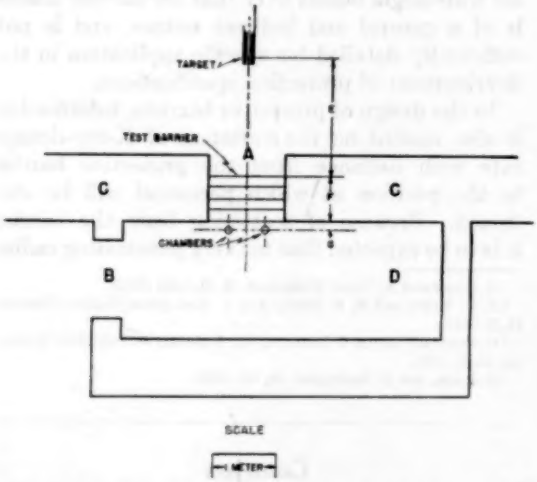


FIGURE 1.—*Experimental arrangement showing two sets of concrete test blocks in place.*

A total of three sets were used.

TABLE 1.—*Ionization chambers*

| Type | Wall material | Inside dimensions | | Volume | r[7] |
|---|---|---|---|---|---|
| | | Diameter | Length | | |
| | | cm | cm | cm³ | |
| CX-1, Cylindrical. | Bakelite | 12.05 | 21.85 | 2490 | 0.2 |
| SX-11, Spherical | Polystyrene | 10.5 | | 624 | .7 |
| D-1, Thimble | Catalin | 0.7 | 2.15 | 0.783 | 1.0 |

[7] Dose in roentgens per scale division of electrometer.

The barrier material consisted of concrete bl of density 130 lb/ft³, measuring 5¾ by 7¾ by in. These were laid in the doorway, *A*, show figure 1. Measurements were made through of double layers of these blocks; one 5¾ in. the other 7¾ in. thick. The layers were stagg so that the planes of the cracks between bl did not pass through either the tube targe ionization chamber. The opening remaining tween the top of the test barrier and the lint the doorway to the maze was filled with lead b For this arrangement both the radiation lea through the doorway, *B*—produced by the scattered through a glass-brick window above main wall, *C*—and that through cracks in the barrier were found to be negligible in compar with the dosage rate at the position of the ionization chambers.

The distance, $E$, in figure 1 was 1.83 m in all cases; is the barrier thickness. This thickness was nverted to thickness of concrete of a density of 7 lb/ft$^3$ before plotting. The wall-to-center-of-amber distance, $G$, varied from 2 to 4 in. for all otted points. The ionization chambers were aced as near as practicable to the radiation rrier. It will be shown later that this position ves the minimum apparent absorption.

The X-ray generator used is the 2-million-volt -ray resonance generator described by Charlton and Westendorp,[7] which is operative at both 1 and 2 million volts. All measurements were made with X-radiation transmitted through the tube target along the axis of the tube. The anode cone consisted of a cylinder with a lead wall 5 cm thick, the end of which was shaped so as to confine the X-ray beam to a cone of radiation measuring approximately 70° at its apex.

[7] E. E. Charlton and W. F. Westendorp, Electronics **17**, 128 (1944). We are indebted to the General Electric Co. and to E. E. Charlton, of their Research Laboratory, for facilities that were made available to us in carrying out these experiments.

# III. Results

The attenuation curves obtained are shown in gure 2. As a check on the reliability of the ethod used, transmission measurements for million-volt radiation through a solid concrete all 42 in. thick of density 152 lb/ft$^3$ were also made. The single point so obtained is plotted in figure 2 at a thickness of about 43 in.

The effect of chamber-to-wall distance on the apparent attenuation is illustrated by the curves in figure 3. The ordinate is in arbitrary units. It is obtained by dividing the dose per milliampere minute by the square of the sum of the distances $E$, $F$, and $G$. The abscissa is the chamber-wall distance, $G$, shown in figure 1. If there were neither scattering in the wall nor absorption in the air, each set of plotted points should give a straight line with zero slope. Actually, because of wall scattering, the value of the ordinate decreases with increase of abscissa. These plotted points

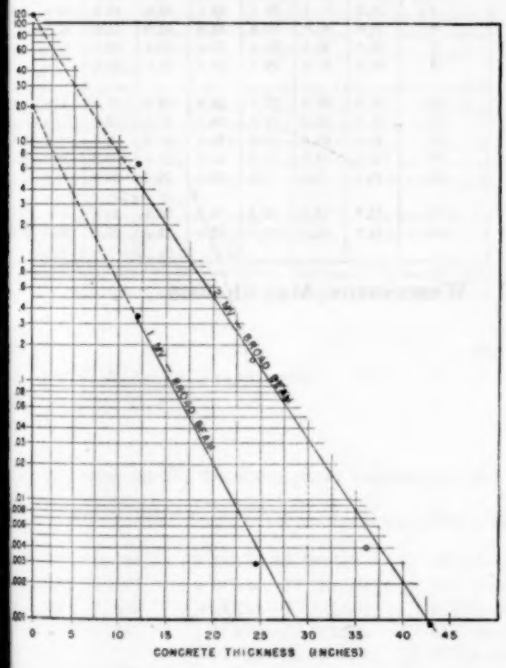


IGURE 2.—*Concrete absorption curves for 70° beams of 1- and 2-million-volt X-rays.*

measurements were made with the radiation transmitted through a ungsten target along the tube axis. A resonance generator was used. The voltage waveform of such generators is sinusoidal. All indicated oltages are peak or crest values.

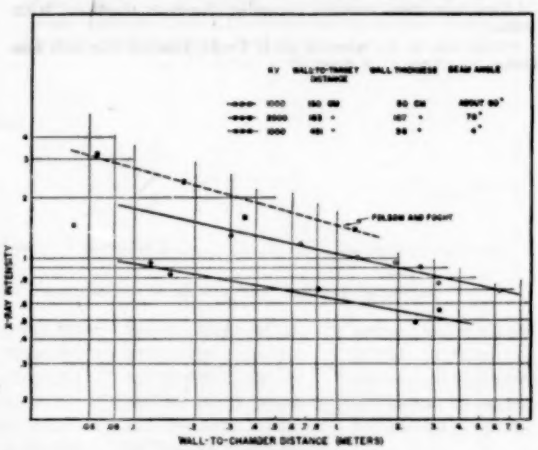


FIGURE 3.—*Variation of X-ray dose with distance from a concrete protective barrier.*

The abscissa is the distance to the ionization chamber measured from the side of the barrier from which the radiation emerges. The ordinate is obtained by dividing the dose per milliampere minute by the square of the distance from the X-ray source to ionization chamber.

fall along a straight line for each experimental setup. The slopes measured on a linear scale—not the logarithmic scale of figure 3—are approximately 0.25. This is so not only for our own 1-million-volt and 2-million-volt data for 70° beams but also for the 1 data on a 4° beam published by Folson and Focht.[8] Accordingly, may be concluded that within these limits beam angle has no important effect on the cha in apparent attenuation with chamber-to-w distance.

[8] Folson and Focht, Am. J. Roentgenol. Radium Therapy 51, 70 (

# IV. Conclusions

From the data presented above it is possible to compute for broad X-ray beams the thickness of concrete barriers necessary for protection against 1- and 2-million-volt X-radiation from targets of the transmission type. Such targets are standard in this quality range. In table 2 the thickness of such barriers is listed for 1- and 2-million-volt X-radiation and for the various tube currents and target distances normally encountered in practice. The tubular values given therein were computed directly from the absorption curves of figure 2. A few points at short distances and high currents required linear extrapolation for their determination. Absorption of X-radiation by air has been neglected. A permissible daily dose of 0.1 r has been assumed.[9, 10] It was further assumed that the dosage rate per milliampere at 1m for a 1-million-volt X-ray generator is 20 r/min and for a 2-million-volt X-ray generator, 120 r/min and th the person to be protected will normally be st tioned near the protective barrier.

TABLE 2.—*Thickness of concrete of density 147 lb/ required for protection against broad beams of X-r for the current, distance, and voltage indicated*

| Target distance | 1-million-volt X-rays | | | | 2-million-volt X-rays | | | |
|---|---|---|---|---|---|---|---|---|
| | 0.5 ma | 1.0 ma | 2.0 ma | 3.0 ma | 0.5 ma | 1.0 ma | 2.0 ma | 3.0 m |
| *Feet* | *In.* | *In.* | *In.* | *In.* | *In.* | *In.* | *In.* | *In.* |
| 4 | 30.5 | 32.5 | 34.5 | 36.0 | 44.5 | 47.0 | 49.5 | 51.0 |
| 5 | 29.5 | 31.5 | 33.5 | 34.5 | 43.0 | 45.5 | 48.0 | 49.5 |
| 6 | 28.0 | 30.0 | 32.5 | 33.5 | 42.0 | 44.5 | 47.0 | 48.5 |
| 8 | 26.5 | 28.5 | 30.5 | 32.0 | 39.5 | 42.0 | 44.5 | 46.0 |
| 10 | 25.0 | 27.0 | 29.5 | 30.5 | 38.0 | 40.5 | 43.0 | 44.5 |
| 15 | 23.0 | 25.0 | 27.0 | 28.0 | 35.0 | 37.5 | 40.0 | 41.5 |
| 20 | 21.0 | 23.0 | 25.0 | 26.5 | 33.0 | 35.5 | 38.0 | 39.5 |
| 30 | 18.5 | 20.5 | 22.5 | 24.0 | 30.0 | 32.5 | 35.0 | 36.5 |
| 40 | 17.0 | 19.0 | 21.0 | 22.0 | 28.0 | 30.5 | 33.0 | 34.5 |
| 50 | 15.5 | 17.5 | 19.5 | 21.0 | 26.0 | 28.5 | 31.0 | 32.5 |
| 75 | 13.5 | 15.5 | 17.5 | 18.5 | 23.0 | 25.5 | 28.0 | 29.5 |
| 100 | 11.5 | 13.5 | 15.5 | 17.0 | 21.0 | 23.5 | 26.0 | 27.5 |

WASHINGTON, May 31, 1946

[9] X-ray protection, National Bureau of Standards Handbook HB20 (1936).

[10] Safety code for the industrial use of X-rays, American Standards Association, New York, N. Y. (1946).

# MATHEMATICAL TABLES

**(Note that prices in parentheses are for countries not extending the franking privilege)**

**Attention is invited to a series of publications prepared by the *Project for the Computation of Mathematical Tables* conducted by the Federal Works Agency, Work Projects Administration for the City of New York, under the sponsorship of the National Bureau of Standards. The tables which have been made available through the National Bureau of Standards are listed below. A list of other WPA tables obtainable elsewhere will be sent by the Bureau on request. There is included in this list a publication of the hypergeometric and Legendre functions (MT15), prepared by the Bureau.**

**Payment is required in advance. Make remittance payable to the "National Bureau of Standards" and send with order, using the blank form below. A mailing list is maintained for those who desire to receive announcements regarding new tables as they become available.**

T1. Table of the First Ten Powers of the Integers From 1 to 1000: 1938) VIII+80 pages; heavy paper cover. Out of print.

T2. Tables of the Exponential Function $e^x$: The ranges and intervals of the argument and the number of decimal places in the entries are given below:

| Range of x | Interval of x | Decimals given |
|---|---|---|
| −2.5000 to 1.0000 | 0.0001 | 18 |
| 1.0000 to 2.5000 | .0001 | 15 |
| 2.500 to 5.000 | .001 | 15 |
| 5.00 to 10.00 | .01 | 12 |

1939) XV+535 pages; bound in buckram, $2.00 ($2.50).

T3. Tables of Circular and Hyperbolic Sines and Cosines for Radian Arguments: Contains 9 decimal place values of sin $x$, cos $x$, sinh $x$, and cosh $x$ for $x$ (in radians) ranging from 0 to 2 at intervals of .0001. (1939) XVII+405 pages; bound in buckram, $2.00 ($2.50).

T4. Tables of Sines and Cosines for Radian Arguments: Contains 8 decimal place values of sines and cosines for radian arguments ranging from 0 to 25 at intervals of 0.001. (1940) XIX+275 pages; bound in buckram, $2.00 ($2.50).

T5. Tables of Sine, Cosine, and Exponential Integrals, Volume I: Values of these functions to 9 places of decimals from 0 to 2 at intervals of .0001. (1940) XXVI+444 pages; bound in buckram, $2.00 ($2.50).

T6. Tables of Sine, Cosine, and Exponential Integrals, Volume II: Values of these functions to 9, 10, or 11 significant figures from 0 to 10 at intervals of 0.001 with auxiliary tables. (1940) XXXVII+225 pages; bound in buckram, $2.00 ($2.50).

T7. Table of Natural Logarithms, Volume I: Logarithms of the integers from 1 to 50,000 to 16 places of decimals. (1941) XVIII+501 pages; bound in buckram, $2.00 ($2.50).

T8. Tables of Probability Functions, Volume I: Values of these functions to 15 places of decimals from 0 to 1 at intervals of 0.0001, and from 1 to 5.6 at intervals of 0.001. (1941) XXVIII+302 pages; bound in buckram, $2.00 ($2.50).

MT9. Table of Natural Logarithms, Volume II: Logarithms of the integers from 50,000 to 100,000 to 16 places of decimals. (1941) XVIII+501 pages; bound in buckram, $2.00 ($2.50).

MT10. Table of Natural Logarithms, Volume III: Logarithms of the decimal numbers from 0.0001 to 5.0000, to 16 places of decimals. (1941) XVIII+501 pages; bound in buckram, $2.00 ($2.50).

MT11. Tables of the Moments of Inertia and Section Moduli of Ordinary Angles, Channels, and Bulb Angles With Certain Plate Combinations: (1941) XIII+197 pages; bound in green cloth. $2.00 ($2.50).

MT12. Table of Natural Logarithms, Volume IV: Logarithms of the decimal numbers from 5.0000 to 10.0000, to 16 places of decimals. (1941) XXII+506 pages; bound in buckram, $2.00 ($2.50).

MT13. Table of Sine and Cosine Integrals for Arguments from 10 to 100. (1942) XXXII+185 pages; bound in buckram, $2.00 ($2.50).

MT14. Tables of Probability Functions, Volume II: Values of these functions to 15 places of decimals from 0 to 1 at intervals of 0.0001 and from 1 to 7.8 at intervals of 0.001. (1942) XXI+344 pages; bound in buckram, $2.00 ($2.50).

MT15. The Hypergeometric and Legendre Functions With Application to Integral Equations of Potential Theory. By Chester Snow, National Bureau of Standards. Reproduced from original handwritten manuscript. (1942) VII+319 pages; bound in heavy paper cover. Out of print.

MT16. Table of Arc Tan x: Table of inverse tangents for positive values of the angle in radians. Second central differences are included for all entries. $x=[0(.001)7(.01)50(.1)300(1)2,000(10)10,000; 12D]$ (1942) XXV+169 pages; bound in buckram, $2.00 ($2.50).

*(Continued on other side)*

(Cut Here)

ATIONAL BUREAU OF STANDARDS
ashington 25, D. C.

Date

Please send me the Mathematical Tables checked below. I enclose $_____ to cover the cost.

CHECK HERE (Note that prices in parentheses are for countries not extending the franking privilege)

| | | | | |
|---|---|---|---|---|
| ☐ MT2—$2 ($2.50) | ☐ MT9—$2 ($2.50) | ☐ MT17—$1.50 ($1.75) | ☐ MT25—$0.25 ($0.30) | ☐ MT32—$0.25 ($0.30) |
| ☐ MT3—$2 ($2.50) | ☐ MT10—$2 ($2.50) | ☐ MT18—$0.25 ($0.30) | ☐ MT26—$0.25 ($0.30) | ☐ MT33—$0.25 ($0.30) |
| ☐ MT4—$2 ($2.50) | ☐ MT11—$2 ($2.50) | ☐ MT19—$0.25 ($0.30) | ☐ MT27—$0.25 ($0.30) | ☐ MT34—$0.25 ($0.30) |
| ☐ MT5—$2 ($2.50) | ☐ MT12—$2 ($2.50) | ☐ MT20—$0.25 ($0.30) | ☐ MT28—$0.25 ($0.30) | ☐ MT35—$0.25 ($0.30) |
| ☐ MT6—$2 ($2.50) | ☐ MT13—$2 ($2.50) | ☐ MT21—$0.25 ($0.30) | ☐ MT29—$0.25 ($0.30) | ☐ MT36—$0.25 ($0.30) |
| ☐ MT7—$2 ($2.50) | ☐ MT14—$2 ($2.50) | ☐ MT22—$0.25 ($0.30) | ☐ MT30—$0.25 ($0.30) | |
| ☐ MT8—$2 ($2.50) | ☐ MT16—$2 ($2.50) | ☐ MT24—$0.25 ($0.30) | ☐ MT31—$0.25 ($0.30) | |

ND ONLY MONEY
RDER OR CHECK
AYABLE TO THE
NATIONAL BUREAU
F STANDARDS" IN
. S. CURRENCY.

_____
(Name)

_____
(Address)

_____
(City, Zone, and State)

## MATHEMATICAL TABLES—*Continued*

**MT17.** Miscellaneous Physical Tables: Planck's Radiation Functions (Originally published in the Journal of the Optical Society of America, February 1940); and Electronic Functions. (1941) VII+58 pages; bound in buckram, $1.50 ($1.75).

**MT18.** Table of the Zeros of the Legendre Polynomials of Order 1-16 and the Weight Coefficients for Gauss' Mechanical Quadrature Formula. (Reprinted from Bul. Amer. Mathematical Society, October 1942.) 5 pages, with cover, 25 cents (30¢).

**MT19.** On the Function $H(m, a, x) = \exp(-ix)F(m+1-ia, 2m+2; 2ix)$; with table of the confluent hypergometric function and its first derivative. (Reprinted from J. Math. Phys., December 1942.) 20 pages, with cover. 25 cents (30¢).

**MT20.** Table of Integrals $\int_0^x J_0(t)dt$ and $\int_0^x Y_0(t)dt$. (Reprinted from J. Math. Phys., May 1943.) 12 pages, with cover, 25 cents (30¢).

**MT21.** Table of $Jis(x) = \int_x^\infty \frac{J_0(t)}{t}dt$ and Related Functions. (Reprinted from J. Math. Phys., June 1943.) 7 pages, with cover, 25 cents (30¢).

**MT22.** Table of Coefficients in Numerical Integration Formulae. (Reprinted from J. Math. Phys., June 1943.) 2 pages, with cover, 25 cents (30¢).

**MT23.** Table of Fourier Coefficients. (Reprinted from J. Math. Phys. Sept. 1943.) 11 pages, with cover. (Out of print.)

**MT24.** Coefficients for Numerical Differentiation With Central Differences. (Reprinted from J. Math. Phys., Sept. 1943.) 21 pages, with cover, 25 cents (30¢).

**MT25.** Seven-Point Lagrangian Integration Formulas. (Reprinted from J. Math. Phys., Dec. 1943.) 4 pages, with cover, 25 cents (30¢).

**MT26.** A Short Table of the First Five Zeros of the Transcendental Equation. $J_\sigma(x)Y_\sigma(kx) - J_\sigma(kx)Y_\sigma(x) = 0$. (Reprinted from J. Math. Phys., Dec. 1943.) 2 pages, with cover, 25 cents (30¢).

**MT27.** Table of Coefficients for Inverse Interpolation With Central Differences. (Reprinted from J. Math. Phys., Dec. 1943.) pages, with cover, 25 cents (30¢).

**MT28.** Table of $J_\sigma(x) = \frac{n!}{(x/2)^n}J_\sigma(x)$. (Reprinted from J. Math. Phys., 1944.) 16 pages, with cover, 25 cents (30¢).

**MT29.** Table of Coefficients for Inverse Interpolation With vancing Differences. (Reprinted from J. Math. Phys., May 19 28 pages, with cover, 25 cents (30¢).

**MT30.** A New Formula for Inverse Interpolation. (Reprinted Bul. Amer. Mathematical Society, Aug. 1944.) 4 pages, with cove cents (30¢).

**MT31.** Coefficients for Interpolation Within a Square Grid in Complex Plane. (Reprinted from J. Math. Phys., Aug. 1944.) 11 pa with cover, 25 cents (30¢).

**MT32.** Table of Coefficients for Differences in Terms of the Du atives. (Reprinted from J. Math. Phys., Nov. 1944.) 4 pages, cover, 25 cents (30¢).

**MT33.** Table of Coefficients for Numerical Integration Wit Differences. (Reprinted from J. Math. Phys., Feb. 1945.) 21 pa with cover, 25 cents (30¢).

**MT34.** Inverse Interpolation for Eight-, Nine-, Ten-, and Elev Point Direct Interpolation. (Reprinted from J. Math. Phys., M 1945.) 3 pages, with cover, 25 cents (30¢).

**MT35.** Table of Coefficients for Double Quadrature Without D ferences, for Integrating Second Order Differential Equati (Reprinted from J. Math. Phys., Nov. 1945.) 6 pages, with cove cents (30¢).

**MT36.** Formulas for Direct and Inverse Interpolation of a Comp Function Tabulated Along Equidistant Circular Arcs. (Repri from J. Math. Phys., Nov. 1945.) 3 pages, with cover, 25 cents (30¢).